Analysis of phenolic compounds by dint of GDH-biosensors and immunoassays

Dissertation

Zur Erlangung des akademischen Grades
Doktor der Naturwissenschaften
(Dr. rer. nat.)
in der Wissenschaftsdisziplin Analytische Biochemie

eingereicht an der
Mathematisch-Naturwissenschaftlichen Fakultät
der Universität Potsdam

von
Andreas Rose

Potsdam, im Juni 2003

Die Zukunft hat viele Namen.
Für die Schwachen ist sie das Unerreichbare.
Für die Furchtsamen ist sie das Unbekannte.
Für die Tapferen ist sie die Chance.

Victor Marie Hugo (1802 - 1885)

Acknowledgements

Specially, I wish to thank Prof. F.W. Scheller who gave me the great opportunity to work in his famous group. Thanks for offering me many helpful advice and for always encouraging me finishing this project.

Jenny, “the boss”, for always supporting and trusting me, for allowing me to spend a lot of fruitful time in her labs, and for not separating me from Catalin, even the noise level increased with the both of us in the same lab.

Prof. P.D. Hansen for taking the job as referee of this thesis. He organized nice workshops in Berlin and was key person at many international meeting on biosensor for environmental monitoring (Barcelona, Cork, Cascais).

I would like to express my gratitude to all the people, who have contributed to the completion of this thesis: Let’s start with the “Luckenwalde/Potsdam” group:

Ulla, my supervisor, who always supported me even we had difficult times and different ideas. Her theoretical way of thinking was the perfect match to my practical ideas.

My thousand thanks Andrea, for helping me through my work as well as through my private life.

Thanks Mak for fruitful discussions about science, life, football and other sports.

Daniela for the nice time in Luckenwalde, Berlin, Potsdam, Sweden, and USA. She wasn’t angry (only surprised) when unannounced visitors came to Salzburg.

Peter for giving me a place during nights when I had missed the last train to Luckenwalde.

Kristian and Moe, the first students I ever led through a practical course in “Analytical Biochemistry”. In the end we spent much time together in the lab, in bars, in cinemas, or watching sports on TV. All past and present members (Katrin, Claudia, Bixia, Fred, Axel, Nenad etc.) of department of Analytical Biochemistry.

The people at Lund University and other places around Europe:

Catalin, my Romanian lab- and roommate in many occasions. The person, that taught me most basics about biosensors, immunoassays, and especially the handling in the lab. Thanks for the great days in Lund, Barcelona, Cascais, Luckenwalde, and Potsdam, including our trips to Berlin, Munich, Salzburg, and Hanover. His lovely wife Mickey. She never complained when I staid as an additional member of the family in their house. You made me very happy asking to become godfather of little Andrea.

The members of the Romanian “Mafia” in Lund for very nice days in the lab, the gym, participating at football tournaments, playing “Siedler” and stuffing me with excellent Romanian food (killer cabbage and cow stomach soup).

People from the Analytical Chemistry Department at Lund University for letting me participate at wonderful Xmas-parties with “Snaps” and food from all over the world.

Thanks to Damia, Arantxa (Columbus egg(s)), Peter, Eva, Natalia, Iannis, and other colleagues from all over Europe. Frank, Anja, Jochen, Jochen, Frank, and Tom my very best friends for the longest time of my life. They supported me throughout the years.

Last not least I want to express my gratitude to my new colleagues at Aventis Pharma Germany. My bosses Hilde and Andrea for the excellent training opportunities and the guidance to perform the step from university to the industrial world. The QAs (Anja, Andreas, Alik, and Joachim) for the coffee, breakfast, and DVDs.

Many thanks to the participants of the Aventis trainee program 2002 for making the start in Frankfurt a nice and easy one.

My beloved family (Heinrich, Inge, Gitta, Kalle, Nils, Heiner, Tina and Jan-Niklas). Without all your help, trust, and support I wouldn't have had all the courage to finish my studies and to become the person I am.

Thanks to the most important person of my present life. Her smile worms my heart; the talks about friends, school, work, and problems opened my eyes a bit more to see all the little things that make a day worth to enjoy it. She encouraged me most of all to finish this thesis even when I wanted to give up.

Vielen lieben Dank Melanie. Ich liebe Dich!

Abbreviations

A	Ampere
Ab	Antibody
ABS	Absorption
Ag/AgCl	Silver-silverchloride reference electrode
ALP	Alkaline phosphatase
AP	Alkylphenol
APE	*4*-Alkylphenolethoxylate
4AP	*4*-Aminophenol
4APG	*4*-Aminophenyl-*ß*-D-Galactopyranoside
BSA	Bovine serum albumin
BST	BioSensor Technologie GmbH, Berlin
ß-Gal	*ß*-Galactosidase
c	concentration
CDH	Cellobiose dehydrogenase
c.e.	Catechol equivalents
CE	Capillary Electrophoresis
CIA	Capillary ImmunoAssay
CPE	Carbon Paste Electrode
DCC	Dicyclohexyl Carbodiimide
DCPIP	Dichlorophenolindophenol
DMF	Dimethylformamid
Dop	Dopamine
EPA	Environmental Protection Agency
EtOH	Ethanol
e	Extinction coefficient
FIA	Flow injection analysis
Fig.	Figure
FIIA	Flow injection immunoassay
GC	Gas chromatography
GDH	Glucose dehydrogenase
Apo-GDH	*Apo*-Glucose dehydrogenase
Holo-GDH	*Holo*-Glucose dehydrogenase
HPLC	High Performance Liquid Chromatography
HOM	*S*-(hydroxyl-5-nitrobenzyl)-propionic acid (nitrophenol derivative)
IA	Immunoassay
KLH	Keyhole limpet hemocyanin
K^*_{app}	Apparent affinity for the antibody tracer interaction

K_{app}	Apparent affinity for the antibody analyte interaction
L	Liter
L-dopa	*ß*-(*3,4*-dihydroxy-phenyl)-L-alanin
LLD	Lower limit of detection
m	Meter
MeOH	Methanol
MS	Mass spectrometry
NHS	*N*-hydroxysuccinimide
NMM	*N*-methylmorpholine
4NPE	*4*-Nonylphenolethoxylate
4NP	*4*-Nonylphenol
$4NO_2P$	*4*-Nitrophenol
$4NO_2PG$	*4*-Nitrophenyl-*ß*-D-Galactopyranoside
4OPE	*4*-Octylphenolethoxylate
4OP	*4*-Octylphenol
PEI	Polyethylene imine
ppm	Parts per million (mg/kg or mg/L)
ppb	Parts per billion (µg/kg or µg/L)
PQQ	Pyrroloquinoline quinone
PSSA	Polystyrene sulfonic acid
Pt	Platinum
PVC	Polyvinylchloride
RT	Room temperature
SGE	Solid graphite electrode
SPCE	Screen printed carbon electrode
Tab.	Table
TFE	Thick film electrode
TNTU	2-(*5*-norbornene-*2,3*-dicarboximido)-*1,1,3,3*-tetramethyl-uronium tetrafluoroborate
Tw	Tween (polyoxyethylenesorbitan monolaureate)
Tyr	Tyrosinase
UV	Ultra violet
vs.	Versus
WWTP	Waste water treatment plant
Prefixes	
k	kilo (10^{3})
m	milli (10^{-3})
µ	micro (10^{-6})

n	nano (10^{-9})
p	pico (10^{-12})
f	femto (10^{-15})
a	atto (10^{-18})

1 Introduction

Environmental monitoring for the detection of pollutants is becoming increasingly important to regulatory agencies, the affected community, and the general public. This is particularly true for those substances that pose a potential risk to human health or to the environment. In the USA the monitoring of hazardous pollutants is primarily driven by the legislation enacted by Congress. The high costs and slow turnaround times associated with the measurement of regulated pollutants clearly indicates a need for environmental screening and monitoring methods, which are fast, portable, and cost effective (Rogers 1995).

Besides the undeniable advantages and constant improvements of conventional analytical techniques, with respect to sensitivity, reliability, automation, etc., they often require sophisticated, expensive instruments operated by skilled personnel and intensive sample pretreatment. As a result, the throughput is low and a delay between sample collection and communication of results back to the sampling site exists. Biosensor systems should allow analysis of a sample by more simple and cost-effective methods resulting in a more frequent, perhaps eventually quasi-continuous analysis, thus reducing the risk for hazardous accidents or criminal poisoning of the environment (Bilitewski and Turner 2000; Nistor and Emnéus 1999).

For many years biochemical methods were mainly applied to medical analysis, which still represents the main market for these techniques.

A market prediction for the period 2001-2004 shows that medical application will continue to dominate the biosensor market. In this sector, the main focus is directed to home diagnostics and point-of care analysis. However, other applications are research, process control (mainly food and beverage industries) as well as environmental analysis. For the latter the highest growth rate (6.8 %) is predicted, as suitable applications for site characterization and clean up (Frost & Sullivan, 1998) evolve.

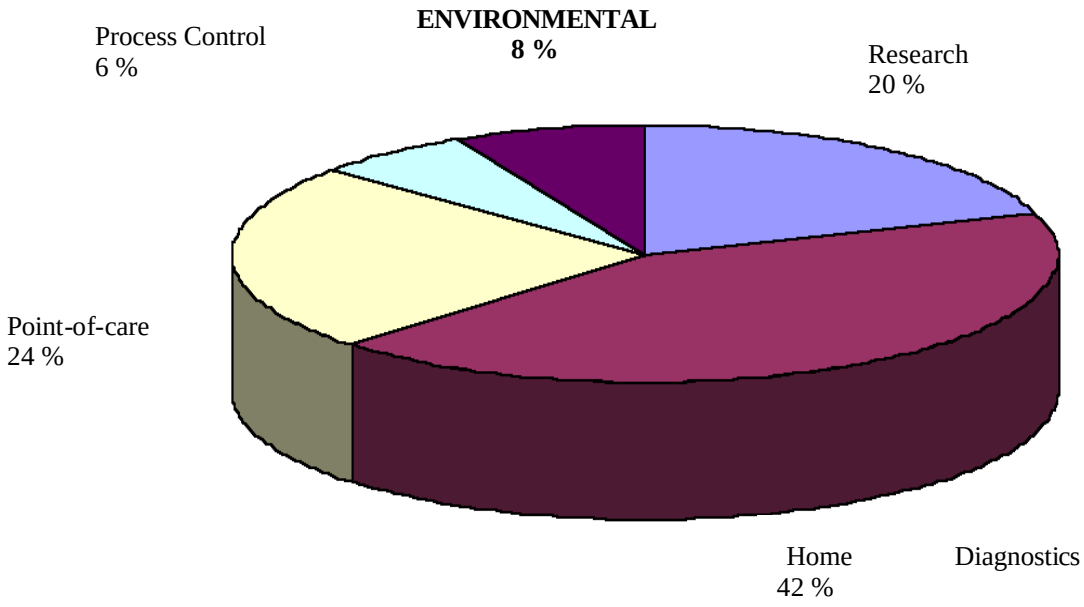

Figure 1.1: Biosensor Market Segments (Frost & Sullivan, 1998)

1.1 Biosensors

In principle, biosensors use biological materials, such as enzymes, antibodies or whole cells immobilized on a physical transducer. This transducer is producing an electrical signal visualizes the recognition of the analyte. This principle is illustrated in **Fig. 1.2**.

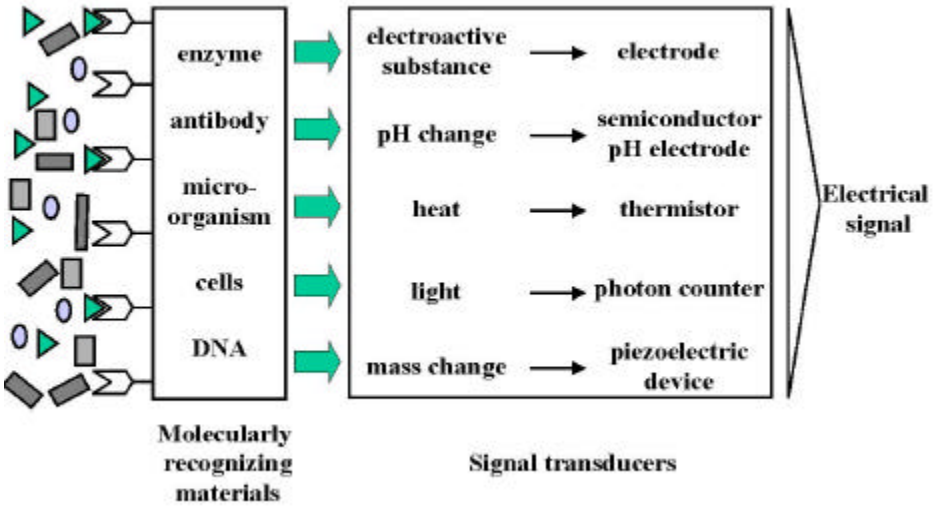

Figure 1.2: Principle of a biosensor

In 1999 the International Union of Pure and Applied Chemistry defined Electrochemical biosensors as follows (Thevenot, Toth et al. 1999).

> *"An electrochemical biosensor is a self-contained integrated device, which is capable of providing specific quantitative or semi-quantitative analytical information using a biological recognition element (biochemical receptor) which is retained in direct spatial contact with an electrochemical transducer element.*
>
> *Because of their ability to be repeatedly calibrated, we recommend that a biosensor should be clearly distinguished from a bioanalytical system, which requires additional processing steps, such as reagent addition. A device that is both disposable after one measurement, i.e. single use, and unable to monitor the analyte concentration continuously or after rapid and reproducible regeneration, should be designated as single use biosensor."*

Since most biosensor devices, such as enzyme or affinity sensors, need the addition of specific reagents, they should be named "bioanalytical systems" in accordance with IUPAC definition.

The enzyme sensors developed in this work would thus not be accepted as biosensors. Therefore we will widen the definition of "biosensor" according to literature (Bier 1998).

> *"**Biosensors** are analytical devices incorporating a **biological material** (eg tissue, microorganisms, organelles, cell receptors, enzymes, antibodies, nucleic acids etc), a **biologically derived material** or a **biomimic one** intimately associated with or integrated within a physicochemical transducer or transducing microsystem, which may be optical, electrochemical, thermometric, piezoelectric or magnetic. They are distinct from **bioassays** where the transducer is not an integral part of the analytical system."*

The American Chemical Society listed the following key terms and concepts in biosensors and related technologies (ACS 1996).

* *Bioanalytical assay: An analytical method that relies on a biorecognition element (e.g., enzymes, antibodies, DNA, microorganisms, tissues).*
* *Biosensor: An analytical device composed of a biological element in intimate contact with a physical transducer, which together relate the concentration of a target analyte to a measurable signal.*
* *Bioaffinity: The process by which a protein or DNA recognizes and binds a particular target compound (one receptor, one binding event).*
* *Biocatalyst (enzyme): The process by which a protein (e.g. enzyme) dramatically increases the rate of a chemical reaction and in which the protein participates in each reaction cycle but is returned to its original state after each cycle (one biocatalyst, many reaction cycles).*
* *Cofactor: A nonprotein element or compound required for the catalytic function.*

In the following the focus was related to enzyme based biosensors.

1.1.1 Enzyme based biosensors

Enzyme biosensors are sensors based on enzymatic biorecognition elements. The consumption of an substrate, or the production of a specific compound generates the signal. Therefore, the immobilization of the enzyme in close proximity to the transducer is important. So far many types of transducers have been described as source for the immobilization in biosensor development (Janata 1990).

1.1.1.1 Electron transfer in amperometric enzyme based biosensors

The first ever designed biosensor was built for the determination of glucose and was based on a Clark-oxygen electrode combined with glucose oxidase (Clark and Lyons 1962). Since the development of this device, the mechanisms behind the electron pathways in amperometric biosensors have received intense interest. The principle of electron transfer is the basis for separating amperometric biosensors in three main groups (generations).

While first generation biosensors depend on the detection of natural co-substrates and products, second generation biosensors utilize redox mediators for the electron transfer. Third generation biosensors depend on direct electron transfer between the prosthetic group of the enzyme and the electrode. In this work, biosensors of the second generation have been employed. The mediated electron transfer is based on redox active compounds that shuttle electrons between the active site of the enzyme and the electrode (Scheller, Schubert et al. 1991).

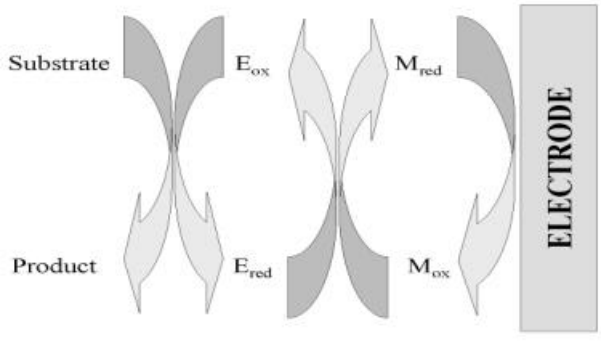

Figure 1.3: Principle for the mediated electron transfer in second generation biosensors

For the applications described in this thesis, the mediator is the molecule of interest. The primary substrate for the enzyme is added in high excess. Thus, the signal is dependent on the concentration of the redox mediator.

1.1.1.2 Amplification principles

There are many possibilities to enhance the properties of enzyme sensors and thus to reach lower detection limits (Wollenberger, Schubert et al. 1993). A very efficient method is signal amplification based on continuous regeneration of the analyte. In a non-amplified enzyme sensor the reaction of the enzyme with one analyte molecule (A) results in one product molecule (B). In this case concentrations in the micromolar range are detectable.

If the substrate A is regenerated, i.e. B is converted back to A, this analyte molecule can enter this more often in the process amplifying the signal.

Ideally, these cycles can be repeated a thousand-fold, potentially resulting in an enhancement at least three orders of magnitude. This makes detection of concentrations down to the nanomolar range feasible.

Substrate recycling can be combined with electrochemical detection in different ways.

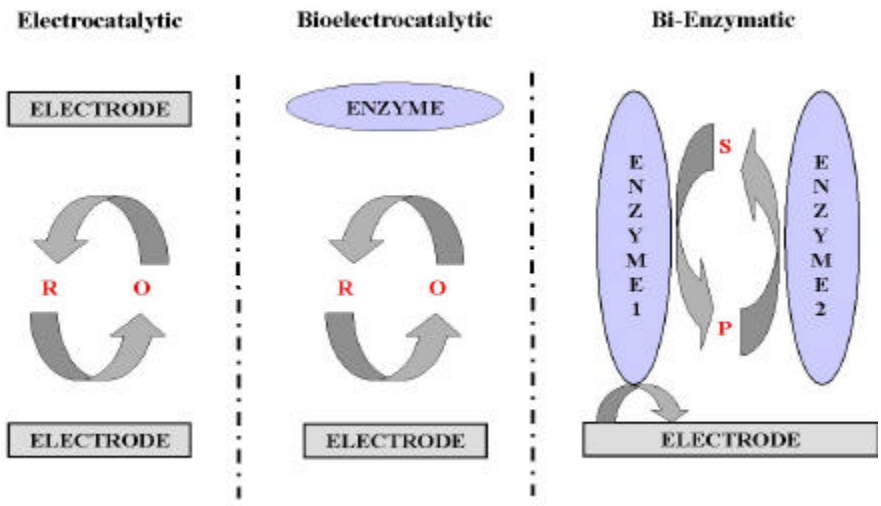

Figure 1.4: Principle of substrate recycling

The first possibility is implemented by electrochemical amplification of the product of an enzymatic reaction. In this case the amplification cycle is based on two electrodes (i.e. interdigitated array electrodes). This can be realized only for substances with reversible redox behavior (Niwa, Morita et al. 1991).

The second possibility (biocatalytic principle) is based on bienzymatic substrate recycling (Schubert, Kirstein et al. 1985). Here, the cycle is implemented between the active centers of two enzymes where one enzyme produces the substrate for the second while a co-reactant is measured directly or in an additional analytical step.

The third variation directly combines the biological and electrochemical mechanisms. In the bioelectrochemical redox system, active substrate molecules are potential analytes. In contrast to the first described principle only one electrode is used in combination with the active redox center of an enzyme (Scheller, Wollenberger et al. 1987). This type of amplification was applied for the biosensors developed in this thesis.

Basic considerations for the fabrication of biosensors, i.e. transducer production, as well as immobilization techniques and possible applications in the area of environmental analysis will be described in the next sections. The combination with immunological techniques will be discussed in more detail.

1.1.1.3 Fabrication of enzyme biosensors

For successful applications in the field of enzyme biosensors a high quality in the production of these devices must be established, i.e. the reproducibility of the features must be guaranteed, while cost efficiency must be realized. The fabrication of biosensors can be divided in two main steps. On the one hand there is the production of the transducer and on the other hand there is the immobilization of the enzyme as biorecognition element.

For traditional electrochemical research, mercury was the most popular material due to the readily renewable clean surface of well-defined geometry. Today, mercury is being displaced by solid metal and carbon electrodes for environmental and health reasons.

The requirements for biosensor electrodes are somewhat different even though the electrocatalytic reaction takes place at the surface of the electrode. Besides being electrically conductive, the electrode material has to serve to immobilize the enzyme and possible mediators.

When choosing electrode material for biosensor construction, variables such as the applied potential, type of enzyme, immobilization method and sample matrix should be taken into consideration. The common electrode materials used for biosensors have been summarized in the following section.

1.1.1.3.1 Conducting salts

Organic conducting salts are prepared by mixing an organic electron donor with an electron acceptor, such that only a partial electron transfer occurs, causing the conductivity. This results in a salt that is insoluble in water and that can be pressed into pellets (Cass 1990). The main advantage of such electrode materials is their mediating properties. Several “mediatorless” biosensors have been based on conductive salt electrodes.

1.1.1.3.2 Conductive Polymers

Conductive polymers are commonly grown electrochemically on other electrode materials, such as platinum (Pt) or glassy carbon. The polymer consists of chains with delocalized electrons (electronically conducting) or bound redox functionalities (redox conducting) that give the material its conductive properties. The best known electronically conducting polymer is polypyrrole, although other such as polyaniline and polyacetylene have been studied. Both enzymes and mediating functionalities can be incorporated into the material for biosensor purposes.

1.1.1.3.3 Noble metals

Noble metals (platinum, gold, and silver) are traditional electrode materials exhibiting good conductivity, wide potential windows, and high corrosion resistance (Koryta, Dvorák et al. 1993; Moseley and Crocker 1996). Biosensors based on noble metals have been generated in a number of ways, such as membrane covered sensors (in which case the enzyme is trapped under a membrane on the electrode surface) (Schmidt, Schuhmann et al. 1992; Schuhmann 1995; Turner, Karube et al. 1987), or sensors with the enzyme physically adsorbed onto protein layers on the surface of the electrode(Du, Anzai et al. 1996). Recently, work on sensors with the enzyme bound to a spacing monolayer deposited on the electrode surface (usually gold electrodes) has been published (Finklea 1996). The spacing (or self assembled monolayer) consists of a single monolayer in which the constituents share a common orientation. These layers depend on molecules with sulfur head groups (e.g. thiols, sulfides and disulfides) and

alkane chains, controlling the spacer length. Such surface modifications allow the orientation of the enzyme which promotes direct electron transfer (Wink, van Zuilen et al. 1997).

1.1.1.3.4 Carbonaceous materials

Carbonaceous materials have been used extensively for electrode fabrication in biosensor research. A wide variety of structures, which are relatively cheap, are available. It offers high purity, relatively low (electro-) chemical reactivity, low thermal expansion, good thermal and electrical conductivity and a wide potential range (Kinoshita 1988; Koryta, Dvorák et al. 1993). The material used for biosensor fabrication can be divided into diamond, carbon black, carbon fibers, glassy carbon, graphite, and carbon composites depending on the structure and degree of order (Kinoshita 1988; McCreery 1991). Due to the size and orientation of the graphite particles (influenced by the manufacturing process) the bulk properties, as well as the surface structure, vary significantly between these materials, which affects the electrode performance (background current, electrode kinetics, etc.) (McCreery 1991).

Glassy carbon or vitreous carbon materials have a black glassy appearance and are prepared by pyrolysis of organic polymers, e.g. phenolic resins. Glassy carbon electrodes are very hard, impermeable to gasses, resistant to heat and chemical attack and they provide the widest potential range of all carbon materials.

Graphite electrodes consist of layers of hexagonal graphite crystals that are loosely bound by van-der-Waals forces. The basal planes are hydrophobic whereas the edge planes are rather hydrophilic and polar. Graphite materials vary in the porous microcrystalline structure between *highly* ordered (pyrolytic carbon) and *randomly* ordered (graphite rods and carbon composites) (Kinoshita 1988; McCreery 1991).

Spetroscopic graphite is a common material for solid graphite electrodes offering high purity and a randomly oriented structure. Moreover, this material allows regeneration of the electrode surface by polishing with fine wet emery paper (Larsson 2001).

Composite electrodes consist of two phases, a conducting carbon phase and an inert non-conducting phase. In principle, composite electrodes can be divided in three main groups:

1. *impregnated electrodes*
2. *carbon/polymer electrodes*
3. *carbon paste electrodes*

Impregnated electrodes are based on solid graphite materials that contain small pores. These pores are filled with wax to remove air resulting in an enhancement of the electrode properties. Carbon/polymer electrodes are prepared by mixing carbon powder with a non-conducting polymer. When the polymer (often epoxy containing monomers) hardens, the result is a solid electrode. Another possibility is the use of commercially available carbon inks, which are often used in screen printing technology (Wang, Tian et al. 1998).

Carbon paste electrodes are a mixture of carbon powder with a binder (pasting liquid) holding the carbon material together. Carbon powders are commercially available form different sources in a wide range of varieties and particle sizes (Kalcher, Wang et al. 1995). Enzymes and stabilizers (e.g. polyelectrolytes) can easily be added during the paste preparation. This type of electrodes was tested in combination with glucose dehydrogenase during biosensor development in this thesis.

1.1.2 Modern biosensor technology

1.1.2.1 New techniques in transducer production

Beside the enzyme immobilization, the manufacturing of electrochemical transducers is of great interest. The manual preparation of electrodes (e.g. carbon pastes) and its processing to the final sensor is highly dependent on the manufacturer. Great differences in sensor behavior can be observed even with standardized protocols. The reproducibility between batches of electrodes is usually poor. Also, this process is time consuming and limits the preparation of electrodes in high numbers.

Screen printing techniques adapted from the computer industry offer the ability to provide very reproducible transducers in high numbers. Semiconducting oxides on alumina substrates were used as chemical sensors with applications in environmental analysis (Traversa, Sadaoka et al. 2000). Screen-printed electrodes were used as basic transducers for many applications of enzyme sensors in environmental analysis (Wang, Nascimento et al. 1996).

Screen printing was applied for the preparation of the platinum based thick-film electrodes obtained from BST BioSensor Technologie, Berlin, which were used for biosensor preparation in this thesis.

1.1.2.2 Immobilization techniques in biosensors development

In the preparation of a biosensor the immobilization is a crucial step. The main purpose is to fix the enzyme in close proximity to the electrode surface thus enabling a long-term usage of the enzyme while maintaining the enzymatic activity. The enzyme substrate must be able to penetrate the layer to access the active site of the enzyme. Moreover, the mass transfer of substrate and product molecules through the immobilized layer should not be hindered.

The general immobilization techniques can be divided in four main classes, namely physical adsorption, physical entrapment, crosslinking and covalent coupling. Combinations (hybrid techniques) of the stated methods are possible, but have usually been shown to be specific for certain applications.

1.1.2.2.1 Physical adsorption

The most simple technique for immobilization is adsorption, since no reagents are required and only a minimal activation is necessary (Dreyhurst, Kadish et al. 1982; Schmidt, Schuhmann et al. 1992). The interactions are based on electrostatic adhesion, hydrophobic and van-der-Waals interaction, or hydrogen bonding. Potential drawbacks are conformational changes and denaturation of the enzyme due to the adsorption process. In addition, desorption can occur due to changes in pH, ionic strength, and temperature. One successful example is the CDH biosensor for phenol detection in flow systems developed at Lund university (Lindgren, Stoica et al. 1999).

1.1.2.2.2 Physical entrapment

This technique can either involve entrapment of the enzyme in a gel, a polymeric network (conducting or non-conducting) or behind a semi-permeable membrane (Schmidt, Schuhmann et al. 1992; Turner, Karube et al. 1987). The pores of the polymeric network should be large enough to allow free diffusion of substrates and products but should retain the enzyme within the network (Palmisano, Zambonin et al. 2000). Conducting polymers can be electronically conducting (e.g. polypyrrole, polyaniline), redox conducting (e.g. Os redox hydrogels, mediator modified nafion), or non-conducting polymers which commonly are polyacrylamide, cellulose, acetate, chitin, gelatine, and starch based (Bartlett and Cooper 1993; Cosnier 1999; Emr and Yacynych 1995; Schuhmann 1995;

Wallace 1999). A combination with screen-printing technique improving the stability for various enzymes was described by Schuhmacher et. al (Schumacher, Münch et al. 1999). The development of sol-gel derived enzyme-containing carbon inks has combined the transducer fabrication and the immobilization into a one-step procedure (Wang, Pamidi et al. 1996). In this thesis a polyurethane membrane was applied for physical entrapment in the biosensors fabrication (Rose, Pfeiffer et al. 2001).

1.1.2.2.3 Covalent coupling

Covalent coupling leads to strong binding of the enzyme and desorption is practically not observed. This is of special interest in flow systems, where the mechanical stress is high. For the binding primary reactive groups are needed, both on the enzyme and the support (Murray 1984; Schmidt, Schuhmann et al. 1992; Turner, Karube et al. 1987). Functional groups on the support (the electrode) such as hydroxyl, carboxyl, thiol, and amino moieties can be treated with suitable reagents (e.g. carbodiimide) allowing the activated surface to bind with amine, thiol, and hydroxyl groups present in the amino side chains of the enzyme. Covalent coupling results in stabile biosensors with less risk of desorption. However, inactivation of the enzyme may occur if functionalities are bound at the active center.

1.1.2.2.4 Crosslinking

Crosslinking of enzymes to a support or other enzymes using intermolecular covalent linkages can increase sensor stability and improve electron transfer. Bifunctional crosslinking agents such as glutaraldehyde, dialdehydes, diisothiocyanates, and poly(ethylene glycol)diglycidyl ether have been used for the linkage (Larsson 2001; Schmidt, Schuhmann et al. 1992; Turner, Karube et al. 1987). This technique is often used in combination with adsorption or entrapment for improved sensor stability and electrochemical performance. Crosslinking of enzymes with redox polymers forming redox hydrogels is one of the most successful examples of this technique (Larsson 2001).

Developments in biosensor research are in large part due to new immobilization techniques and improved transducers as a result of advances in microfabrication, silicon technology.

1.2 Immunological methods

1.2.1 Historical overview

Svante Arrhenius can be regarded as the initiator of quantitative immunology. He elaborated the “Application of physical chemistry on the theory of physiological antibodies”(Arrhenius 1907). His work attracted criticism from many colleagues who were convinced that immunological systems could not explained with basic laws of natural sciences. Karl Landsteiner (also known for the discovery of blood groups) was working on the systematic characterization of AB reactivity and their development and production. He first synthesized hapten conjugates in order to investigate the chemical and structural relations between ABs and antigens (Landsteiner 1933). Thus many basic immunological rules are based on his work, for example that haptens should be coupled at the side most distant to their most important structural feature. Also, the ability of ABs to distinguish between stereoisomers and even enantiomers was first published by Landsteiner (Hofstetter, Hofstetter et al. 1999; Hofstetter, Hofstetter et al. 1998). He also performed the first competitive immunoassy using a precipitation format.

In the 1960s the breakthrough of IA detection began due to the development of radioactive labeling (Berson and Yalow 1959; Ekins 1960). In the beginning of the 70s the restriction to safety laboratories was lifted due to the introduction of enzyme labels (Engvall, Jonson et al. 1971; Engvall and Perlmann 1971).

The reason for the intensifying research within this area was the inherent advantages associated with immunoassays such as high sensitivity, simplicity, and cost effectiveness. Additionally, virtually any type of compound is nowadays capable of inducing an immunological response. With the continuous progress in antibody production and antibody engineering the general use of both monoclonal and polyclonal antibodies for the development of immunoassays has increased.

1.2.2 Terminology

Here the most common terms used in immunoassays used in this thesis are presented:

Antibody - *Protein of immunoglobulin type that binds to foreign molecules in the body*

Antigen - *Structure (molecule, organism, etc.) to which an antibody binds selectively*

Label - *Compound covalently coupled to an immunoreagent, which is used for the indirect detection of the antigen-antibody reaction*

Tracer - *Covalent conjugate between an antigen, hapten or antibody with a label compound*

Protein A/G - *Proteins with high affinity for the constant region of immunoglobulins*

Figure 1.5: Common terms in immunoassay.

1.2.3 Structure and function of the antibody

The body of vertebrates is protected by the immune system, which can neutralize and destroy certain undesirable cells, viruses, or macromolecules. For example, when an individual is exposed to infectious microbes, the immune response is activated and B-lymphocytes start to produce specific receptor proteins called antibodies.

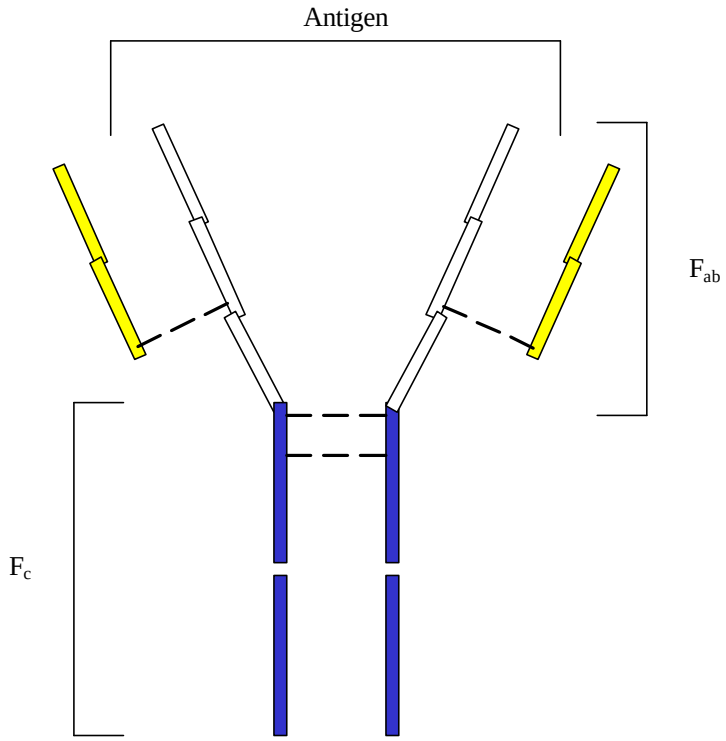

Figure 1.6: Schematic structure of an IgG antibody. The F_c part is shown in blue and the two F_{ab} fragments are displayed in white and yellow. The yellow part shows the two light chains, while the heavy chains are drawn in blue and white.

Antibodies are glycoproteins that belong to the immunoglobuline (Ig) family. There are five major categories of antibodies (IgG, IgA, IgM, IgD and IgE) that differ in size, charge, aminoacid composition and carbohydrate content.

The IgG is the most frequently used antibody for immunoassay development. All IgGs have the same basic structure with an approximate molecular weight of 150 Kda. The basic structural unit of all IgGs is a symmetric four-chain heterodimer made of two identical heavy chains (H, MW 50000 Da each) and two identical light chains (L, MW 25000 Da), which form the characteristicY-shape illustrated in **Fig 1.6**.

Each L chain binds a H chain with one or more disulfide (-S-S-) bonds. Likewise, the two H chains are bound by one or more disulfide bonds in the "hinge" region, all of which contribute to the chemical stability of immunoglobulin molecules (Wild 1994). The antigen-binding domain (paratop) is located at the aminoterminated end of the F_{ab} fragments.

1.2.4 Antigens

An antigen is usually a foreign molecule (exception is autoimmune answer) that causes the humoral immune defense system to produce antibodies, therefore functioning as a so-called immunogen. The region of an antigen that binds to an antibody is called the epitope or antigenic determinant. Haptens are small antigen molecules with a molecular weight of = 1000 Dalton, which are incapable of inducing any antibody production on their own. Haptens have to be covalently linked to a carrier protein (e.g. BSA, KHL) before they can be used as immunogens (Harrison, Goodrow et al. 1991).

1.2.5 Theory of immunoassays

The interaction between an antigen and an antibody is similar to an enzyme/substrate interaction. According to x-ray crystallographic studies, 15-22 amino acids residues in the antigen-binding site are involved in the binding of the antigen but only 3-6 of them contribute to the free energy of the binding (Savies 1994). Comparable to enzyme/substrate recognition, it is the three dimensional conformation that governs the antigen/antibody interaction. This interaction occurs through multiple non-covalent bonds, such as hydrogen bonds, or electrostatic, hydrophobic, and van der Waals interactions. Typical dissociation constants for antigen-antibody reactions are > 10^9 mol/L (Wild 1994).

The immunoassay is an analytical tool that is based on the distribution of free antigens (the analyte) in relation to the antigen bound to its corresponding antibody. In this manner, quantitative data can be obtained.

The ***law of mass action*** can be used to describe the reaction between an antigen and antibody, (Hock, Dankwardt et al. 1995) i.e.,

$$[Ag] + [Ab] \underset{K_2}{\overset{K_1}{\rightleftharpoons}} [AgAb] \qquad K = [AgAb]/[Ag][Ab]$$

Where

[Ag]	is the antigen concentration
[Ab]	is the antibody concentration
[AgAb]	is the antigen-antibody complex concentration
K_1	is the association rate constant
K_2	is the dissociation rate constant
K	is the equilibrium constant of the immunoreaction

The following assumptions were made:

* the antigen is present in a homogeneous form consisting of only one chemical species
* the antibody is homogeneous
* the antigen possesses only one epitope for one binding
* the antibody has a single binding site for one epitope of the antigen
* the reaction is at equilibrium
* the separation of bound fraction from free antigen is complete
* there should be no non-specific binding.

Although it is hardly possible to meet all these criteria in practice, the law of mass actions has still been used (Wild 1994).

Quality criteria for the immunoassay are its sensitivity (the difference in concentration that can be determined), its midpoint (IC_{50}) (concentration of analyte, which leads to 50 % of the initial tracer signal), and the detection limit (lowest concentration, which leads to a signal significantly bigger than the noise threshold) (Ekins and Edwards 1997; Ekins and Edwards 1998; Pardue 1997).

1.2.6 Labels in immunoassays

In the development of the first immunoassays, radioisotopes were most commonly used as labels. However, less hazardous electrochemical, fluorescent, chemiluminescent, and enzyme labels have been introduced. One of the most popular approaches today is the use of enzyme labels (Sittampalam and Wilson 1984).

The most common enzymes used in EIAs as labels are: glucose oxidase (Ekins and Chu 1997), alkaline phosphatase (Ishikawa 1987), peroxidase (Thorpe, Kricka et al. 1985), and ß-D-galactosidase (Oellerich 1984).

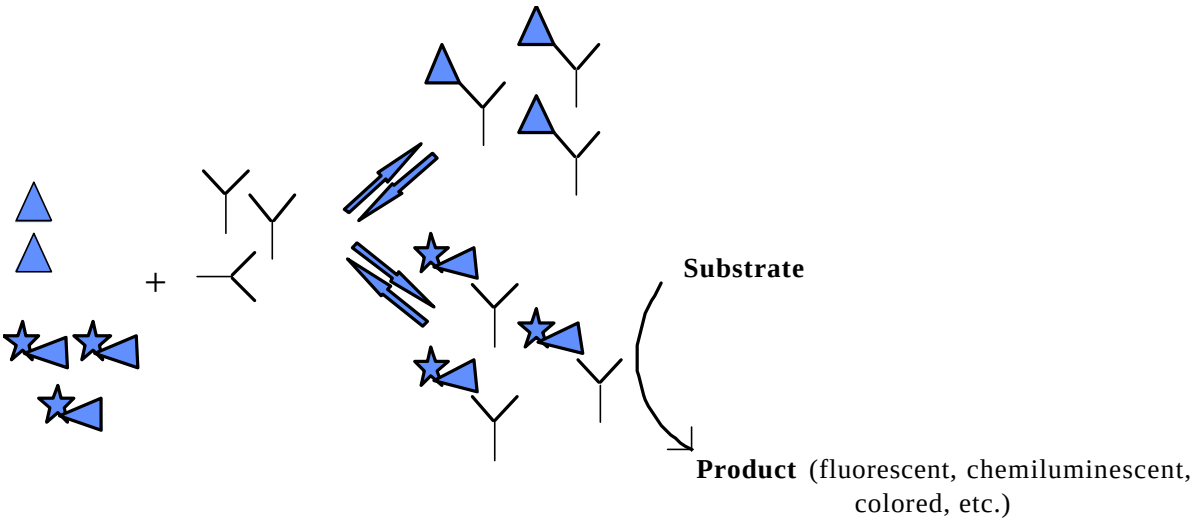

Figure 1.7: An enzyme immunoassay, making use of an enzyme label: (△) labeled analyte(tracer); (△) analyte; (Y) antibody. The antibodies react with analyte and tracer and the result is an unlabeled immunocomplex and a labeled immunocomplex; the analytical signal is proportional to the labeled immunocomplex.

The enzyme can be covalently coupled to either the antigen or the antibody. In **Fig. 1.7** an example of an EIA (enzyme immunoassay), using an enzyme labeled antigen (a *tracer*), is shown.

$$(1) \qquad E + S \underset{k_{-1}}{\overset{k_1}{\rightleftharpoons}} ES \xrightarrow{k_2} E + P$$

The kinetics of such an enzyme-catalyzed reaction can be described best using the Michaelis-Menten equation:

$$(2) \qquad v_0 = \frac{v_{max} * [S_0]}{[S_0] + K_m}$$

Here, the initial velocity v_0 is a function of the initial substrate concentration $[S_0]$, the maximum velocity v_{max} and the Michaelis constant K_m.

For the equation to be valid, the following assumptions must be fulfilled:

* the enzyme concentration is constant
* the enzyme concentration is much smaller than the substrate concentration
* the overall rate limiting step is the decomposition of the enzyme/substrate complex ($k_1 >> k_{-1} >> k_2$)
* the measurement takes place in the initial period of the reaction when concentration of the product is still close to zero (no need to consider any constant k_{-2})

From this equation it follows that enzymes with high v_{max} and low K_m will be the most sensitive labels (Barman 1969; Maggio 1980).

Table 1.1: *Assay methods for some important enzymes used as labels in immunoassays.*

	Assay method	**Substrate, mediator etc.**	**References**
ALP	Colorimetric	*4*-nitrophenyl-phosphate	(Eremenko, Bauer et al. 1998) (Ishikawa 1987)
	Electrochemical	*p*-substituted phenyl phosphates	(Kreuzer, O'Sullivan et al. 1999)
		naphthyl-phosphate	(Del Carlo, Lionti et al. 1997)
		phenyl-phosphate	(Eremenko, Bauer et al. 1998; Nistor and Emnéus 1998) (Bauer, Eremenko et al. 1998; Bauer, Eremenko et al. 1998)
		4-aminophenyl-phosphate	(Ding, Zhou et al. 1999) (Wijayawardhana, Purushothama et al. 1999) (Zhang, Heineman et al. 1999)
	Fluorimetric	*5*-fluorosalicyl-phosphate	(Christopoulos and Diamandis 1992)
		4-methyllumbelliferyl-phosphate	(Lindgren, Emnéus et al. 1998)
ß-Gal	Colorimetric	*2*-nitrophenyl-galactoside	(Ishikawa 1987)
	Electrochemical	*4*-aminophenyl-galactoside	(Másson, M. 1995)
	Fluorimetric	*4*-methylumbellifery-galactoside	(Labrousse and Avrameas 1987)
POD	Colorimetric	H_2O_2 and tetramethylbenzidine	(Wittmann, Bier et al. 1996)
		H_2O_2 and o-phenylenediamine	(Li, Woodward et al. 2000)
	Electrochemical	ferroceneacetic acid	(Del Carlo and Mascini 1996)
	Fluorimetric	*3*-(p-hydroxyphenyl)-propionic acid	(Lindgren, Emnéus et al. 1998)
	Luminometric	Luminol	(Thorpe, Kricka et al. 1985)

ALP: alkaline phosphatase; POD: peroxidase; ß-Gal: ß-galactosidase

The versatility of enzymes as labeling substances is largely dependent on the methods by which enzymes activity is measured. A wide variety of assays have been developed for each of the well-established, widely used labeling enzymes **(Tab. 1.1)**.

1.2.7 Immunoassay configurations

The main classes of immunoassay are shown in **Fig. 1.8**.

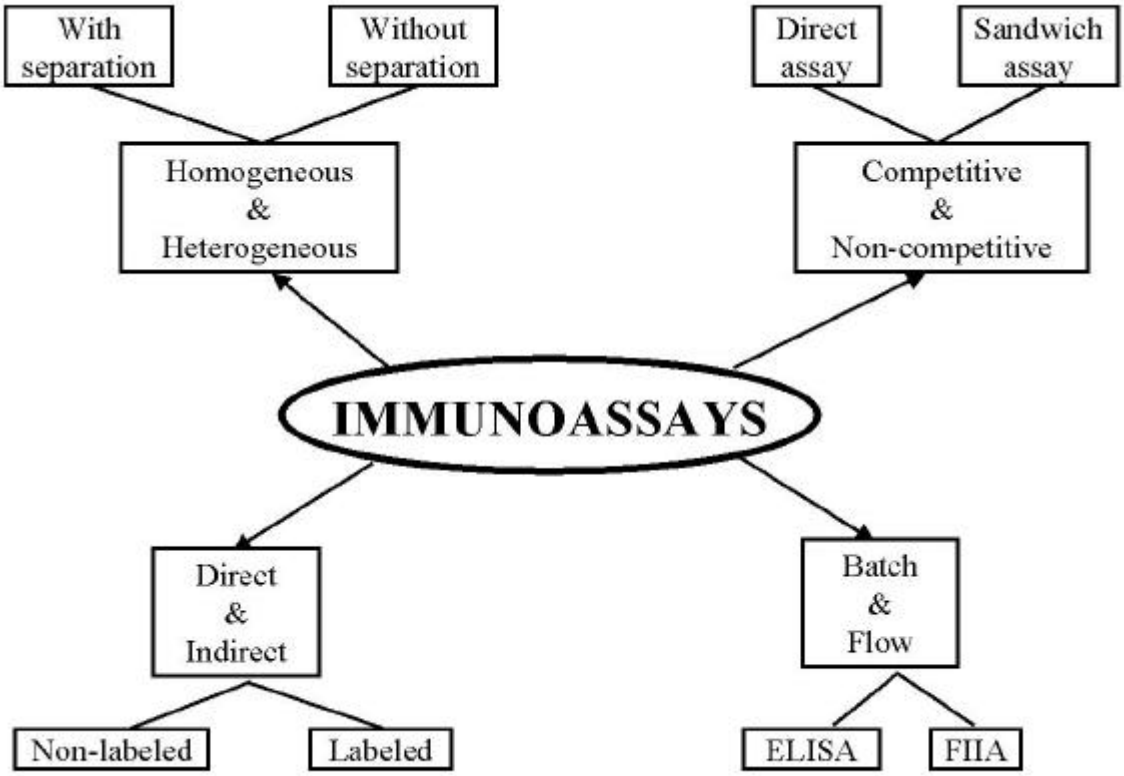

Figure 1.8: Classification of immunoassays

1.2.7.1 Competitive-non competitive immunoassays

Immunoassay techniques can be divided into two major groups:

* the “limited reagent“ method (competitive immunoassay)
* the “reagent excess“ method (non-competitive immunoassay)

1.2.7.1.1 Competitive immunoassays

In this type of immunoassay, either the antibody (direct assay) or the antigen (indirect assay) is immobilized covalently or by physical adsorption onto a solid support (e.g. polystyrene microtiter wells, polymer beads, tube walls, etc.) either. The excess binding sites on the solid phase are then blocked using a protein solution, e.g. bovine serum albumin (BSA). **Fig. 1.9** shows a direct assay, using immobilized antibodies. In this direct assay a labeled analyte is used as a so-called tracer. The sample is pipetted onto the solid phase together with the tracer. Therefore, the analyte competes with the tracer for a limited number of immobilized antibodies binding sites. After a certain incubation time, the unbound reagents are removed by washing of the solid support. Finally, the signal generated from the bound tracer is measured.

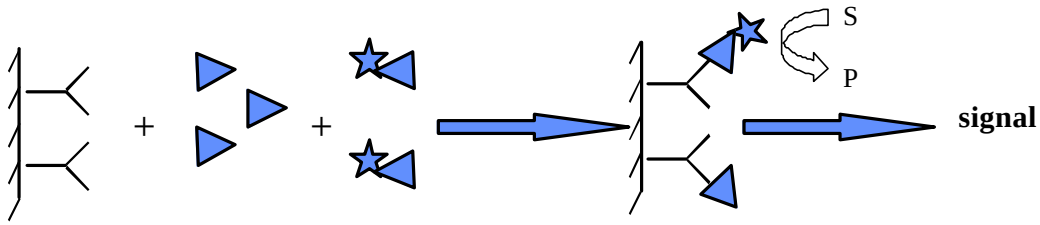

Figure 1.9: Configuration of the competitive immunoassay using an immobilized antibody; symbols as **Fig. 1.7**.

The other competitive immunoassay configuration, the indirect assay, is shown in **Fig. 10.** Here, the antigen is immobilized on the solid phase and the analyte from the sample competes with immobilized analyte for binding to soluble labeled antibody molecules.

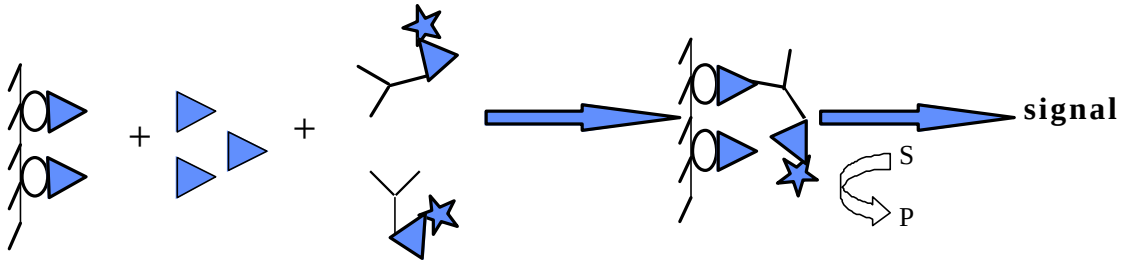

Figure 1.10: Configuration of a competitive immunoassay, using an immobilized antigen: the immobilized antigen. For other symbols refer to **Fig. 1.7**.

In both types of competitive immunoassay described, the signal is inversely related to the analyte concentration (Diamandis and Christopoulos 1996).

1.2.7.1.2 Non-competitive immunoassays

Most often in these types of assays, diluted test serum is added to excess antigen immobilized on a solid phase (sp-Ag). The amount of specific antibody that binds (sp-Ag-Ab) may be quantified by labelled antibodies. These specially bind to the constant region of the anti-antigen antibody (or immunoglobulin class) of interest (sp-Ag-IgG_1-Ab-enzyme).

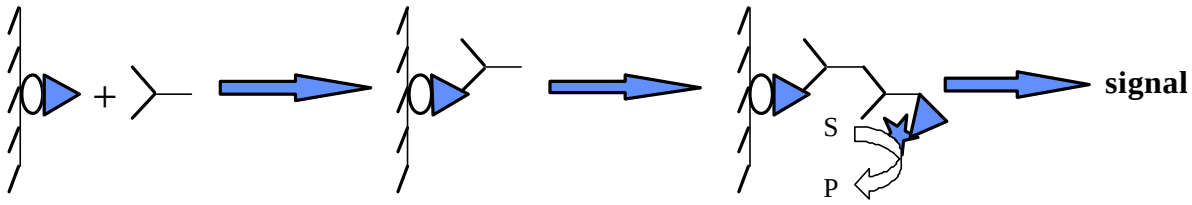

Figure 1.11: A non-competitive immunoassay for the quantification of an antibody. For symbols refer to **Fig 1.10**.

Much less frequently, an antigen capture approach may be employed. In some cases, these types of assays can be applied to the determination of macromolecular antigens, when the antigen is able to bind two antibodies simultaneously, for example when the antigen has two antibody binding epitopes.

Non-competitive immunoassays offer higher sensitivity than competitive ones. The ultimate detectability of the analyte in competitive immunoassays is limited by the affinity constant of the antibody used. In non-competitive assays the ultimate sensitivity of the assay is determined from the nonspecific binding of the labeled immunoreactants. Thus, non-competitive assays have high potential for single molecule detection, by using easily detected tracers and at the same time offering low nonspecific binding (Jackson and Ekins 1986).

1.2.7.2 Heterogeneous - homogeneous Immunoassays

There are two major types of immunoassays, namely heterogeneous and homogeneous versions.

A ***homogeneous immunoassay*** requires no physical separation of bound and unbound antigen. Most homogeneous immunoassays take advantage of the size difference between the unbound antigen (which is small) and antigen bound antibody complex (large). Since there is no separation step before the signal detection, interferences may compete with the binding site.

In the ***heterogeneous system***, the antigen-antibody reaction does not affect the activity of the enzyme label. A heterogeneous immunoassay is more versatile. With a physical separation step it eliminates most interfering substances present in the sample. The separation step, together with the potential of using larger sample size, improves sensitivity. The immunometric assay tends to have a broader dynamic range of the standard curve. The term "ELISA" (enzyme-linked immunosorbent assay) denotes a heterogeneous enzyme assay in which one of the reactants is immobilized onto a solid-phase matrix. ELISA can be formatted in various configurations and the enzymatic activity in the bound or free fraction is quantified by the enzyme-catalyzed conversion of a relatively non-chromatic or non-fluorescent substrate to a highly chromatic or fluorescent product.

1.2.7.3 Flow injection immunoassays (FIIA)

Traditional microtiter ELISAs are associated with drawbacks such as long incubation times, washing and mixing steps. FIIA offers a simplified system of automation, the possibility of real-time monitoring, on-line sampling, sample pre-treatment and enrichment. A flow injection immunoassay is performed using a small reusable immunoreactor and a continuously flowing buffer stream into which samples and necessary reagents are introduced by valves or by injection (Blake and Gould 1984). These systems are flexible in detection methods. The separation of immunoreactants in a heterogeneous FIIA is performed on-line, typically making use of a solid phase. There are a number of examples of FIIAs in the literature.

1.2.7.3.1 Separation in flow

In order to separate the antibody bound fraction of the analyte (AbAg) and tracer (AbAg*) from the free analyte (Ag) and free tracer (Ag*) fractions in a heterogeneous FIIA, a separation column based on e.g. immobilized affinity reagents such as protein A or G (Fernandez-Hernando and Miller 1991; Kronkvist, Lövgren et al. 1993), thiophilic gels (T-gels) (Palmer and Miller 1995), immobilized antibody (Maiolini, Ferrua et al. 1975), antigen (Clark and Adams 1977; Engvall and Perlmann 1972), or a chromatographic column containing restricted access material (Önnerfjord, Eremin et al. 1998) have been used.

Protein A/G and T-gels remove the antibody fraction from the mixture by binding the Fc-part of the antibody (protein A and G) or by adsorption due to interaction of aromatic amino acid side chains of the antibody with sulfone groups in the adsorbent (T-gels).

Immobilized antibody or antigen columns are based on the direct binding to the excess of labeled antigen or antibody, respectively, while the immunocomplex is detected (Burestedt, Kjellström et al. 2000). Here, the immuno-enzymometric assays using the separation via an immobilized antigen column led to highly sensitive determination of cocaine (Bauer, Eremenko et al. 1998).

The restricted access material contains inner cavities modified with hydrophobic materials e.g. C-18, C-8 or C-4. These inner pores exclude molecules lager than 15 Kda (Boos, Walfort et al. 1991). When restricted access columns

are used in a flow immunoassay, the antibody-tracer complex is detected and the free tracer is trapped in the hydrophobic cavities of the material.

Protein G is a cell wall protein isolated from group G streptococcus bacteria. Like protein A from Staphylococcus aureus, protein G binds to most mammalian IgGs, primarily through their F_c regions (Akerstrom and Bjorck 1986; Bjorck and Kronvall 1984; Bjorck, Miorner et al. 1984). A column with immobilized protein G allows the passage of free analyte (Ag) and tracer fractions (Ag*) but traps the antibody bound analyte and tracer fractions (AbAg and AbAg*) (Fig. 8). Depending on the (e.g. fluorescent) label quantification of the free fraction or of the bound fraction is possible. The use of enzyme labels allows both possibilities. The analysis of the free fraction is more rapid while better sensitivity is gained by quantifying the bound fraction. This is due to the prolonged enzymatic reaction.

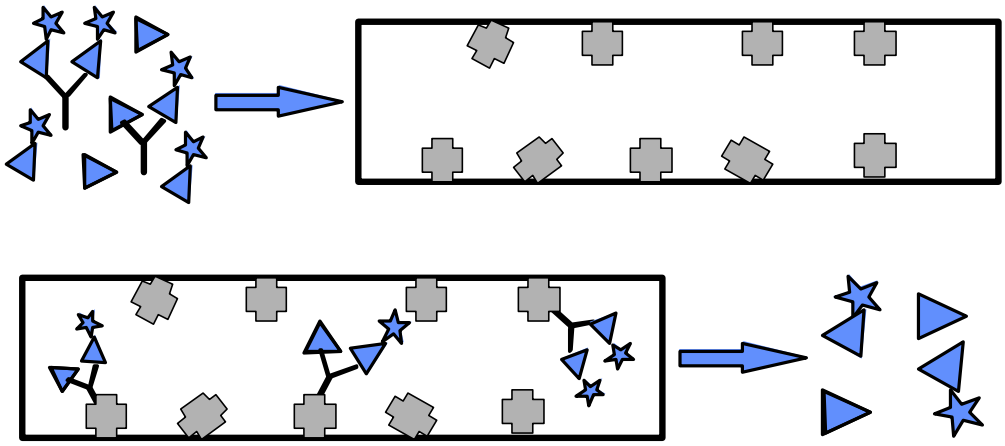

Figure 1.8: Separation in the flow using immobilized Protein G. The sample is mixed off-line with tracer and antibody for preincubation. After the equilibrium is established this mixtures passes the protein G column. The antibody fraction is captured via the F_c region by the immobilized protein G. Free tracer and analyte molecules pass through the column. Quantification can be based on the passing fraction as well as on the trapped fraction. Immobilized protein G. Other symbols as in **Fig. 1.6**.

The effectiveness of the protein A/G – antibody interaction was demonstrated for the manufacturing of an optical biosensor (Anderson, Magan et al. 1997).

1.2.7.3.2 Flow injection immunoassays using substrate recycling enzyme biosensors as detection units

Both the antibody affinity and the sensitivity of the detector towards the label are essential in deciding the final characteristics of a heterogeneous immunoassay. A supplementary enhancement of the signal generated by using an enzyme label can be obtained, e.g. by including the product of the enzymatic reaction in an additional amplification cycle during the detection step performed on an amperometric biosensor. Substrate recycling, enzyme-based biosensors can also be applied for immunoassays using redox active molecules as the label compound, e.g. redox active dyes.

The coupling of an immunoreaction with an electrode based on substrate recycling combines the advantages of the specific recognition of the analyte with a highly sensitive detection. The most commonly utilized label enzymes are alkaline phosphatase (ALP) and ß-galactosidase (ß-Gal) (Scheller, Bauer et al. 2001).

The biosensors based on horseradish peroxidase, tyrosinase, glucose dehydrogenase, or cellobiose dehydrogenase were successfully utilized as label detectors in flow immunoassays.

For the determination of ALP one method has become particularly useful. *p*-Aminophenyl phosphate dephosphorylates to *4*-aminophenol, which can be measured amperometrically at low oxidation potential. This work has been pioneered by Heineman and Halsall (Tang, Lunte et al. 1988). Also, a biosensor based on horseradish peroxidase was applied for the analysis of ALP activity using an indolyl phosphate derivative (Ho, Athey et al. 1995). Tyrosinase based biosensors were used for the detection of phenol, generated from phenylphosphate by the use of ALP (Nistor and Emnéus 1998). Very sensitive detection systems based on the bi-enzymatic substrate recycling were successfully used in our working group in combination with immunoassays (Bauer, Eremenko et al. 1998; Bauer, Eremenko et al. 1998; Bier, Förster-Ehrentreich et al. 1996).

ALP has an optimal working range above pH 9. Thus, either the enzyme used in the detection step must be able to work sufficiently at this pH, or the solution must be rebuffered to lower pH.

ß-Gal instead works best at neutral pH. It was successfully applied for immunoassays using cellobiose dehydrogenase, tyrosinase, and glucose dehydrogenase as biorecognition elements for the sensor preparation (Bier, Förster-Ehrentreich et al. 1996; Burestedt, Nistor et al. 2000; Nistor, Rose et al. 2002).

1.2.8 Immunoassays for environmental applications

The question remains whether there is any information available while using an immunoassay for the analysis of an unknown sample….

1. *if only **one substance** is present in the sample that binds to the antibody => ideal case!*

The results should be identical (within the error range) to conventional analytical methods. The same conclusion is expected if the crossreactivity is very low or crossreacting compounds are present in very low concentrations.

2. *if **more cross reacting substances** are present in the sample ...*

All substances have a similar crossreactivity leading to a virtual sum value for this class of analytes. Unfortunately, it is very difficult - for small haptens almost impossible - to realize such a kind of assay. Mixing of different ABs in a competitive format does not lead to success due to mechanistic reasons (Weller 2000).

3. *if **small amounts of different substances** with different crossreactivity are present in the sample ...*

In this case chemometric methods can be used in combination with a microtiter plate assay using several antibodies. It is possible to identify and quantify the analytes (Schneider, Weil et al. 1992). Also, variation of pH-value (Weller, Weil et al. 1996), amount of surfactants (Stangl, Weller et al. 1995), and/or content of organic solvents might lead to additional information (Stöcklein, Rhode et al. 2000).

4. *if **a variety of different substances** with varying crossreactivity are present in the sample (most common and most difficult case, often present in real samples) ...*

It is nevertheless possible to obtain information about a certain value/limit. This is of special interest in the case of "negative-screening" (where most of the expected sample will not contain the analyte). Since IA **not lead to false-negatives** (only in rare exceptions, i.e. measurement of the bound fraction when the AB is inhibited) the use for screening purposes indicates the absence of certain pollutants (hereby saving time and money for conventional analyses). Only in case of a positive test result a conventional measurement would be necessary (Weller 2000).

1.3 Environmental analytical chemistry

Environmental analytical chemistry can be divided in three major application fields according to the different main matrices, namely air, soil and water analysis. In this work only the analysis of water samples was performed and thus only related methods are described. The conventional analytical methods such as gas or liquid chromatographic with various detection principles, mass spectrometry, and inorganic analytical chemistry were reviewed in recent years showing the increasing amount of publications in this field (Clement and Wang 1997; Clement and Wang 1999). In the cited reviews the main focus lies on methods for the identification of analytes. However, toxicity tests were also mentioned. Here an interesting trend exists, which reflects the increasing interest in this field: While in 1997 only eleven citations were made in this area in 1999 the number increased to 30 citations on toxicity tests and bio-indication. Additionally, a new sector was added dealing with the analysis of endocrine disrupting compounds.

One main disadvantage of conventional analytical methods is their dependence on a laboratory setup. Thus, the cost is tremendous due to sampling, transportation and storage combined with intensive sample pretreatment. A rapidly growing area is the „field analytical chemistry" in which the analytical measurements are completed entirely at the site of interest. Various methods applicable in „field analytical chemistry" were reviewed in 1997 (Lopez-Avila and Hill 1997). This article demonstrates impressively (using 32 citations dealing with biosensors and another 64 citations on immunochemical methods) the applicability of biochemical analytical techniques in this area of environmental analysis.

Researchers of the U.S. Environmental Protection Agency (EPA) described biosensors and especially electrochemical immunosensors (as well as the growing impact of bioseparation and bioanalytical techniques in environmental monitoring) (Rogers 1995; van Emon, Gerlach et al. 1998; van Emon, Gerlach et al. 1997). In 1992 Hansen described biosensors for on-line monitoring of surface waters (Hansen 1992). Bioanalytical tools for monitoring polar pollutants in environmental samples were reported by Nistor and Emnéus in 1999 (Nistor and Emnéus 1999). The evolution of environmental immunochemistry was summarized in 2001 (van Emon 2001). Methods for biological pesticide monitoring were reviewed recently (Aprea, Colosio et al. 2002). An overview on bioindication in aquatic ecosystems was published in 1994 (Gunkel 1994).

The application of enzyme-based biosensors for environmental analysis was recently reviewed, and included a section dealing with the utilization of enzyme inhibition (Karube and Nomura 2000). There are many examples using the inhibition of cholinesterase, urease, tyrosinase, etc. for detection of pollutants (Cowell, Dowman et al. 1995; Starodub, Kanjuk et al. 1999; Wang, Nascimento et al. 1996).

Special applications for biological and biochemical methods can be seen in the field of ecotoxicity and environmental risk assessment (Hansen 1995; Hansen and von Usedom 1997). Cytotoxicity was estimated by bioluminescence inhibition (*Vibrio fisheri*-based assays) (Castillo, Alonso et al. 2001; Farré, García et al. 2001). A bacterial biosensor based on *E. Coli* was utilized for the toxicity assessment of organic pollutants in wastewaters (Farré, Pasini et al. 2001). These methods are much more cost- and time-efficient and are also clearly more sensitive to ethical aspects when compared with traditional fish tests. Monitoring of xenoestrogens with biological assays (e.g. DNA-binding, reporter-binding, and reporter-gene assays) describes another application area (Oosterkamp, Hock et al. 1997). Moreover, the potential of DNA as a tool in environmental analysis was described (Wang, Rivas et al. 1997).

1.4 Phenolic pollutants in the environment

In recent years there has been a growing concern regarding the consequences of exposure of wildlife and humans to xenobiotics (Castillo and Barceló 1997; Crisp, Clegg et al. 1998; Rivas, Olea et al. 1997). A considerable number of these organic pollutants have phenol-derived structures. The occurrence of phenols as industrial pollutants in surface waters is quite common due to the un-checked release of by-products in the petrochemical industry, coal liquefaction plants, production of plastics and dyes, as well as in the pulp industry (Bately 1987; Lindstrom and Nordin 1976; Neilson, Ellard et al. 1991; Ogan and Katz 1981). This source of contamination outbalances the natural formation pathways of phenols, often derived from farm waste, biodegradation of humic acids, tannins and lignins. Another minor source are pesticides, i.e. chlorinated phenoxyacids and organophosphorus insecticides that yield chloro- and nitrophenols as major degradation products (Marcheterre, Choundry et al. 1988).

Phenolic compounds as metabolites of natural organic substances, such as humic acids, tannins and lignins are of great danger upon entering the food chain. They are toxic for living beings by easily penetrating through natural membranes, thereby causing a broad spectrum of genotoxic, mutagenic and hepatotoxic effects. They are also known to modulate biocatalyzed reactions in respiration and photosynthesis (Brodfuehrer, Chapman et al. 1990; Yager, Eastmond et al. 1990).

Because of their toxicity, as well as their unpleasant organoleptic properties (concentrations in the low µg/L range affect the taste and odor of water and fish), phenols have been included in the priority pollutant list of the EEC and US-EPA (EPA-Method 604; EPA-Method 625; EPA-Method 8041; Hennion, Pishon et al. 1994; Vincent 1991).

1.4.1 Traditional analytical methods for phenols

Traditional analytical methods for determination of phenols are mainly based on high-performance liquid chromatography (HPLC) (Brouwer and Brinkman 1994; Jáuregui, Moyano et al. 1997; Puig and Barceló 1995; Puig and Barceló 1997; Wissiask, Rosenberg et al. 2000) or capillary electrophoresis (CE) (Arce, Ríos et al. 1998; Gonnord and Collet 1993; Jáuregui, Moyano et al. 2000; Morales and Cela 2000). Various detection methods such as electrochemistry (Lacorte, Fraisse et al. 1999; Piangerelli, Nerini et al. 1993; Pocurull, Marcé et al. 1996), spectrometry (García-Viguera and Bridle 1995; Vinas, Lopez-Erroz et al. 2000), fluorescence (Markhem, McNett et al. 1998; Vinas, Lopez-Erroz et al. 2000), or mass-spectrometry (MS) (Busto, Olucha et al. 1991; Furtmann 1994) were described in the literature.

Also, gas chromatography (GC) with flame-ionization (FID) (Ortner and Rower 1999), electron-capture (ECD), MS (Jahr 1998; Ng, Lafontaine et al. 2000), or microwave-induced plasma emission spectroscopy (MIP-ES) detection are common tools for the analysis of phenols (Cardwell, Hamilton et al. 1986; Christophersen and Cardwell 1996). Liquid-liquid extraction (LLE) has represented a suitable alternative for pre-concentration of phenolic compounds from the original water samples, adopted in standard analysis methods (1984; Powley and Carloson 1999; Realini 1981). However, there has been an increasing trend of replacing LLE with solid-phase extraction (Jahr 1998) or solid-phase micro-extraction (Arthur, Potter et al. 1992). Although the above analytical techniques are under constant improvement, extensive sample clean-up and pre-concentration steps (when dealing with environmental samples) are usually necessary before detection. As a result, the sample throughput is low and there is a long delay between sample collection and the communication of results back to the sampling site. Therefore, as a complement to already existing techniques, there is a need for developing faster screening methods. These should be technically simple and useful for routine analysis of large numbers of samples.

1.4.2 Surfactants based on phenolic structures

Alkylphenolethoxylates (APE) are non-ionic surfactants which are used in a variety of industrial applications, such as in the manufacturing of pulp and paper, metals, textiles, paints, resins, adhesives, latex, rubber and plastics. The most commonly used compounds are nonylphenolethoxylates (NPE) (80 %), 15 % octylphenolethoxylates (OPE) and the remainder as dodecylphenol and dinonylphenolethoxylates (Naylor 1995). For NPE the APE-research council to be as high as 340 million pounds with the demand growing by 2% annually in recent years (APE research council 2001) estimated the production. The distinct APE can differ in carbon chain length, structural and ring isomers (Weinheimer and Varineau 1998).

Since these compounds are used in aqueous solutions, they primarily enter in the environment *via* sewage and industrial wastewater treatment plants. The APE can be biodegraded through an iterative loss of ethoxy groups to form less ethoxylated congeners and carboxylated products. Alkylphenol, its mono- and diethoxylated derivatives, as well as alkylphenoxy carboxylic acids remain as the most persistent metabolites, and can accumulate in sediments under anaerobic conditions (Ahel and Giger 1985; Ahel, Giger et al. 1994; Valsecchi, Polesello et al. 2001).

1.4.2.1 NP belongs to the group of xenoestrogens

One main component, nonylphenol (NP) exhibits low toxicity if swallowed (LD_{50} > 2 g/kg body weight) but causes severe skin and eye irritation (Talmage 1994). Moreover, NP and NPE have been recognized as having reproductive and endocrine disrupting effects, for example leading to a notable decrease in sperm production (Sharpe and Skakkebaek 1993). NP was also found to initiate the growth of estrogen-dependant MCF-7 cells in vitro, and to stimulate vitellogenin production in cultured trout hepatocytes. It has also been shown to reduce weight and to accelerate vaginal opening in rats (Chapin, Delaney et al. 1999; Soto, Justicia et al. 1991; White, Jobling et al. 1994).

This has led to the inclusion of nonyl- and octylphenol in the list of priority substances in the field of water policy (**Tab. 1.2**).

Table 1.2: *Extract from the list of priority substances in the field of water policy ([1])*

CAS number[2]	**EU number[3]**	**Name of priority substance**	**Identified as priority hazardous substance**
25154-52-3	246-672-0	Nonylphenols	X
104-40-5	203-199-4	(*4*-(para)-nonylphenol)	
1806-26-4	217-302-5	Octylphenols	(X)[4]
140-66-9	n.a.	(para-tert-octylphenol)	

n.a. not applicable

1. *Where groups of substances have been selected, typical individual representatives are listed as indicative parameters (in brackets and without number). The establishment of controls will be targeted to these individual substances, without prejudicing the inclusion of other individual representatives, where appropriate.*
2. *CAS: Chemical Abstract Services*
3. *EU number: European Inventory of Existing Commercial Chemical Substances (EINECS) or European List of Notified Chemical Substances (ELINCS)*
4. *This priority substance is subject to a review for identification as possible "priority hazardous substance". The Commission will make a proposal to the European Parliament and Council for its final classification not later than 12 months after adoption of this list. The timetable laid down in Article 16 of Directive 2000/60/EC for the Commission's proposals of controls is not affected by this review.*

Because of the formation of persistent metabolites, the OSPAR member states (The Oslo and Paris Commissions) in their "Convention for the Protection of the Marine Environment of the North-East Atlantic" decided to phase out the use of APE by the year of 2000 (de Voogt, de Beer et al. 1997). Nevertheless a sufficient monitoring with respect to alkylphenolethoxylates will be necessary for the coming years.

1.4.2.2 Traditional analytical methods for APE

The initial complexity and the multitude of aerobic and anaerobic degradation pathways result in an immense amount of metabolic compounds present in an environmental sample. Identification of single compounds is therefore leading to very complicate analyses. One possibility to overcome these difficulties is to concentrate the analytical methodology, and identify substances based on their classes. Simple, relatively fast and inexpensive, quantitative or semi-quantitative methods based on titrimetric or spectrophotometric methods have been commonly used. However, these techniques have obvious drawbacks (Scullion, Clench et al. 1996).

Major developments have been reviewed in the identification and quantification of non-ionic surfactants by gas chromatography (GC) and high-performance liquid chromatography (HPLC) (de Voogt, de Beer et al. 1997; Kiewiet and de Voogt 1996; Marcomini and Zanette 1996).

These chromatographic methods were coupled with pretreatment steps including solid-phase extraction, pressurized liquid extraction, accelerated solvent extraction or supercritical fluid extraction (Bennett and Metcalfe 1998; Kreisselmeier and Dürbeck 1997; Scullion, Clench et al. 1996; Valsecchi, Polesello et al. 2001)

GC analysis was successfully applied to low molecular mass oligomers with up to two or three ethoxylate groups. High molecular mass derivatives require additional derivatization (to increase volatility) and the use of sophisticated instrumentation (high temperature columns). Applicable detection methods are mass spectrometry (MS) or electron capture detection (ECD) after suitable derivatization (Bennie, Sullivan et al. 1997; Blackburn, Kirby et al. 1999; Bolz, Körner et al. 2000; Hawrelak, Bennet et al. 1999.; Rudel, Melly et al. 1998).

The obvious drawbacks in GC separation of high molecular APE lead to an intensive research in HPLC. In this field normal phase (np) as well as reversed phase (rp) columns were used for the separation of the homologues and isomers. rp-HPLC provides information about the length of the alkyl chain whereas np-HPLC resolves the ethoxylate oligomers (Kiewiet and de Voogt 1996).

The used detection methods vary widely, including UV, fluorescence, and MS (Bennie, Sullivan et al. 1997; de Voogt, de Beer et al. 1997; Marcomini and Giger 1987; Zhao, van der Wielen et al. 1999). Especially the combination of HPLC and MS using various interfaces and ionization methods has been described in the literature recently (Castillo, Ventura et al. 1999; Ferguson, Iden et al. 2000; Takino, Daishima et al. 2000). A high resolution in terms of ethoxylate groups was achieved using adsorption HPLC in combination with an evaporative light scattering detector (Kibbey, Yavaraski et al. 1996).

As another separation technique for APE, capillary electrophoresis combined with UV detection was applied but the high efficiency of separation of anionic surfactants could not be achieved due to the lack of charge (Heinig, Vogt et al. 1996.). Very recently micellar electrokinetic chromatography as a new separation tool was applied to the analysis of APE, but the detection limits still have to be improved (Herrero-Martínez, Fernández-Martí et al. 2001).

Although these analytical techniques are under constant improvement, extensive sample clean up and preconcentration is usually necessary before detection when dealing with environmental samples. As a result, the sample throughput is low and no possibility of an early-alert-system has been brought forward so far.

1.4.2.3 Alternative analytical methods for APE

Wastewater toxicity was related to non-ionic surfactants using bioluminescence inhibition assays (Farré, García et al. 2001). These methods do not allow any identification of the compounds but can deliver helpful information in combination with conventional analysis (Castillo, Alonso et al. 2001). A bacterial biosensor based on *E. coli* was also used for toxicity assessment for NP and NPE (Farré, Pasini et al. 2001). Since the estrogenic properties of APE are known, receptor based screening can be used (Körner, Bolz et al. 2000). All these techniques do not provide further information about the involved pollutants.

As a complement to already existing techniques, there is a need for developing screening methods that should be technically simple. An application for routine analysis of a large number of samples as well as integration in a portable device for on-the-spot measurements would be desirable. Immunoassay techniques are potential candidates for fulfilling these requirements due to the high selectivity of antibodies, the good sensitivity of such systems and the fact that antibodies can be raised against virtually any compound.

During an inter-laboratory test the Takeda Industries APE ELISA kit was compared with conventional techniques (Castillo, Riu et al. 2000.). On one hand the parallelism of the analysis allows a high sample throughput. On the other hand the time-consuming washing and development steps are the major drawbacks, especially when only one sample should be analyzed at one time. This makes most ELISAs less applicable for on-the-spot measurements.

2. Objectives

The development of fast and reliable biochemical tools for on-site screening in environmental analysis was the main target of the present work. Due to various hazardous effects such as endocrine disruption and toxicity phenolic compounds are key analytes in environmental analysis and thus were chosen as model analytes.

2.1. Three different methods should be developed

For the enzymatic detection of phenols in environmental samples an enzyme-based biosensor should be developed. In contrast to reported work using tyrosinase or peroxidases, we developed a biosensor based on glucose dehydrogenase as biorecognition element. This biosensor was devoted for an application in a laboratory flow system as well as in a portable device for on-site measurements.

This enzymatic detection is applicable only for a limited number of phenols due to substrate specificity of the enzyme. For other relevant compounds based on a phenolic structure (i.e. nitrophenol, alkylphenols and alkylphenol ethoxylates) immunological methods must be developed. Electrochemical biosensors should be used as the label detector in these immunoassays.

Two heterogeneous immunoassays should be developed where enzymes are used as the label. An electrochemical method for the determination of the marker enzyme activity must be processed. The separation step should be realized with protein A/G columns (laboratory flow system) or by direct immobilization of the antibodies in small disposable capillaries (on-site analysis).

All methods were targeted on the contemporary analysis of small numbers of samples.

3 Materials and methods

3.1 Reagents

Table 3.1: *Reagents*

Company	Reagent
Avocado (Lancaster, UK)	*4*-Nitrophenyl-*ß*-D-Galactopyranoside
Fluka (Deisenhofen, Germany)	*4*-Aminophenyl-*ß*-D-Galactopyranoside graphite mineral oil PEI PQQ
Merck (Darmstadt, Germany)	Calcium chloride Citric acid monohydrate Glucose Potassium chloride Potassium phosphate
Ringsdorff Werke (Germany)	Spectroscopic graphite rod (i.d. 3.05.mm, RW 001)
Serva (Heidelberg, Germany)	Tris-(hydroxymethyl)-aminomethan [Tris] N-morpholinopropanesulfonic acid [Mops] PSSA
Sigma (Deisenhofen, Germany)	Polyoxyethylenesorbitan monolaureate (Tween 20)
Mirka-Schleifmittel (Kronberg, Germany)	Fine emery paper (P1200)
Roth (Karlsruhe, Germany)	Ethanol Methanol N-(*2*-hydroxyethyl)-piperazine-N´-(*2*-ethanesulfonic acid) [HEPES]

Table 3.2: *Phenolic compounds used as model analytes*

Company	Reagent
AGBAR, Barcelona, Spain	Nonylphenol ethoxylates
Alldrich (Deisenhofen, Germany)	*4*-methylcatechol *4*-nitrocatechol *ß*-(*3,4*-dihydroxy-phenyl)-L-alanin (L-Dopa) *4*-nonylphenol *4*-octylphenol octylphenol ethoxylates (Triton X-100)
Avocado (Lancaster, UK)	noradrenaline
Fluka (Deisenhofen, Germany)	DichlorophenolinDophenol (DCPIP) L-adrenaline
Merck (Darmstadt, Germany)	*1,2*-benzenediol (catechol) phenol, *2,4,6*-trichlorophenol
Sigma (Deisenhofen, Germany)	*4*-aminophenol *2,5*-dihydroxyphenyl-acetic acid *3,4*-dihydroxyphenyl-acetic acid, *1,4*-benzenediol (hydroquinone), *1,2*-benzenediol (catechol) *p*-benzoquinone dopamin *4*-nitrophenol

All phenolic analytes were of analytical grade.

3.1.1 Enzymes

Apo-glucose dehydrogenase (Apo-GDH) from a recombinant *E. coli* (gene of perisplasmatic glucose dehydrogenase from Acinetobacter calcoaceticus, EC 1.1.99.17; GDH) was a kind gift of Roche (Indianapolis, USA).

ß-galactosidase (enzyme immunoassay grade from *E. coli*) was obtained from Boehringer (Mannheim, Germany).

3.1.2 Antibodies and haptens

Anti-nitrophenol antibodies (raised in rabbit with HOM covalently coupled to KLH), were kindly placed at our disposal by Mrs. Maria Pilar-Marco, Barcelona.

4-nitrophenol derivative (*3*-[S-(*2*-hydroxy-*5*-nitrobenzyl)]-propionic acid (HOM)) was synthesized by EMP-Biotech GmbH, Germany.

The Bio-Rad protein assay was from Bio-Rad, Munich, Germany.

The APE-hapten (C_9H_{19}-C_6H_4-0-$(CH_2CH_2O)_5$-$COCH_2CH_2$-COOH), anti-APE antibodies (raised in mice with APE-hapten covalently linked to Keyhole limpet hemocyanin (KLH)), and the ELISA test kits for the determination of APE were kindly placed at our disposal by Mr. Shin Dosho, Takeda Industries (Osaka, Japan).

3.1.3 Buffer solutions

Sörensen buffer: 11.88 g/L Na_2HPO_4 and 9.08 g/L KH_2PO_4 were mixed to obtain the final pH-value. The final concentration of $CaCl_2$ was 1 mmol/L.

Davis buffer solution: 21.01 g/L citric acid monohydrate, 13.61 g/L KH_2PO_4, 19.07 g/L $Na_2B_4O_7$, 12.11 g/L TRIS, and 7.4 g/L KCl were mixed and the pH-value was adjusted with either HCl or NaOH. The buffer was diluted to a total concentration of buffer salt of 112.5 mmol/L. The final concentration of $CaCl_2$ was 1 mmol/L.

HBS: HEPES and KCl were mixed and the pH-value was adjusted with NaOH. The final concentration of $CaCl_2$ was 1 mmol/L.

TRIS: *2*-amino-*2*-(hydroxymethyl)-*1,3*-propanediol and KCl were mixed and the pH-value was adjusted with NaOH. The final concentration of $CaCl_2$ was 1 mmol/L.

MOPS: N-morpholinopropanesulfonic acid and KCl were mixed and the pH-value was adjusted with NaOH. The final concentration of $CaCl_2$ was 1 mmol/L.

3.2 Instrumentation

3.2.1 Biosensor measurements

3.2.1.1 Instruments and electrodes

Potentiostats	Biometra	Göttingen, Germany
	Enza	University of Potsdam, Germany
	Zäta Electronics	Lund, Sweden
Ag/AgCl reference electrode	ELBAU	Berlin, Germany

3.2.1.2 Data aqusition

Chart Recorder	Kipp&Zonen	Delft; The Netherlands
Interface box	Knauer	Berlin, Germany
Eurochrom software	Knauer	Berlin, Germany
Chromstar 4.06	Chromatographie und Prozess-Analytik	Stuhr, Switzerland
Unipoint Software	Gilson	Villiers-le-Bel, France

3.2.1.3 Automated flow systems

3.2.1.3.1 Flow system I (EVA-System)

peristaltic pump	Eppendorf	Hamburg, Germany
8-port injection valve	Eppendorf	Hamburg, Germany

The pump and the valve were programmed by their keypads.

3.2.1.3.2 Flow system II

6-port injection valve	Rheodyne	Berkley, USA
Minipuls 3peristaltic pump	Gilson	Villiers-le-Bel, France

3.2.1.3.3 Flow system III

HPLC pump 2150	LKB	Bromma, Sweden
6-port injection valve(7010)	Rheodyne	Berkeley, CA, USA
ASTED autosampler233 XL	Gilson	Villers-Le-Bel, France

The autosampler was controlled by a Gilson keypad including the software 720 Sampler Controller version V2.01

3.2.1.3.4 Flow system IV

Minipuls 3peristaltic pump	Gilson	Villiers-le-Bel, France
6-port injection valve(7010)	Rheodyne	Berkeley, CA, USA
ASTED XL autosampler	Gilson	Villiers-le-Bel, France

The autosampler was controlled by a Gilson Unipoint Software (version 1.07).

3.2.2 Further instrumentation

Balance	Sartorius	Göttingen, Germany
pH-meter	Knick	Berlin, Germany
Polyvinyl chloride capillaries	KABE Labortechnik	Nümbrecht-Elsenroth, Germany
UV-Vis spectrophotometer	DU 640; Beckmann Instruments Inc.	Fullerton, CA, USA
Microtiter plates reader	SLT340 ATTC; SLT Lab Instruments Multiskan MCC 340; Thermo Labsystems	Crailsheim, Germany Helsinki, Finland
Microtiter plates	Maxisorp; Nunc	Roskilde, Denmark

3.2.3 Carbon paste electrodes (CPE)

For the preparation of these electrodes plastic (PVC) capillaries were filled with enzyme free carbon paste. To obtain electrical contact a steel wire was inserted from the backside into the paste. At the outer tip 3 mm were kept empty to be filled with the GDH-modified carbon paste (**Fig. 3.1**).

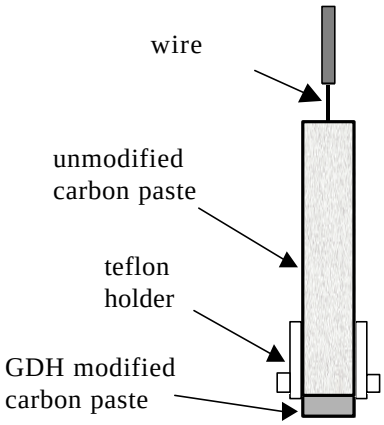

Figure 3.1: Schematic draw of a GDH carbon paste electrode in PVC capillary.

Enzyme free carbon paste for the bulk was prepared using 350 mg graphite and 100 mg mineral oil. The graphite was pre-treated in an oven at 600°C for 20 s.

Three carbon pastes were prepared containing polyethyleneimine (PEI), poly-(sodium-*4*-styrene sulfonate) (PSSA) with a MW above 70000 g/mol, and a mixture of both.

CPE1: 13.2 mg graphite were mixed with 200 µL PEI (0.4 % in H_2O)

CPE2: 13.2 mg graphite were mixed with 200 µL PSSA (10 mg/mL H_2O)

CPE3: 13.2 mg graphite were mixed with 100 µL PEI (0.4 % in H_2O) and 100 µL PSSA (10 mg/mL H_2O)

These mixtures were dried overnight in a vacuum centrifuge and 15 mg of each were afterwards mixed with 4.5 mg mineral oil.

3.2.3.1 GDH modified carbon paste

The GDH-modified carbon pastes were prepared by mixing 5 mg GDH with 5 µL $CaCl_2$, 100 mmol/L, and 60 µL PQQ 2 mmol/L.

This mixture was added to:

1) *200 µL deionize water*
2) *20 µL PEI (0.2 % in H2O)*
3) *20 µL PSSA (10 mg/mL H2O)*
4) *100 µL PEI (0.4 % in H2O) and 100 µL PSSA (10 mg/mL H2O)*

The resulted solution was added to 13.2 mg graphite and homogenized. The mixture was placed in the vacuum centrifuge for 3 h at 4°C and afterwards 15 mg were mixed with 4.5 mg mineral oil.

3.2.4 Solid graphite electrodes

GDH biosensors were prepared by applying 10 µl of enzyme solution (0.84 mg/L) on the top of a spectroscopic graphite rod (i.d. 3.05 mm, RW001, Ringsdorff Werke, Bonn, Germany), previously polished on wet fine emery paper (P1200) and washed with deionized water. The electrodes were placed in a glass beaker covered with sealing film, and the immobilization was allowed to proceed for 20 h at 4°C. Before use, the electrodes were thoroughly rinsed with deionized water to remove the enzyme that was not immobilized.

3.2.5 Screen-printed carbon electrodes

Screen-printed electrodes were obtained from Cambridge Life Science. The transducer consisted of a three-electrode system; a carbon based working electrode, a Ag/AgCl reference electrode and a platinum counter electrode. The GDH was immobilized on the working electrode by adsorption. 2mg GDH were mixed with 2 mmol/L PQQ (in H_20) and diluted 1:10 with 50 mmol/L potassium phosphate buffer pH 7, containing 100 mmol/L KCl, and 1 mmol/L $CaCl_2$. 5 µl of this solution were placed dropwize on the working electrode and allowed to dry over night at 4°C.

3.2.6 Platinum based thick-film electrodes

The screen-printed electrodes from BST-BiosensorTechnologie (Berlin, Germany) consist of a platinum based working electrode and an Ag/AgCl reference/counter electrode.

For the biosensor preparation GDH was suspended in different polyurethane solution (BST-BiosensorTechnologie Berlin). The electrodes were prepared using the apo-enzyme in the absence or presence of PQQ (**Tab. 3.3**).

In the latter case 1.5 µL aqueous PQQ solution (1 mg in 175 µL H_2O) were added to the enzyme-polymer mixture and stirred for 15 min at room temperature. Defined volumes of this solution were immobilized on the platinum working electrode. The electrodes were dried at room temperature for 24 h at controlled humidity (50 %). For storage the electrodes were wrapped and kept in the refrigerator at 4°C.

Table 3.3: *Preparation of GDH-TFE biosensors*

Type	**m (GDH) [mg]**	**PU**		**PQQ**	**immobilized volume [µL per sensor]**
		type	**volume [µL]**		
A	1	I	20	no	2
B	1	I	20	no	4
C	1	I	20	yes	2
D	1	I	20	yes	4
E	1	II	20	no	2
F	1	II	20	no	4
G	1	II	20	yes	2
H	1	II	20	yes	4
I	1	III	20	yes	4
J	1	III	20	no	4

3.2.7 Measuring cells

For this thesis experiments were performed in batch systems as well as in flow systems. The various measuring cells are listed in this section.

3.2.7.1 Stirred batch cells

Two different batch cells were used. The cell for carbonpaste electrodes was equipped with an additional Ag/AgCl reference electrode from ELBAU (Germany). These reference electrodes were filled with KCl (1 mol/L) and were separated from the cell by a diaphragm. The steel outlet was used as the counter electrode.

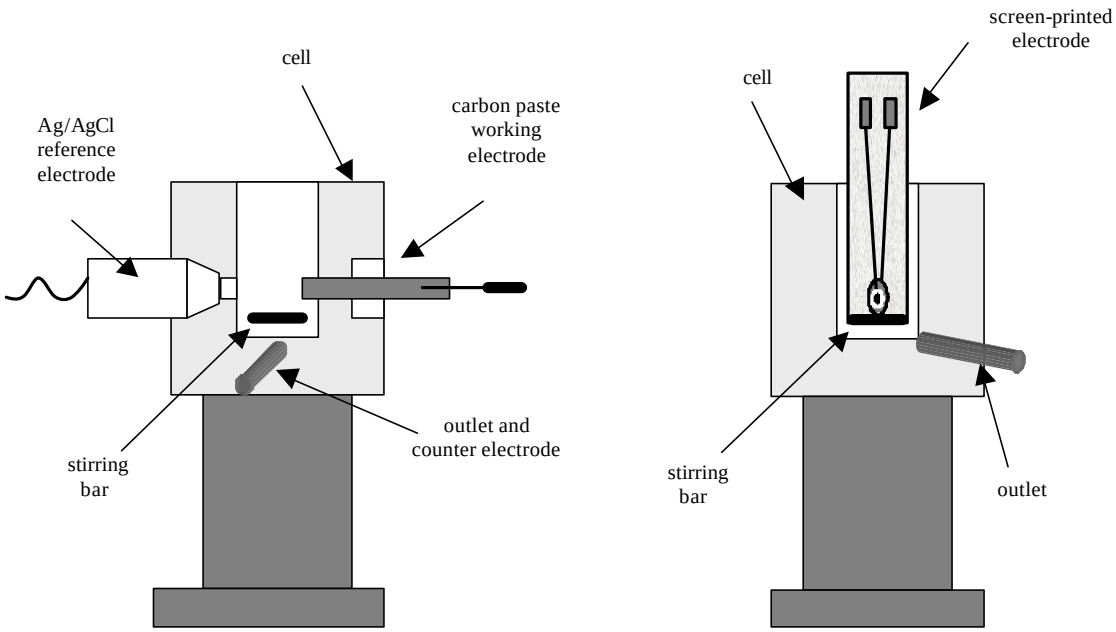

Figure 3.2: Schematic drawing of the stirred batch cells. The left is for carbon paste electrodes and the right is equipped with screen-printed electrode.

The cell designed for the screen-printed electrodes was not equipped with any additional electrodes since the reference/counter electrode was integrated on the transducer.

Both cells had a total volume of 1 mL and were equipped with a magnetic stirring bar. The cell was filled with buffer for equilibration and the working potential was applied. After a constant current signal was measured, the sample solution was added to obtain a final dilution of 1:100 and the resulting change of the current was recorded. In the batch experiments a steady state current was used for data evaluation.

3.2.7.2 Flow through cells

For the experiments with the solid graphite electrodes as well as for investigations of the carbon paste electrodes in a flow system a wall-jet cell was used (**Fig. 3.3**).

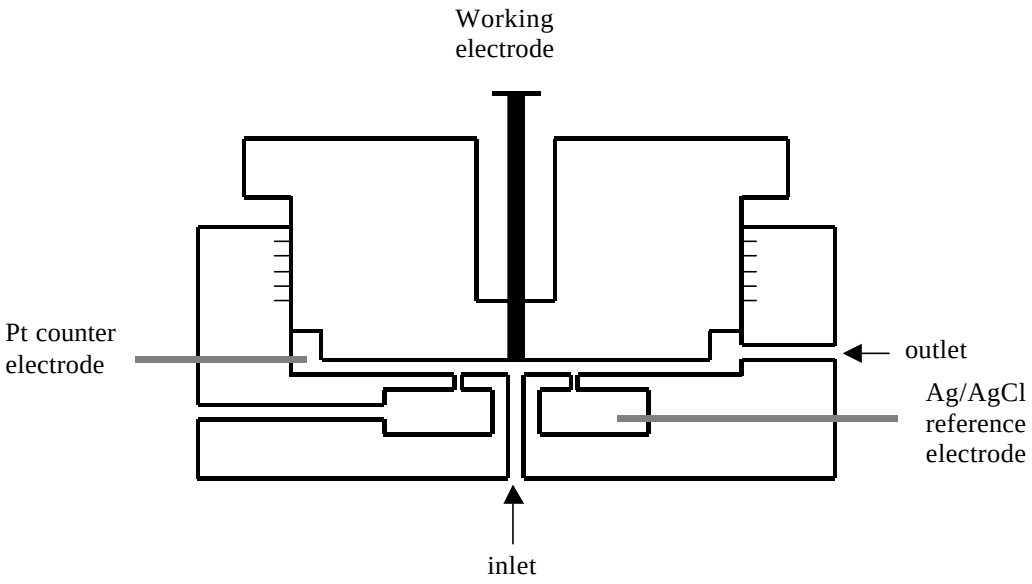

Figure 3.3: Schematic drawing of the flow-through wall-jet cell (Appelqvist, Marko-Varga et al. 1985)

The experiments with the screen-printed electrodes were performed with the flow cell shown in **Fig. 3.4**. The inlet and the outlet consisted of a platinum tube with an inner diameter of 0.5 mm. The flow channel was cut into the Plexiglas with a depth of 1 mm. A rubber seal was used to prevent leaking and the electrode was kept in place by a screw from the backside.

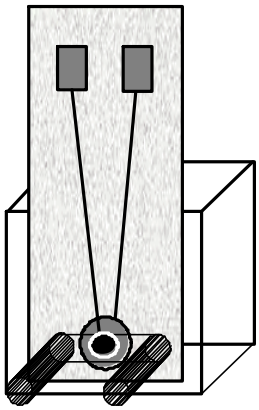

Figure 3.4: Schematic draw of the flow cell used in combination with the screen-printed electrodes.

The flow system consisted of the flow through cell, the two channel peristaltic pump and the 8-port injection valve programmable EVA-System from Eppendorf (Hamburg, Germany) (**Fig. 3.5**). All tubings were made from Teflon with an inner diameter of 0.8 mm. The sample channel was used for filling the tubing with the respective analyte solution and was switched off when starting the analysis.

The program included an equilibration time of 1 min before the first measurement of a series. Then the valve was switched to injection and back to flush with buffer again. The injection volume was determined by the flow rate and time of the valve set into ”inject” position. Numerous injections of the same sample were performed automatically.

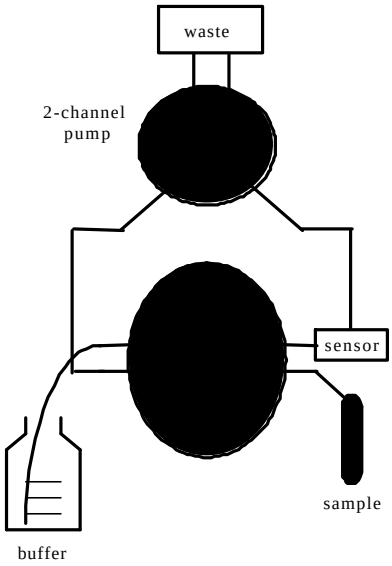

Figure 3.5: Flow system used for the experiments during biosensor development based on thick-film electrodes. The valve is shown in the “inject” position.

This system was used for most flow injection experiments during the development and optimization of the GDH-biosensors based screen-printed carbon and platinum based thick-film sensors. Only for the optimization of the injection volume this flow system was equipped with a manual 6-port injection valve (Rheodyne).

3.3 GDH-biosensor in the portable device

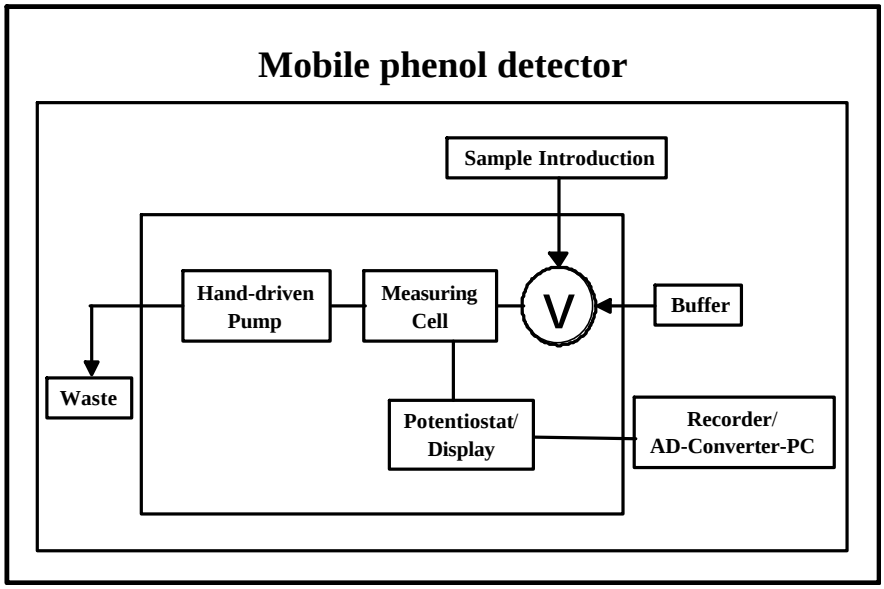

Figure 3.6: Portable measuring system for on-site analysis for phenolic pollutants.

The portable measuring system consisted of the integrated flow system based on a hand-driven peristaltic pump, the measuring cell for the platinum based thick-film electrodes, and the injection valve. Containers for the buffer and the waste were connected at the outer wall. The potential was applied by an external potentiostat ENZA. The signals were recorded on a computer using an interface box and Eurochrom software for data acquisition.

3.3.1 Experiments performed during the workshop in the "La Llagosta" WWTP, Barcelona

The biosensor was placed into a flow cell as described in **Fig. 3.4.**. and integrated into the portable system used for in-field analysis. The buffer was pumped inside the measuring cell with the help of the manually-driven pump. A PVC capillary with a volume of 20 µL was used for handling and injecting the sample into the carrier buffer via valve V. The sample was sucked in the device when the valve was switched to the position "INJECT". To minimize the dispersion of the sample in the carrier, the injected plug was separated from the buffer by introducing small air bubbles before and after sample injection.

The buffer contained 20 mM N-(2-hydroxyethyl)-piperazine-N´-(2-ethanesulfonic acid), 20 mM potassium chloride, 1 mM calcium chloride and 10 mM glucose, all from Merck, was used during the experiments based on the GDH biosensor.

3.3.1.1 Standards

Catechol (Merck) was used as the standard analyte both for sensor calibration and spiking of real water samples. Stock solutions of phenol, nitrophenols and chlorophenols were prepared at 10 mg/L in methanol from pure standards obtained from Aldrich. Standard mixtures of chlorophenols, phenols and nitrophenols were prepared in methanol at 200 µg/L by appropriate dilution from the individual stock solutions.

The individual polyethoxylate surfactants were mixtures with a certain average number of ethoxy groups, provided by Kao Corporation (Barcelona, Spain). The standards of alcohol ethoxylates (AEO) were individual pure C_{10} to C_{16} ethoxylates with an average of 4 ethoxy units per molecule. The standard of nonylphenol polyethoxylate (NPEO)

contained chain isomers and oligomers with an average of 6 ethoxy units per molecule. The mixture of coconut fatty acid diethanol amides (CDEA) was kindly supplied by H. Fr. Schroeder. The proportional composition of the different homologues was C_7 (7%), C_9 (7.5%), C_{11} (60.9%), C_{13} (18%) and C_{15} (6.6%). High purity (98 %) standard of *4*-tert-octylphenol (OP) was obtained from Aldrich (Milwaukee, WI, USA). Standards of *4*-nonylphenol (NP) and nonylphenol carboxylate (NPEC) were kindly supplied by AGBAR, Barcelona, Spain. Commercial linear alkylbenzene sulphonates (LAS) with a low dialkyltetralinsulfonates (DATS) content (<0.5%) were supplied by Petroquimica Española S.A. (Barcelona, Spain) in a single standard mixture with the proportional composition of the different homologues, as follows: C_{10}, 3.9%; C_{11}, 37.4%; C_{12}, 35.4% and C_{13}, 23.1%. Bisphenol A (BPA) and phtalate esters (diethyl-, dibutyl-, bis(2-diethylhexyl)-) were from Aldrich. Standard stock solutions of estradiol and ethinyl estradiol were prepared at 10 g/L in methanol from pure standards purchased from Sigma. Carbaryl (99,4% purity) was from Dr. Ehrenstorfen, Augsburg, Germany. PA-grade acetic acid (Panreac, Barcelona, Spain) and sulfuric acid (95-97%, Merck) were used.

Filter membranes were from Scharlau (Barcelona, Spain). HPLC-grade methanol, and water were purchased from Merck (Darmstadt, Germany).

3.3.1.2 Sampling

24-h composite samples were collected from the raw influent, from the effluent, and at an intermediate stage - after primary settlement and before biological treatment -, of two wastewater treatment plants located in the municipalities of “La Llagosta” and “Igualada” (Barcelona, Spain), which receive mainly industrial discharges and to a lesser extent urban wastewater. Filtered samples were collected in Pyrex borosilicate amber glass containers previously rinsed with tap water and with high-purity water. Immediately after sampling and until extraction, which took place within 48 h after collection, samples were stored at 4 °C.

3.3.1.3 Analysis

For the analysis using the GDH biosensor, the filtered samples were diluted 1:1 (v/v) with doubled concentrated buffer (40 mM HEPES, 40 mM KCl, 2 mM $CaCl_2$ and 20 mM glucose), then injected into the systems. If the signal recorded on the biosensor was outside its dynamic response range, the sample was further diluted using the carrier buffer (20 mM HEPES, 20 mM KCl, 1 mM $CaCl_2$ and 10 mM glucose).

At least two different dilutions of the water samples that gave signals within the working range of the sensor were further spiked with catechol (final concentrations: 10, 50, 100 µg/L), injected into the system, and the signal was further recorded.

The stability tests for the GDH-biosensor were performed by successive injections of 10, 50 and 100 µg/L catechol in the carrier buffer after analysis of each water sample.

3.4 Activity measurements for free ß-Gal and the synthesized conjugates

Activity measurements were performed with a Beckman 640 spectrophotometer (Beckman Instruments Inc., Fullerton, CA, USA). Batch activity measurements were carried out spectrophotometrically at 405 nm by monitoring the 4NP released by ß-Gal hydrolysis of 4NPG, at the conditions specified by the enzyme supplier (Roche-Industries 1999). The activity of the tracers was determined either spectrophotometrically or electrochemically using the GDH-FI-system.

3.4.1 Spectrophotometric method

The optical measurements were performed at 405 nm and a temperature of 22 ± 1 °C using a glass cuvette (path length 10 mm) and HBS20 buffer, containing 10 mmol/L 4NPG and glucose. A U-1100 spectrophotometer (Hitachi, Tokyo, Japan) coupled to a Kipp&Zonen (Delft, The Netherlands) chart recorder was used to obtain kinetic information.

The autohydrolysis of the 4NPG substrate was monitored during 10 minutes, however, no increasing of the background was visible. The extinction coefficient for 4NP in the substrate buffer was calculated, according to Lambert-Beer's law, at concentrations between 10 and 90 µmol/L. For the concentration dependence a linear fit through origin (y = ax) was performed using Origin 5.0 (Microcal Software, Northhampton US).

The initial activity of the free ß-Gal was determined. ß-Gal solutions of 5, 10, and 20 mg/L in HBS20 with 10 mmol/L glucose in the absence of 4NPG were prepared. 10 µL of these free ß-Gal solutions were mixed in the cuvette with 990 µL of HBS20 containing 10 mmol/L 4NPG and the change in A_{450} with time was recorded. To estimate the enzyme activity of the ß-Gal tracer, three dilutions 1:10000, 1:20000, and 1:50000 of the tracer stock solution were prepared and the measuring procedure was the same as described for the free ß-Gal. These results were used for comparison with the bioelectrochemical method, described below.

3.4.2 Bioelectrochemical method using the GDH-FI system

The free ß-Gal and the ß-Gal tracer were characterised by their ability to hydrolyse the 4APG substrate where the resulting 4AP was quantified with the GDH-FI system, described above, at a temperature of 22 ±1 °C. The calibration of the GDH biosensor with 4AP (10 to 500 nmol/L) was performed in HBS20 in the presence and the absence of 2 mmol/L 4APG to determine the influence of the 4APG. Each concentration of 4AP was injected in triplicates, the peak height of the resulting oxidation current was recorded, and the sensitivity was calculated using a linear fit. Additionally the background current at various concentrations (20 to 2000 µmol/L 4APG) was recorded.

The activity of the free ß-Gal, diluted in HBS20 with 10 mmol/L glucose in the absence of 4APG, was tested for three different ß-Gal concentrations (10, 20, and 50 µg/L). To start the activity measurement 990 µL of HBS20 containing 2 mmol/L 4APG were mixed with 10 µL of the enzyme solution and the reaction time was controlled. The enzyme substrate mixture was placed in the autosampler of the GDH-FI system and triplicate injections of 50 µL were made within 10 min. The resulting increase of the biosensor oxidation current corresponded to the amount of 4AP produced by the ß-Gal. Three identical experiments were performed for each enzyme dilution. The activities were calculated from the slope of the linear current-time relation. In the same way as above the activity of the ß-Gal tracer, diluted in HBS20 with 10 mmol/L glucose in the absence of 4APG, was estimated three times for triplicate injections of a mixture of 990 µL of HBS20 containing 2 mmol/L 4APG and 10 µL of three dilutions of the tracer stock solution (1:500000, 1:1000000, and 1:2000000, respectively).

3.5 Heterogeneous Immunoassays for *4*-nitrophenol

3.5.1 Synthesis of the *4*-nitrophenol (4NP) tracers

HOM and *ß*-Gal were employed for tracer synthesis according to the following steps:

Step 1)

The carboxyl group of the HOM derivative was pre-activated by reaction of 15 µmols of HOM (3.86 mg) with activation reagents. Two different activation procedures were used:

* *Activation procedure I (Fig. 3.7):*

8.62 mg N-hydroxysuccinimide and 29.1 mg dicyclohexylcarbodiimide were dissolved in 50 µl dry DMF and added to 3.9 mg HOM in 50 µl dry DMF. The mixture was stirred for 1 h at room temperature and the resulting white precipitate of dicyclohexyl urea was removed by centrifugation for 10 min at 10000 rpm, while the supernatant was used for further conjugation.

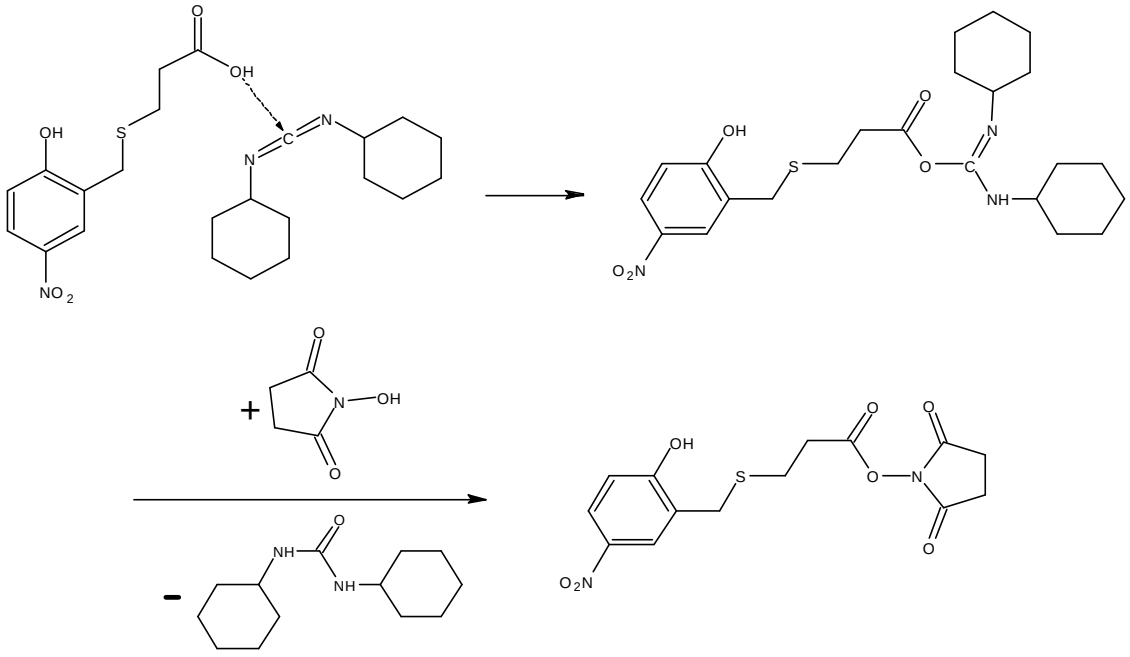

Figure 3.7: Activation with NHS/DCC method. In the first step a nucleophilic attack of the HOM occurs at the positively charged carbon atom of the DCC. In the second step a displacement with NHS leads to the activated ester.

* *Activation procedure II (Fig. 3.8):*

50 µl dry DMF, containing 5.48 mg *2*-(*5*-norbornene-*2,3*-dicarboximido)-*1,1,3,3*-tetramethyl-uronium tetra-fluoro-borate and 1.52 mg N-methylmorpholin were added under stirring to 50 µl dry DMF, containing 3.9 mg HOM and the mixture was stirred for an additional 15 min at room temperature. A clear solution containing the activated HOM was obtained, and used for further conjugation without additional purification.

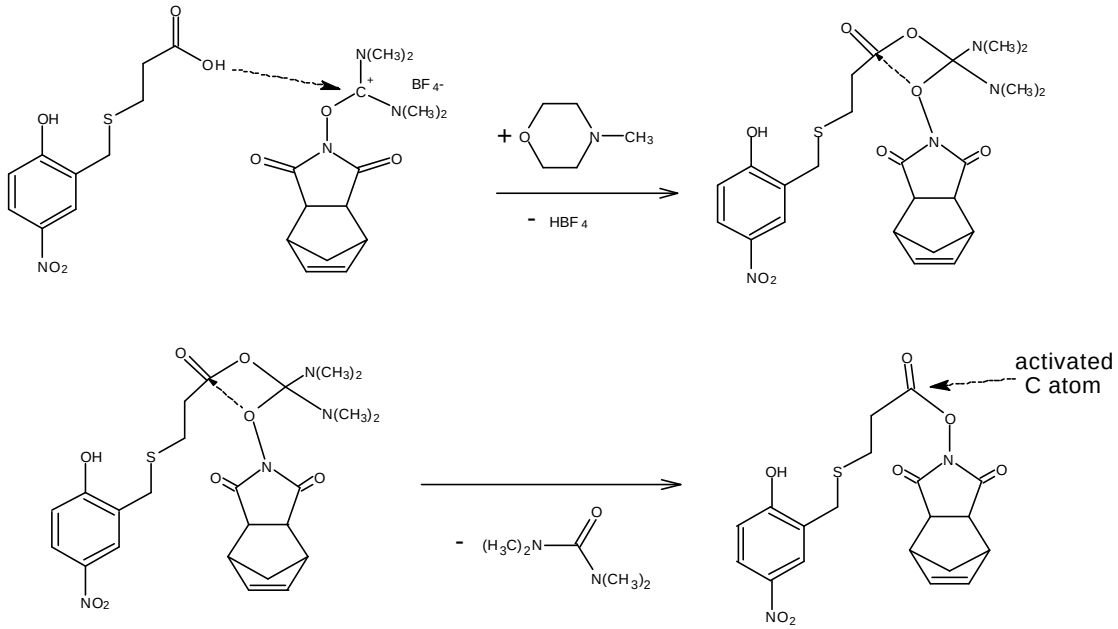

Figure 3.8: Schematic drawing of activation procedure II (NMM/TNTU method). In the first step a nucleophilic attack of the HOM occurs at the positively charged carbon atom of the TNTU. This happens in the presence of NMM as catalyst to preserve the basic nature of the solution. In the second step an intra-molecular displacement leads to the activated ester under separation of urea.

Step 2)

The two pre-activated HOM derivatives were coupled to ß-Gal according to the following procedure: to obtain tracers with initial molar ratio of 1000 mols HOM to 1 mol of ß-Gal, 10 µL each of the NHS and TNTU activated HOM conjugates were added dropwize and under stirring to each 4.05 mg ß-Gal dissolved in 200 µL 0.1 mol/L carbonate buffer pH 8.3.

For preparation of the tracers with initial molar ratios of 100/1, 10/1 and 1/1 HOM to ß-Gal the activated HOM solutions were diluted to 1:9, 1:99 and 1:999 (v/v), respectively, with dry DMF. Then, 10 µl of each resulting solution were added dropwize to 200 µL ß-Gal solution. All the coupling reactions were allowed to proceed over night at 4°C.

Step 3)

Purification of the tracers from the unconjugated HOM derivative was performed by dialysis (Molecular Weight Cut-Off 10 KDa) against 2 L of 0.1 mol/L tris-(hydroxymethyl)-aminomethan buffer (TRIS), pH 7.5, containing 1 mmol/L $MgCl_2$.

3.5.2 Tracer Characterization

The tracers were characterized in terms of HOM to ß-Gal molar ratio by estimation of protein concentration using the method described by Bradford (Bradford 1976). The HOM concentration was determined by measuring the specific absorbency at 420 nm (e_{420} = 1.18 cm^2/µmol).

3.5.2.1 Protein determination using the Bradford method

Protein concentration was determined using the Bio-Rad Protein Assays according to Bradford. 25 µL reagent A solution was added to 200 µL reagent B solution and mixed with 5 µL of the protein sample. Incubation lasted for 20 min in the dark. The extinction was measured at 750 nm. BSA samples of known concentrations were used as standards.

3.5.3 Enzyme Flow ImmunoAssay (EFIA)

The detection of the analyte was based on the off-line competition between the analyte and tracer molecules for the binding sites of the antibody. The discrimination between the antibody-bound fraction and the free analyte and tracer molecules was realized by separation using a protein G column.

In principle, two types of experiments were performed for each of the synthesized tracers: *Optimization of the antibody concentration, i.e.*, generation of an antibody dilution curve, was carried out by incubation of different concentrations of antibody (Ab) with a minimal and constant concentration of tracer (Ag*). After incubation, the mixture was introduced into the flow system and the amount of trapped Ag* was monitored as described below. The *antigen calibration curve* was accomplished similarly, except that the reaction mixture consisted of different concentrations of antigen mixed with the optimized and constant concentrations of tracer and antibody determined above.

After 15 minutes competitive off-line incubation of the analyte ($4NO_2P$), *ß*-Gal tracer, and Ab36, this mixture was injected into the flow system via a 50 µl injection loop connected to a manually-driven six port injection valve. The sample was transported by a peristaltic pump, continuously pumping a carrier buffer containing 20 mmol/L HEPES buffer at pH 7.5, 20 mmol/L KCl (Merck), 1 mmol/L $CaCl_2$, 1 mmol/L $MgCl_2$, 10 mmol/L glucose 0.01 % (v/v) Tween 20, and 50 µmol/L *4*-aminophenyl-*ß*-D-galactopyranoside (4APG), at a flow rate of 0.5 mL/min. The unbound analyte and tracer were separated from the formed antibody-antigen and antibody-tracer complexes by trapping the immuno complexes in a column (0.2 x 2.5 cm) filled with protein G immobilized on sepharose. This column was placed instead of an injection loop in a second six-port injection valve, allowing it to be switched in or out from the carrier flow for regeneration between runs with 0.1 mol/L glycine buffer, adjusted to pH 2.5 with HCl. After injection of the sample mixture, the protein G column was washed for 2 min with carrier buffer containing the enzyme substrate, then the flow through the protein G column was stopped for 5 min. During this time, the enzyme tracer trapped inside the column converted 4APG to *4*-aminophenol (4AP). When the flow was re-started, the formed 4AP was eluted by the carrier flow and electrochemically detected downstream on the screen-printed GDH-biosensor.

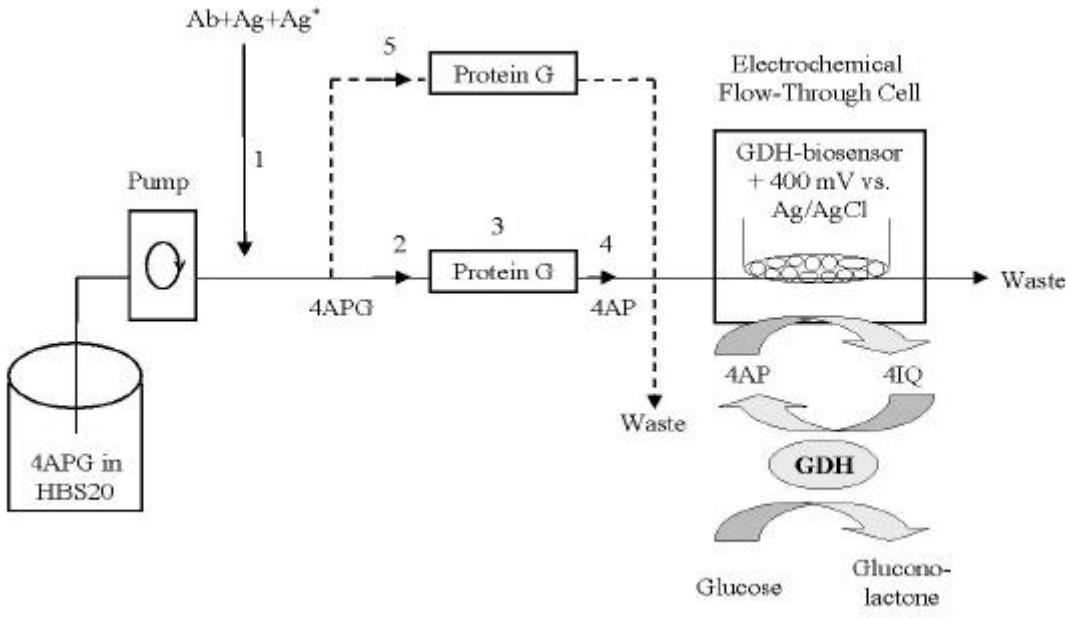

Figure 3.9: Schematic representation of the flow-injection system and the working mechanism of the GDH-biosensor. 1) Injection of the sample mixture containing the analyte, tracer and antibody at equilibrium; 2) Trapping the antibody-complexed analyte and tracer on the protein G column, and removal of the free fractions; 3) the carrier flow through the protein G column and the GDH-biosensor equipped measuring cell is stopped; 4) the carrier flow is restarted and the 4AP produced is transported into the measuring cell and quantified on the GDH biosensor; 5) the protein G column is disconnected and regenerated, while the carrier buffer continuously passes the GDH-biosensor.

3.5.4 Microtiter plate Enzyme-Linked ImmunoSorbent Assay (ELISA) for *4*-nitrophenol

A direct competitive ELISA was performed by first coating microtiter plates with Ab by incubation 100 µL/well, containing 10 µg/mL Ab36 in 0.1 mol/L carbonate buffer at pH 9.6. The adsorption was allowed to take place over night at 4°C. The excess of unbound Ab36 was washed away 3 times with 300µL/well phosphate buffer saline (PBST) at pH 7.2, containing 40 mmol/L Na_2HPO_4/KH_2PO_4, 137 mmol/L NaCl, 3 mmol/L KCl, and 0.05 % (v/v) Tween 20. The free unspecific binding sites were blocked by addition of 100 µL/well, containing 0.5% bovine serum albumin (BSA, Sigma) in 0.1 mol/L carbonate buffer at pH 9.6, and incubated at room temperature for 2 h. The excess of BSA was removed by washing the plate with PBST. The competition step was accomplished by addition of different concentrations of analyte (4NP) and fixed concentrations of *ß*-Gal tracers dissolved in 50 mmol/L phosphate buffer at pH 7.0, and incubation for 60 min. After washing away the unbound reagents with PBST, 300 µL/well of 4.15 mmol/L of the *ß*-Gal substrate *4*-nitrophenyl-*ß*-D-galactopyranoside in 0.1 mol/L phosphate buffer containing 0.1 mol/L NaCl and 1 mmol/L $MgCl_2$ at pH 7.5, was added and incubated with the bound tracer fraction. The liberated 4NP was monitored over a period of 20 h at 405 nm using a SLT340 ATTC microtiter plate reader.

3.6 Heterogeneous Immunoassay for alkylphenols and their ethoxylates

3.6.1 Synthesis of the NPE–ß-Gal conjugate

The synthesis of the 4NPE-ß-Gal tracer was performed using the TNTU/NMM-activation method (**Fig. 3.10**) in accordance with the protocol described below.

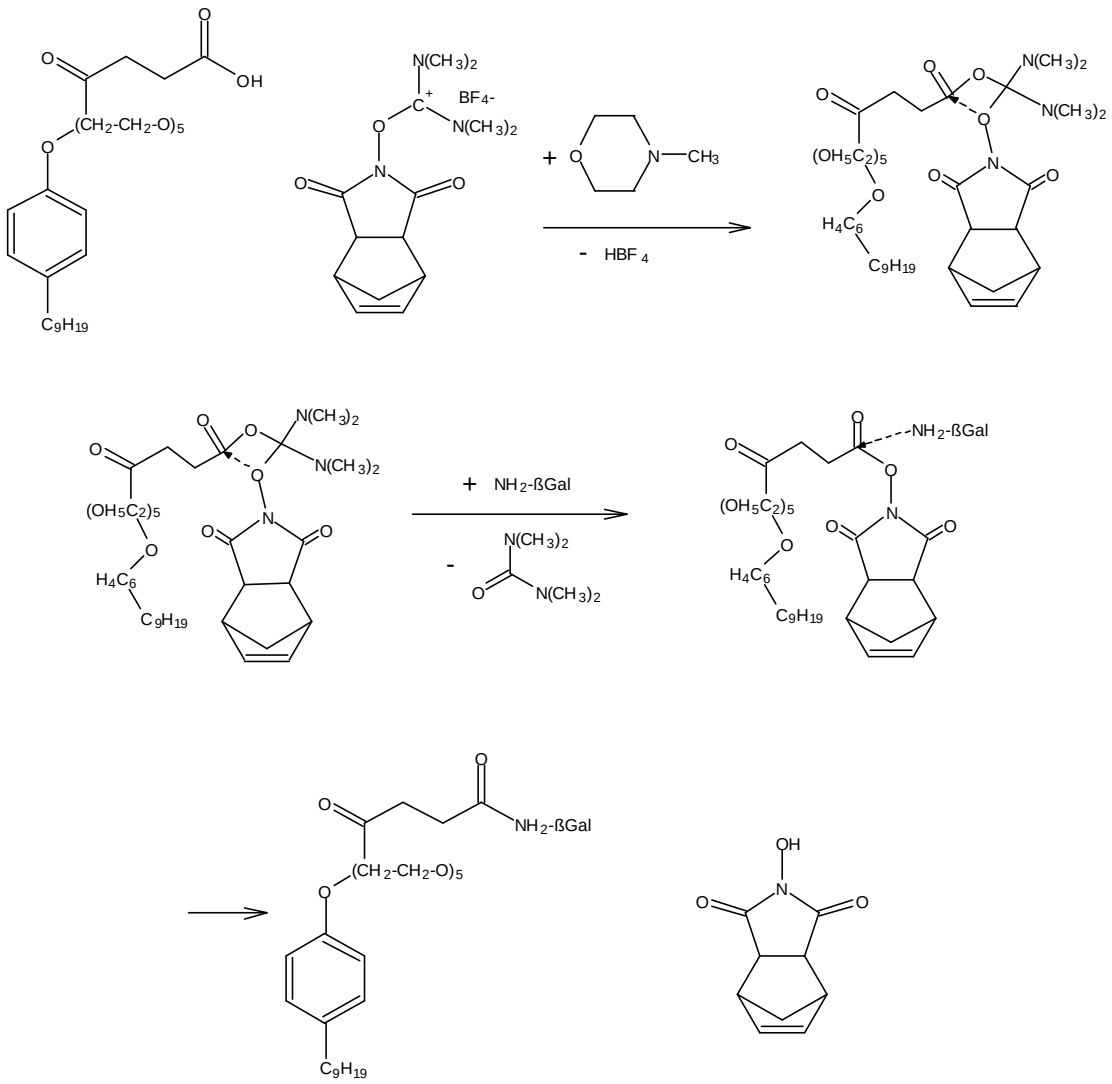

Figure 3.10: Schematic illustration of the tracer synthesis. Coupling of the APE derivative to ß-Gal using the NMM/TNTU method. In the first step a nucleophilic attack of the APE derivative occurs at the positively charged carbon atom of the TNTU. This happens in the presence of NMM as catalyst to preserve the basic nature of the solution. In the second step an intra-molecular displacement leads to the activated ester under separation of urea. In the last step a nucleophilic attack of the free electron pair at the amino groups of the enzyme towards the carbon atom of the ester function leads to the APE-enzyme conjugate.

Step 1)

For the activation of the 4NPE hapten derivative 5 µL NMM were dissolved in 450 µl of dry DMF. 100 µL of this solution were mixed with 100 µL dry DMF containing 3.65 mg TNTU. This mixture was added dropwize to 100 µL stirred solution containing 2.7 mg (5 µmols) of the APE in dry DMF. The mixture was stirred for 30 min and a clear solution was obtained.

Step 2)

75 µL of the resulting solution were added dropwize to 450 µL ß-Gal solution (66,7 µg/µL solid) in carbonate buffer, pH 8.3, 0.1 mol/L. The mixture was stirred in a closed vial for 4 hours at room temperature.

Step 3)

The unconjugated APE hapten was removed using a Microcon ultrafiltration unit (Millipore, Bedford, US) with molecular weight cut off 50000 Da. The tracer was removed from the filter with HEPES buffer, consisting of 20 mmol/L HEPES, 20 mmol/L KCl, 1 mmol/L $CaCl_2$ and 1 mmol/L $MgCl_2$ with an adjusted pH of 7.5, to a final volume of approximately 450 µL. When not in use the tracer was stored in the refrigerator at 4°C.

3.6.2 Microtiter plate ELISA for APE

For comparative reasons and for testing the binding properties of the synthesized tracer, an ELISA was performed, using commercially available 96 wells ELISA plates coated with monoclonal anti-APE antibodies (no details known), obtained from Takeda Chemical Industries (Japan). For quantification of the results a Multiskan MCC 340 microtiter plate reader was used. The plate was loaded with 100 µL/well of the ß-Gal tracer stock solution, diluted 1:20000. 100 µL aliquots of various concentrations of NPE, OPE, NP, and OP prepared in HBS20, were added. The concentration range for the APEs was between 1 and 1024 µg/L and for the APs between 8 and 8192 µg/L because of the lower affinity of the antibody for the latter (Takeda-Industries 2000). The mixture was allowed to compete for 1 h. After three washing steps using 300 µL/well of the washing buffer (HBS20 containing 0.05 % Tween 20), 100 µL of substrate buffer (HBS20 containing 0.05 % Tween 20 and 10 mmol/L 4NPG) was added. The microtiter plate was covered and placed into a reader and absorbance at 450 nm was measured frequently over a period of 4 h.

3.6.3 Immunoassay in disposable PVC capillaries

A competitive immunoassay was developed for alkylphenols and alkylphenol ethoxylates. The detection of the analytes was based on the competition between the analyte and tracer molecules for the binding sites of anti-alkylphenol ethoxylate antibodies. The sample, containing APE, was incubated off-line with a fixed amount of ß-Gal tracer. This mixture was then introduced into a disposable antibody-coated capillary, where the competition of tracer and analyte for the antibody binding sites took place. The assay conditions and capillary reproducibility were optimzed by introducing the capillary into a flow injection system serving as an injection loop.

3.6.3.1 Pre-treatment of the plastic capillaries

The polyvinyl chloride capillaries were pre-treated with 5 % NaOH for 30 min. Connecting 50 capillaries, one after the other, using connecting tubing with a minimum dead volume, performed the practical mode of washing. The solution was flushed continuously through the capillaries at a flow rate of 1 mL/min. Afterwards the capillaries were flushed for 15 min with distilled water until a neutral pH was observed. The capillaries were dried in a nitrogen stream.

3.6.3.2 Immobilization of the antibody

Monoclonal anti-APE antibodies (Takeda Industries, Japan) were adsorbed to the inner surface of the pre-treated capillaries. Therefore 25 µg antibody were added to 500 µL carbonate buffer pH 9.6. The resulting solution was filled into the capillaries carefully to avoid air bubbles. The immobilization proceeded over a period of 4 h at room temperature. Afterwards the capillaries were washed with 2 mL HBS20 containing 0.05 % Tween 20. The free binding sites were blocked overnight with 1 % BSA in carbonate buffer, pH 9.6. To distinguish between specific

and unspecific binding, reference capillaries were coated with 1 % BSA only. The immobilization procedure was performed by connecting 25 capillaries, one after the other, with connecting tubing and pumping all reagent solutions through, using a peristaltic pump that was stopped during specific time frames for the reactions to take place as specified above. This was done in order to obtain as reproducible protein coatings as possible on the capillaries. At the end the protein solution was removed and the capillaries were carefully dried in a nitrogen stream. After the coating the capillaries were manually cut into halves (final length of 25 mm, V= 10 µL) using a razor blade. The coated capillaries were stored dry in Eppendorf vials at 4°C. During the day of use the capillaries were kept at room temperature.

3.6.4 Capillary Immunoassay (CIA)

The methodology of the CIA is illustrated in **Fig. 3.11**. The sample is mixed in advance with a fixed amount of tracer (1) and introduced into the capillary (2). The filling of the capillary was performed manually by aspiration using an Eppendorf pipette with an adjusted volume of 12 µL. The competition between the analyte and tracer molecules for the limited amount of antibody binding sites took place inside the capillary (3). After a fixed incubation time, unbound analyte, tracer and matrix molecules were washed away manually by repetitive flushing (3 times) with 50 µL washing buffer (HBS20 containing 0.05 %Tween 20) (4). Then the capillary was mounted into the loop of the 6-port-injection valve of the automated GDH-FI system described above, the system in which the following steps were performed.

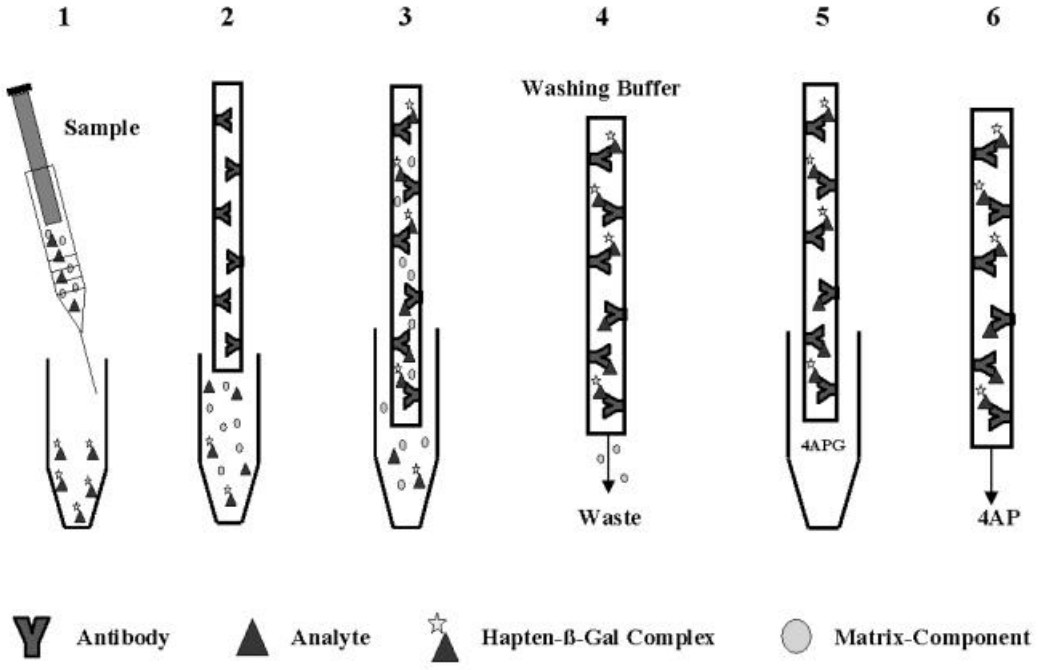

Figure 3.11: Schematic drawing of the steps performed in the capillary immunoassay

First the capillary was flushed in ”inject” position with the substrate buffer (HBS20 buffer containing 4APG) for 60 s. When the valve was switched to ”load” position the buffer flow stopped in the capillary to allow the conversion of the substrate for a pre-set time of 150 s (5). The valve was then switched to ”inject” position the substrate/product plug was passed during 30 s to the GDH biosensor, where the produced 4AP was quantified (6) using the peak height of the oxidation current. Three repetitive injections were performed and the mean was used for quantification. Three capillaries were used for each calibration point if not otherwise stated.

4 Results and discussion

4.1 GDH-biosensors

4.1.1 Measuring principles

Glucose dehydrogenase catalyses the oxidation of glucose to gluconolactone in the presence of a suitable electron acceptor. This enzyme is able to shuttle the electron to the surface of the electrode. An enzymatic substrate recycling leads to an amplification of the signal (**Fig. 4.1**). The electrode is poised at a constant positive potential, thus insuring the oxidation of the analyte. The anodic current from the oxidation will then be used as the analytic signal.

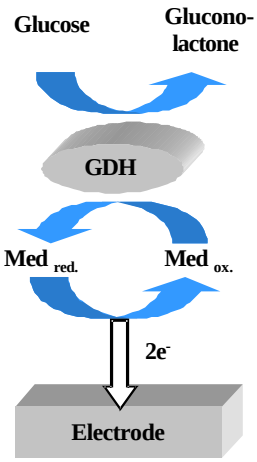

Figure 4.1: Schematic drawing of the amplification cycle of GDH.

This principle shows that only the oxidized analytes are suitable substrates for the GDH. In order to simplify the terminology used within this thesis, the phenolic analytes have been stated as substrates without further specifying their oxidation state.

One main advantage of the GDH catalysis is that this reaction is oxygen independent. This reaction can be used for determination of glucose if the redox mediator is present in high excess and therefore does not limit the reaction. For our purposes, the sensor should be used for the quantification of the mediator, so a high excess of glucose should be present during the experiments. Suitable electron acceptors can be metal complexes, redox active dyes, or phenolic compounds. Our interest was focused on phenolic compounds of analytical interest as well as phenolic compounds liberated during the catalytic process of enzyme-based immunoassays.

To design a biosensor based on this enzymatic reaction an efficient electron transfer must be achieved. Therefore, the enzyme has to be immobilized in close proximity to the transducer, and its initial activity must be preserved. Various basic transducers and immobilization techniques were tested for applications in batch and flow systems.

A typical signal vs. time curve for the batch system is shown in **Fig. 4.2**. The GDH-biosensor is mounted into the stirred measuring cell, the glucose free buffer is added, and a constant potential is applied. After equilibration, a constant background current is obtained (A). The analyte is added into the cell and the oxidation current is recorded. The analyte reaches the polyurethane membrane, diffuses towards the electrode and is oxidized. In the absence of glucose, the oxidized analyte diffuses back into the bulk phase. The current stabilizes when the steady state between the electrode reaction and the diffusion is reached (B). The current would finally decrease again, only when the concentration in the bulk decreases.

By flushing the cell with buffer, the current falls back to the background level (C). If glucose is added to the buffer solution, a constant steady state current is obtained (D). An addition of the analyte in the presence of glucose results in a steady state current (E). As a result of flushing the cell with glucose-containing buffer, the current returns to the steady state value obtained before the addition of analyte. The stepwise addition of small analyte quantities are shown in trace F. By flushing the cell with glucose-free buffer the initial background current is measured. In the batch system the steady state current was used for the quantification of the analyte.

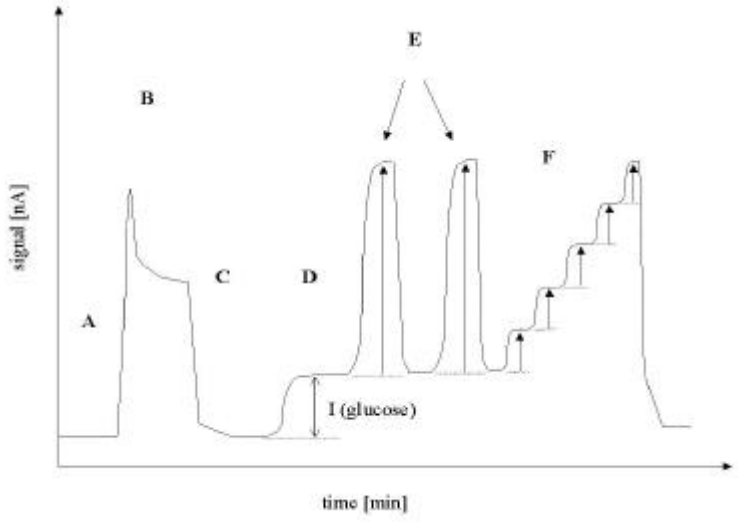

Figure 4.2: Typical signal vs. time plot for a stirred batch system. I (glucose) represents the current difference in the absence and the presence of glucose in the buffer. Signal A (measured in the absence of glucose) resembles a much higher concentration of the analyte than the injections performed in the presence of glucose.

A typical signal vs. time curve for the flow injection system is shown in **Fig. 4.3**.

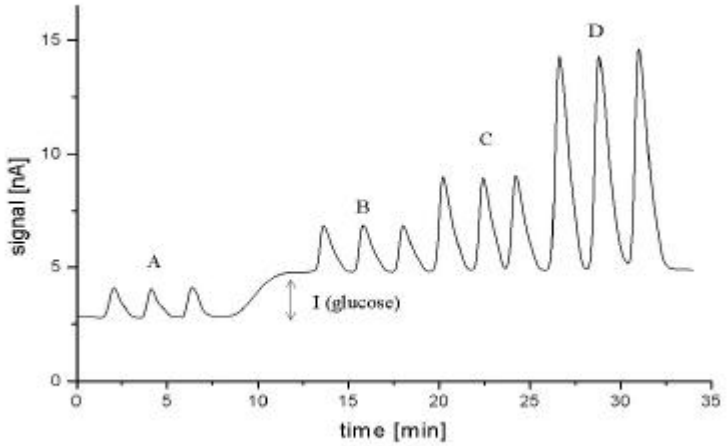

Figure 4.3: Typical signal vs. time plot for the flow injection analysis of dopamine using a GDH-biosensor. I(glucose) represents the current difference in the absence and the presence of glucose in the buffer. Signal groups A-D typical flow-injection peaks resulting each from three injections of the analyte. Signal A is produced by the same concentration as D, while the different peak height is a result of the enzymatic amplification.

The GDH-biosensor is mounted into the measuring cell, the glucose free buffer is pumped trough, and a constant potential is applied. After equilibration, a constant background current is obtained. The addition of analyte results in a typical flow injection peak. When glucose is added to the buffer, an increased background current occurs. The

addition of analyte in the presence of glucose yields increased signals due to the catalytic amplification of the GDH. For data acquisition the peak height will be used throughout this thesis if not otherwise stated.

4.1.2 GDH carbon paste electrodes (GDH-CPE)

Our group demonstrated the application of GDH-modified carbon paste electrodes for the detection of phenolic compounds in 1997 (Wollenberger and Neumann 1997). These GDH-modified carbon paste electrodes using polyethylene-imine as polyelectrolyte showed low detection limits, high sensitivity and extended linear range in stationary stirred devices.

Table 4.1: *Characteristics of GDH-CPE published by Wollenberger et al. (Wollenberger and Neumann 1997).*

Compound	LLD [nmol/L]	Measuring range [nmol/L]
4AP	0.2	0.5-200
Dop	5	5-2500
HQ	0.5	0.5-200

Starting from this experimental evidence, experiments were performed using *4*-aminophenol (4AP) and dopamine (Dop) as model analytes. 4AP was chosen as a phenolic compound liberated in many electrochemical enzyme-based immunoassays. Dop was chosen to represent the phenolic neurotransmitters. Additionally, Dop offers the amino-functionality in the side chain, where basic coupling chemistry could be applied. Therefore, Dop is interesting as a possible redox label in immunoassays. Other phenols such as catechol, hydroquinone, and cresol were also tested later as phenolic analytes of environmental interest.

4.1.2.1 Carbon paste electrodes in the stationary system

4.1.2.1.1 Equilibration time

The GDH-PEI-CPE was mounted into the measuring cell and a potential of 400 mV was applied. A very high, rapidly decreasing, oxidation current was measured. However, a time of about 10 h was necessary to reach the stable background current, required to start the measurements. In order to investigate whether a swelling process of the paste caused this behavior, the GDH-PEI-CPE was mounted into the cell to allow the contact with the buffer solution, without applying a potential. Subsequently, swelling was allowed to take place overnight and the potential was applied the next day. The same behavior recorded before was observed, and only after 10 h the first measurements were possible. Therefore, the GDH-PEI-CPE were prepared and allowed to stabilize overnight poised at 400 mV.

4.1.2.1.2 Optimization of measuring conditions

4.1.2.1.2.1 Oxidation potential

The first experiments were performed under stirring by using GDH-modified carbon paste electrodes with PEI in Sörensen phosphate buffer containing 1mmol/L $CaCl_2$ at pH 7. The graph in **Fig. 4.4** shows that 4AP is more easily oxidized than Dop. However, a potential of 400 mV was sufficient for the oxidation of both analytes and was used for the experiments during buffer optimization.

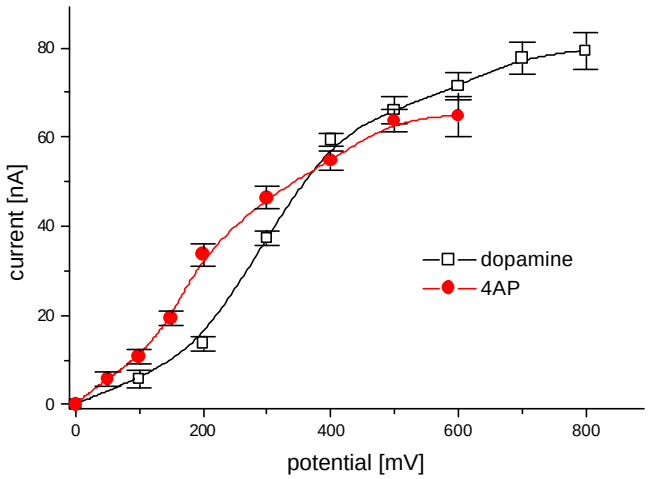

Figure 4.4: Hydrodynamic voltamograms for Dop and *4*-aminophenol (both 5 µmol/L) obtained with GDH-PEI-CPE. Measurements were performed in batch system with Sörensen phosphate buffer containing 1mmol/L $CaCl_2$ at pH 7. No glucose was present during these measurements.

4.1.2.1.2.2 Glucose concentration in the buffer

The influence of the glucose concentration on the signal was studied with Dop as model analyte. Sörensen buffer containing 1mmol/L $CaCl_2$ at pH 7 was used during these measurements.

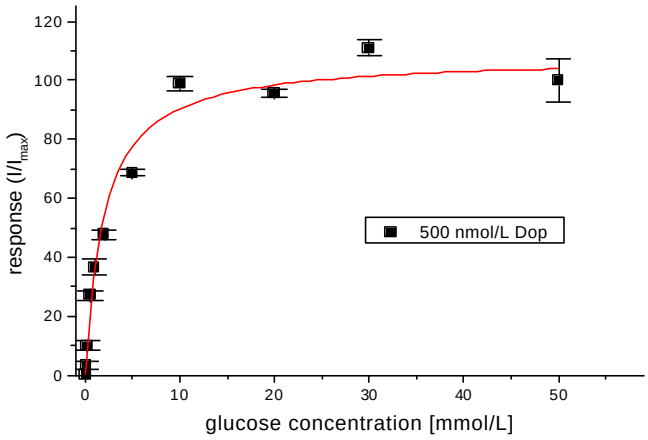

Figure 4.5: Influence of the glucose concentration on the signal for 500 nmol/L Dop. GDH-modified PEI-CPE were used with an applied potential of 400 mV. Measurements were performed in batch system with Sörensen buffer at pH 7 containing 1 mmol/L $CaCl_2$.

From **Fig 4.5** it can be deduced that a concentration of 10 mmol/L glucose allows maximum amplification of the signal. Therefore a glucose concentration of 10 mmol/L was present in all buffer solutions, if not otherwise stated.

Since the enzymatic catalysis is pH sensitive, an optimum pH range had to be established for the GDH-biosensor. Different buffer systems and the influence of the ionic strength had to be investigated as well. All experiments were performed in the batch system with an applied potential of 400 mV using Dop as the model analyte.

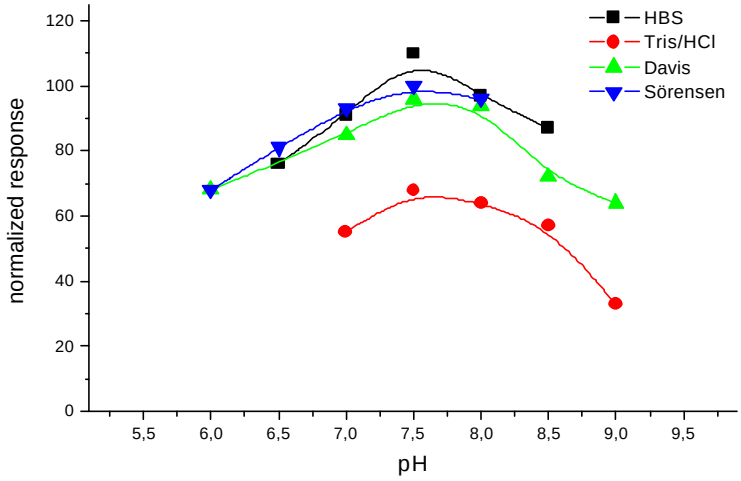

Figure 4.6: pH and buffer dependence of GDH-modified PEI-carbon paste electrodes. Four different buffer systems were tested: 0.1 mol/L HBS, 0.1 mol/L Davis, 0.1 mol/L Tris/HCl, Sörensen phosphate buffer. 1 mmol/L $CaCl_2$ and 10 mmol/L glucose were present in all buffers. For other experimental conditions refer to **Fig. 4.5**.

Fig 4.6. shows that the optimum pH value is 7.5. The highest response was obtained for HBS. This buffer consisted of 100 mmol/L HEPES and 100 mmol/L KCl. Additionally 1 mmol/L $CaCl_2$ was present during these experiments. This buffer at pH 7.5 is referred to as HBS100 throughout the following experiments.

Based on this experiments, the characteristics of the GDH-modified PEI-carbon paste electrode were investigated.

4.1.2.1.2.3 Response behavior towards phenolic compounds

The GDH-PEI-CPE were tested for the detection of Dop and 4AP.

Table 4.2: *Characteristics of the GDH-PEI-CPE in the stirred measuring cell*

Compound	LLD [nmol/L]	Measuring range [nmol/L]	Amplification factor*	Response time for 100 nmol/L [s]	Cycle time [min]
Dop	5	15-1000	95	60	4
4AP	1	3-400	160	40	3

* The amplification factor was calculated by dividing the current obtained in the presence of glucose by the current obtained in the absence of glucose.

As shown in **Tab. 4.2** the GDH-PEI-CPE detects both analytes but the sensitivity for 4AP was higher than for Dop. The GDH showed a better amplification of the 4AP signal (1.7 times). The response times are both below 1 min and the cycle times including the washing step and restabilization of the background current are 3 and 4 min, respectively. These characteristics make the GDH-PEI-CPE a promising tool for phenol detection in the stirred measuring device.

4.1.2.1.2.4 Reproducibility of sensor preparation

To test the reproducibility of the sensor preparation, three electrodes were prepared with the same carbon paste. These electrodes were tested with 100 nmol/L Dop as model analyte.

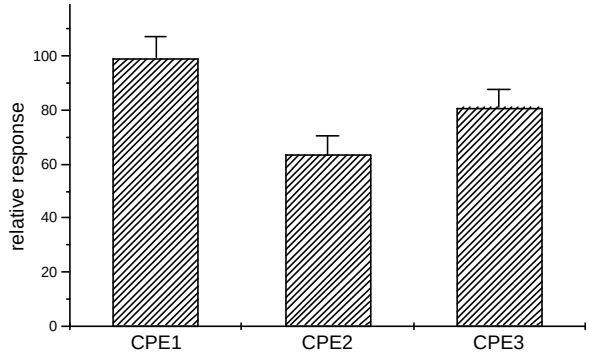

Figure 4.7: Comparison of the response of three carbon paste electrodes resulting from 8 injections of 100 nmol/L Dop. These experiments were performed in HBS100 in the presence of 10 mmol/L glucose with an applied potential of 400 mV.

The three different carbon paste electrodes were prepared from the same paste. Nevertheless, the differences for the quantification of Dop presented in **Fig. 4.7** are enormous. The error bars of each column give the repeatability for all three electrodes. Their values differ between 6.5 and 8 %. The differences between the electrodes can be seen from the mean value. The signal obtained with CPE2 was only 63 % of the value recorded for CPE1.

Another set of experiments was performed by using electrodes prepared with three different carbon pastes manufactured following the same protocol.

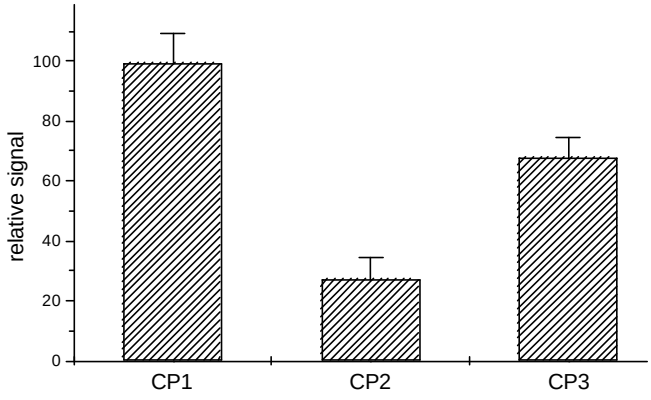

Figure 4.8: Comparison of the response of three electrodes towards 100 nmol/L Dop. The CPE were prepared with three different GDH-modified PEI-carbon pastes. For experimental conditions refer to **Fig. 4.7**.

The data presented in **Fig. 4.8** suggested that the reproducibility decreased when different batches of carbon pastes were used during sensor preparation. The response of CPE2 was 4 times, respectively 2.5 times, smaller than that arising from the other two GDH-electrodes. This cannot be tolerated for sensor preparation in mass production.

Besides the low reproducibility, the long equilibration times proved to be the main problem of the electrodes based on PEI-carbon paste. Therefore, the composition of the carbon paste was further investigated. Pastes without any polyelectrolyte, with poly-(sodium-*4*-styrenesulfonate) (PSSA), and a mixture of PEI and PSSA were studied. PSSA is more negatively charged than PEI.

Table 4.3: *Equilibration time of carbon paste electrodes modified with different poylelectrolytes*

	PEI	PSSA	PEI/PSSA	wo. polyelectrolyte
Equilibration time [h]	10	2	3	3

The shortest equilibration time was found for the PSSA modified carbon paste, while the PEI stretches equilibration time drastically. The characteristics of the different GDH-CPE-biosensors were determined for Dop.

Table 4.4: *Characteristics of the GDH-CPE in the stirred measuring cell towards Dop*

	LLD [nmol/L]	Measuring range [nmol/L]	Amplification factor*	Response time for 100 nmol/L [s]	Cycle time [min]
PEI	5	15-1000	95	60	4
PSSA	2	6-1200	95	40	3
PEI/PSSA	3	9-1200	95	60	4
wo.	15	45->1000	60	60	4

* The amplification factor was calculated by dividing the current obtained in the presence of glucose by the current obtained in the absence of glucose.

The PSSA-CPE shows the best performance for the Dop detection. The lowest detection limit and the fastest response were obtained with these electrodes. This is possibly due to the negatively charged PSSA, which improves the accumulation of Dop at the electrode surface. Adoption of PSSA allowed the reduction of the cycle time for one measurement down to 3 min. Carbon paste electrodes without addition of polyelectrolyte showed the highest LLD and a lower amplification factor.

The use of PSSA reduced significantly the equilibration time of the sensor and improved the response time, the detection limit, and the measuring range.

4.1.2.2 Carbon paste electrodes in the flow system

The experiments in the flow system were performed using a wall-jet cell. The same optimized experimental conditions used with the stirred cell were adopted. HBS100 buffer at pH 7.5 was employed. The applied potential was fixed at 400 mV. Dop was used as the model analyte.

4.1.2.2.1 Optimization of the flow conditions

GDH-PEI-CPE were analyzed first. For the flow system the injection volume and the flow rate had to be optimized first. A constant volume of 50 or 100 µL was injected to investigate the influence of the flow rate.

The graph presented in **Fig. 4.9** shows that a bigger injection volume led to higher response of the GDH-biosensor. This indicates that the steady state cannot be reached with 50 µL of injected Dop solution. This conclusion is remarked by observing that a higher flow rate led to lower signals. The contact time between the sample and the sensor is directly proportional to the flow rate, if the volume is constant. The decreasing signals show that in this experiments the contact time is not sufficiently long for reaching the steady state even by injecting 100 µL of the sample.

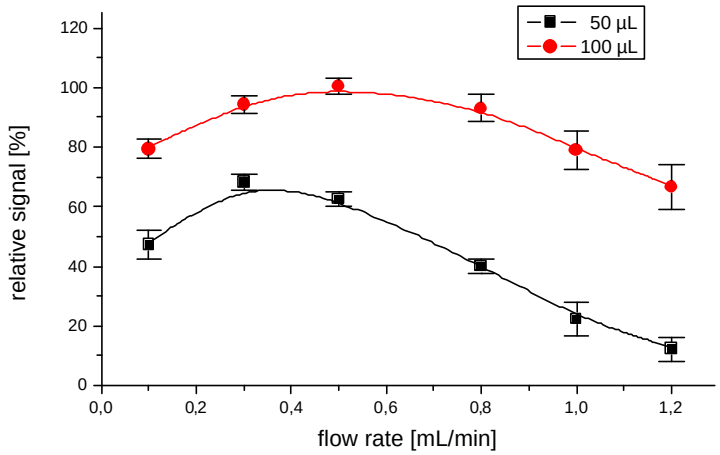

Figure 4.9: Influence of the flow rate on the signal for 100 nmol/L Dop using the GDH-PEI-CPE. Triplicate injections were performed for each point. For experimental conditions refer to **Fig. 4.7**.

The influence of the injected volume was further investigated and the results are shown in **Fig. 4.10.** A bigger injected volume implies a longer contact time between the sample and the sensor at a constant flow rate. By increasing the sample volume and thus allowing longer contact time, the signal increased almost linearly. This demonstrates that the steady state was not reached under this condition even with an injected volume of 1 mL. This means that the response time in this flow set-up is above 2 min. Also, the time needed for stabilization of the background after the injection was more than 2 min for injections of 100 µL, with the time increasing with increasing sample volume. For application in an automated flow system, the response behavior of the GDH-PEI-CPE was therefore not acceptable.

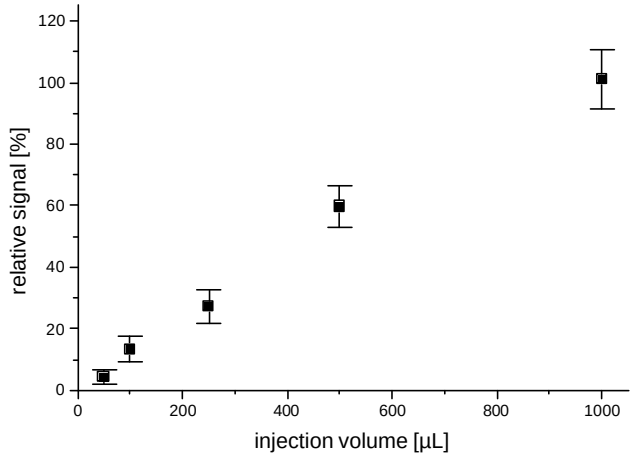

Figure 4.10: Influence of the injected sample volume at a constant flow rate of 0.5 mL/min. Triplicate injection of 100 nmol/L Dop were performed in all cases. For experimental conditions refer to **Fig. 4.7**.

The GDH-CPE modified with PSSA and the mixture of PEI/PSSA were tested for their application in the flow system. A constant flow rate of 0.5 mL/min was used and the influence of the sample volume was tested.

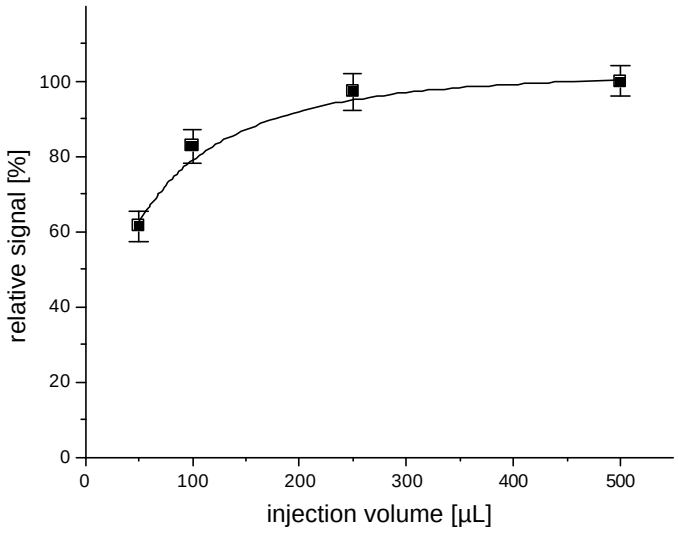

Figure 4.11: Influence of the injection volume at a constant flow of 0.5 mL/min was tested with GDH-PSSA-CPE. 100 nmol/L Dop were injected as triplicates. For experimental conditions refer to **Fig. 4.7**.

The response of the GDH-PSSA-CPE showed little influence of the injected sample volume, due to a much faster response of the electrode. A contact time of 30 s (for 250 µL sample at a flow rate of 0.5 mL/min) was sufficient to reach the maximum signal for 100 nmol/L Dop. Injections of this sample were possible every 5 min.

The GDH-PEI/PSSA-CPE was tested under similar conditions. Here, the maximum signal for Dop was reached with an injected volume of 500 µL at a flow rate of 0.5 mL/min. This implies a contact time of 1 min. The addition of PSSA to the carbon paste showed an improvement on the performance of the sensor in the flow system. For Dop the electrode with only PSSA exhibited the best performance. To further explain these experiments, the three different carbon pastes were tested for the detection of hydroquinone as well.

Avoiding the addition of glucose to the buffer eliminated the influence of the enzyme specificity in these experiments.

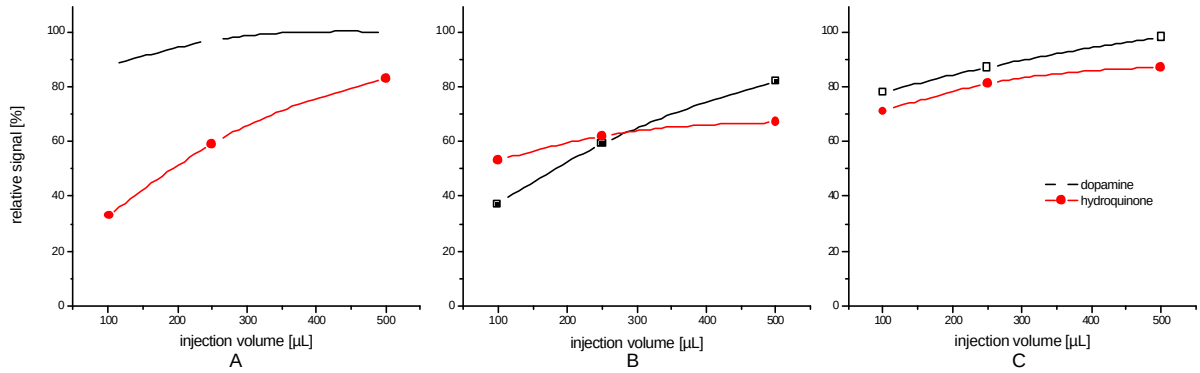

Figure 4.12: Influence of the injection volume at constant flow rate of 0.5 ml/min for samples containing 1 µmol/L Dop or hydroquinone, respectively. These measurements were performed HBS100 in the absence of glucose and the applied potential was 400 mV. PSSA-CPE (A); PEI-CPE (B), and PEI/PSSA-CPE (C). The currents are given as relative values related to the current obtained for the injection of 500 µL sample on PSSA-CPE.

Fig. 4.12, trace A, shows that the maximum signal for Dop was reached with an injected volume of 250 µL. For hydroquinone the steady state current is not reached with this contact time. The opposite behavior is observed with the PEI-CPE. Here, an injection of 250 µL hydroquinone is sufficient to reach the maximum current, while even 500 µL of Dop sample was not sufficient to reach the steady state (B). The sensor prepared with the mixture of both polyelectrolytes showed a similar picture for both analytes. The steady state current was reached after 1 min (500µL) for both Dop and hydroquinone, respectively. 4AP was tested with the three different CPE as well and it was observed that PSSA was preferable for the detection of 4AP. The influence of the carbon paste was not that pronounced since 4AP was detected rapidly on all the electrodes. Therefore, 4AP was additionally tested with injection volumes of 25 and 50 µL. This allows only qualitative comparison.

These results show that the composition of the carbon paste has an influence on the response behavior. The negatively charged PSSA allows better detection of the Dop, while the detection of hydroquinone is at the same time hindered. Using PEI-CPE the detection of Dop is slower, while hydroquinone is detected more rapidly. Since these results were obtained without addition of glucose in the buffer solution there was no influence by the GDH. A correlation between the analyte and its tendency to diffuse towards the electrode surface should also be found. Therefore we calculate the logP-value of the two compounds calculated with the software ACD/pKa version 4.03. This parameter reflects the octanol/water distribution coefficient and allows the evaluation of the hydrophobic properties of a certain compound.

We calculated a logP-value of 0.12 ± 0.3 for Dop and 0.64 ± 0.2 for hydroquinone. For analytes with lower logP-value like Dop it seems preferable to use polyelectrolytes that produce a more negatively charged surface. This should speed up the increase of the analyte concentration in close to the surface of the electrode. A higher logP-value suggests the use of a more positively charged surface. This could be realized by addition of PEI to the carbon paste. For 4AP the calculated logP-value was -0.29 ± 0.2. This requires for a negatively charged surface. The use of PSSA in the CPE preparation improved the response behavior of the electrode towards 4AP. Thus, the analyte enrichment obtained by the right choice of the added polyelectrolyte has to be considered during sensor preparation. Addition of polyelectrolyte can be used for optimizing the response behavior to the analyte of interest and thus for fine-tuning the selectivity of the biosensor.

In our case we focused on Dop during the investigation of the PSSA-CPE in the flow system. The optimum flow rate for an injection of 250 µL Dop (100 nmol/L) was determined in the presence of glucose. As shown in **Fig. 4.13** almost no influence of the flow rate on the resulting current was found between 0.5 and 1 ml/min. By increasing the flow rate the repeatability of the injections decreased. The standard deviation for 5 injections was 2.7 % at 0.5 mL/min and increased to about 8 % at 0.75 and 1 mL/min. Smaller flow rates resulted in broad peaks and longer washing time between injections thus lowering the sample throughput. For the following experiments a flow of 0.5 mL/min was used and reiteration of the injections every 4 min was possible. Adopting these conditions the GDH-PSSA-CPE was further characterized.

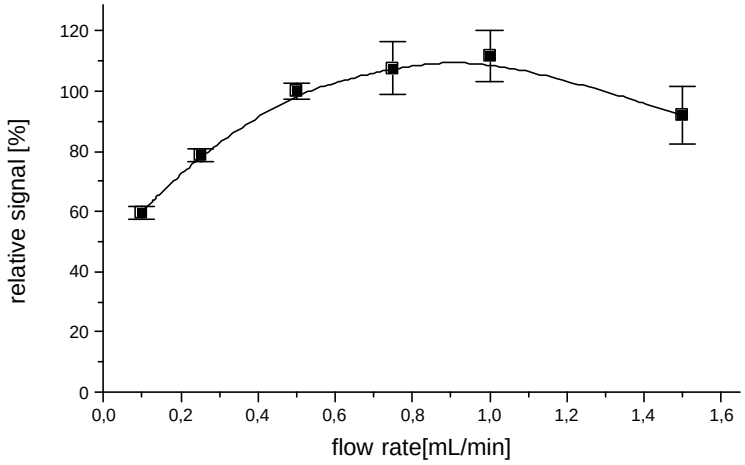

Figure 4.13: Optimization of the flow rate for the injection of 250 µL of 100 nmol/L Dop. The signal obtained at a flow rate of 0.5 mL/min was set to 100 % and all other signals are normalized to this peak. Conditions as stated in **Fig. 4.12** with additional 10 mmol/L glucose in the buffer. Triplicate injections were performed in all cases.

4.1.2.2.2 Characterization of the GDH-PSSA-CPE in the flow system

The GDH-PSSA-CPE showed the most promising results for the application in the flow system. Thus, the use of these electrodes for the determination of Dop was studied intensively. In these experiments a constant potential of 400 mV was applied. HBS100 was used as the carrier buffer and for sample dilution. The flow was set to 0.5 mL/min and the injection volume was maintained constant at 250 µL.

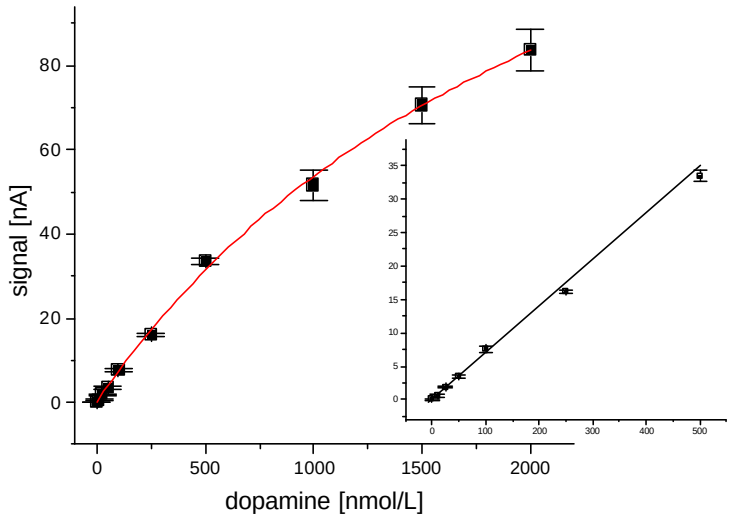

Figure 4.14: Concentration dependence of enzyme amplified determination of Dop with GDH-PSSA-CPE. Flow rate was set to 0.5 mL/min and the injection volume was 250 µL. For the general experimental conditions refer to **Fig. 4.13**.

The LLD of GDH-PSSA-CPE for Dop was 10 nmol/L and the linear range was between 10 and 500 nmol/L. The standard deviation arising from consecutive injections within the linear range was <4.3 % [n = 3]. Under the optimized flow conditions for Dop the electrodes were tested with other analytes and the results are presented in **Tab. 4.5**.

Table 4.5: *Characteristics of the GDH-PSSA-CPE in the flow system. For the general experimental conditions refer to Fig. 4.14.*

Compound	LLD [nmol/L]	Linear range [nmol/L]	Amplification factor[1]	Response time for 100 nmol/L [s]	Cycle time [min]
Dop	10	10-500	65	30	4
4AP	2	2-300	140	20	3
HQ	25	25-500	40	> 30 [3]	4
BQ	25	25-500	n.d.[2]	> 30 [3]	4

1 The amplification factor was calculated by dividing the current obtained in the presence of glucose by the current obtained in the absence of glucose.
2 The amplification factor for BQ can not be determined since it is already oxidized and thus gives no signal in the absence of glucose.
3 250 µL were not sufficient to reach the steady state current for these analytes under the given conditions.

As shown in **Tab. 4.5** the GDH-PSSA-CPE allow the quantification of phenolic compounds in the lower nanomolar range. The flow system was optimized for the detection of Dop and the results obtained for HQ and BQ could be improved by using higher sample volume or by modifying the flow conditions.

Fig. 4.15 shows the reproducibility of the PSSA-CPE in the flow system. The preparation of different electrodes with the same carbon paste led to variations in the response for Dop that were comparable with the results described for the PEI-CPE in the stirred cell. The repeatability of the single injections increased slightly.

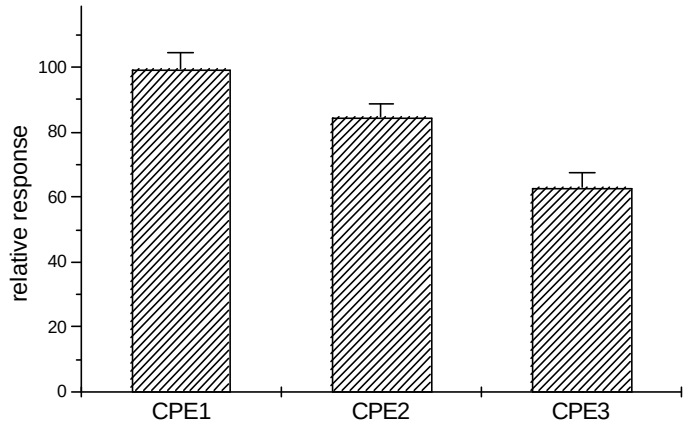

Figure 4.15: Reproducibility of different GDH-PSSA-CPE prepared from one paste tested in the flow system with injections of 100 nmol/L Dop.

However, the large difference caused by the complex manual sensor preparation makes the CPE not suitable for the manufacturing of a high number of standardized biosensors. An equilibration time of 2 h for these electrodes still remains too long for customers to accept, even though the adoption of the PSSA-CPE produced a significant improvement compared with 10 h needed with PEI-CPE. Thus, other basic transducers were tested for the preparation of a GDH-biosensor.

4.1.2.3 Summary of results obtained with GDH carbon paste electrodes

Based on previous work GDH carbon paste electrodes were prepared with PEI as polyelectrolyte. These electrodes were characterized in a stationary and a flow injection system to obtain information such as equilibration time, oxidation potential, pH dependency, response behavior to various analytes and reproducibility of sensor preparation.

The electrodes showed high sensitivity with LLDs in the lower nanomolar range in the stationary system. Obvious drawbacks were found concerning long equilibration times and reproducibility of the manufacturing process. Moreover, the experiments in the flow system showed that the response of the GDH-PEI-CPE was very slow and thus not applicable in practice. Subsequently, the modification of the carbon paste composition was tested. The application of the more negatively charged PSSA shortened the equilibration time from 10 to 2 h and led to better reproducibility of sensor preparation. Also, the response behavior was improved for Dop. The experiments showed a dependence of the response behavior towards the analyte from the composition of the carbon paste, and the charge of the electrode surface. For Dop (more hydrophilic) the influence of the negatively charged PSSA was positive while for the determination of hydroquinone (more hydrophobic) the PEI-CPE showed faster response. This observation will be taken into an account during further immobilization experiments.

With the use of GDH-PSSA-CPE Dop and 4AP were determined in the flow system within 4 and 3 min, respectively, per sample. The LLDs 10 and 2 nmol/L combined with a linear range up to 500 and 300 nmol/L.

Nevertheless, the optimization of the GDH-CPE composition and the flow system did not lead to an acceptable reproducibility of the GDH-biosensor preparation.

4.1.3 GDH adsorbed on spectroscopic graphite

After adsorption of the GDH over night the electrode was mounted in the wall-jet flow cell and integrated in the flow injection system. The electrode was polarized at constant potential of 400 mV vs. Ag/AgCl. Then, HBS100 without glucose was pumped through the cell with a flow rate of 0.5 mL/min. After 15 min a constant background current of 12.3 nA was measured. Dop at a concentration of 1 µmol/L was injected resulting in an oxidation current of 5.3 nA. To determine the amplification factor, 10 mmol/L glucose was added to the buffer. No increasing background current was observed after 5 min stabilization. Again 1 µmol/L Dop was injected. The same peak height was recorded corresponding to a signal of 5.3 nA. These experiments show that no enzymatic amplification occurred with the applied immobilization technique.

In contrast to CDH as biorecognition element, GDH cannot be simply absorbed on solid graphite using the described procedure. The GDH is poorly adsorbed or can easily be removed from the electrode's surface when the biosensor is placed into the measuring cell.

4.1.4 GDH adsorbed on screen-printed carbon electrodes (GDH-SPCE)

Screen-printed carbon electrodes from Cambridge Life Science (CLS-SPCE) were used as basic transducers for the preparation of GDH-biosensors by simply adsorbing the enzyme on top of the working electrode. The experiments were performed in the stirred measuring cell with GDH-modified SPCE in HBS100. The equilibration time before the measurement was kept to 45 to 60 min after the electrode was poised at 400 mV. No glucose was present during these experiments.

The data presented in **Fig. 4.16** demonstrates that 4AP is much more easily oxidized than Dop or hydroquinone. Nevertheless, a potential of 400 mV is sufficient for the oxidation of all three analytes and was used for the experiments during characterization of the system. HBS100 was used as the working buffer.

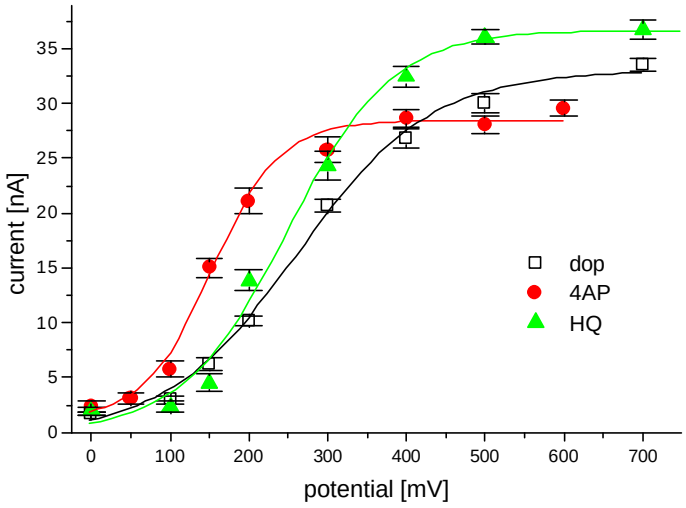

Figure 4.16: Hydrodynamic voltamograms for Dop, *4*-aminophenol, and hydroquinone (all 2.5 µmol/L) obtained with GDH-SPCE in the absence of glucose. Measurements were performed in the batch system with HBS100.

The addition of 10 mmol/L glucose led to an increased background current, which reached a stable value within 5 min. The characteristics of the biosensor for analyzing HQ, BQ, Dop, and 4AP were determined.

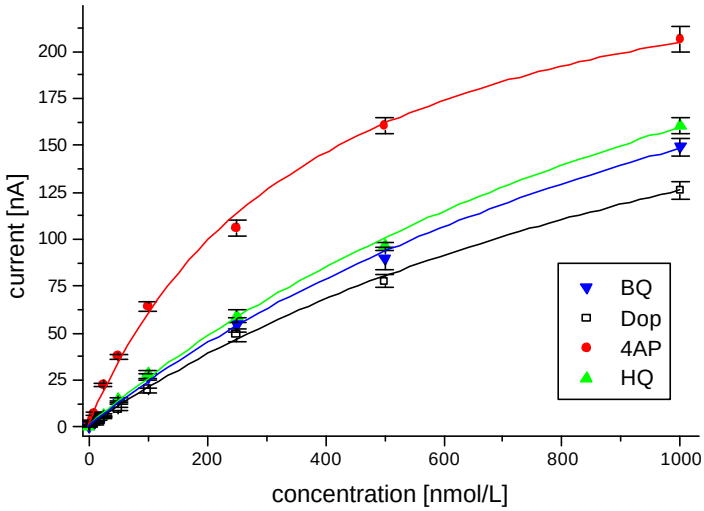

Figure 4.17: Concentration dependence of 4 substrates on GDH-SPCE in stirred measuring cell. The applied potential was 400 mV and 10 mmol/L glucose were present. For other conditions refer to **Fig. 4.16**.

As shown in **Fig. 4.17** the GDH-SPCE could be used to quantify the 4 different phenolic compounds. The highest sensitivity was found for 4AP (600 nA·L/µmol), while Dop was detected worst (190 nA·L/µmol). The data are shown in **Tab. 4.6**.

Table 4.6: *Characteristics of the GDH-SPCE in the stirred batch system on the first day of use. For experimental conditions refer to Fig. 4.16.*

Compound	LLD [nmol/L]	Sensitivity [nA·L/µmol]	Linear range [nmol/L]	Amplification factor[1]	Response time for 100 nmol/L [s]	Cycle time [min]
Dop	15	190	10-250	30	30	4
4AP	1.5	600	1.5-100	90	15	2
HQ	10	280	5-200	25	20	3
BQ	10	270	5-200	n.d.[2]	20	3

[1] The amplification factor was calculated by dividing the current obtained in the presence of glucose by the current obtained in the absence of glucose.
[2] The amplification factor for BQ cannot be determined since it is already oxidized and thus gives no signal in the absence of glucose.

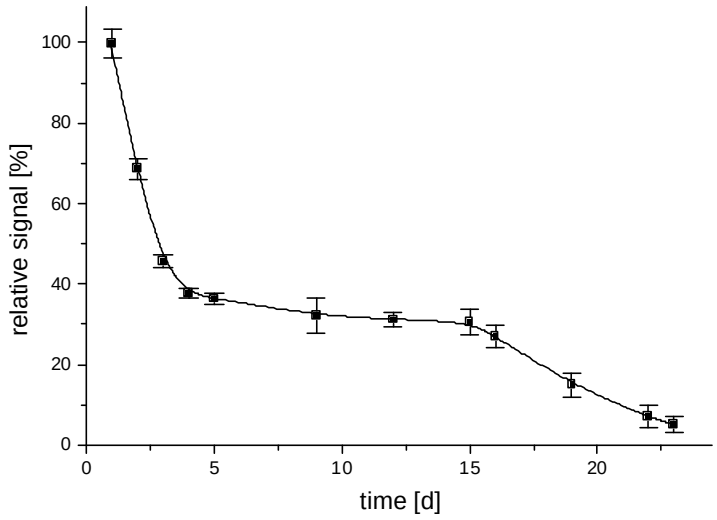

Figure 4.18: Stability of the GDH-SPCE tested with 100 nmol/L Dop in the batch system. For experimental conditions refer to **Fig. 4.17**.

As visualized in **Fig. 4.18**, the response of the GDH-SPCE towards Dop decreased rapidly in the first days of use. After 4 days the activity stabilized at 35 % of the initial value. After 15 days a further reduction was observed and the last values are equal to the values expected for non-amplified detection of Dop. The loss of GDH activity was emphasized by decreasing amplification factors determined during that period (data not presented).

4.1.4.1 Summary of results obtained with GDH screen-printed carbon electrodes

The GDH-SPCE were tested only in a batch system. The equilibration time before the first measurement was shorter (only 5 min) than found with the carbon paste electrodes, but the LLD for Dop (15 nmol/L) was worse. The ease of preparation was an obvious advantage, but the resulting stability was not satisfying.

4.1.5 GDH immobilized on platinum based thick-film electrodes (GDH-TFE)

The immobilization of GDH on carbon based electrodes showed many disadvantages, especially for the application in flow systems. Therefore another type of transducers based on a platinum working electrode and a Ag/AgCl counter/reference electrode was tested.

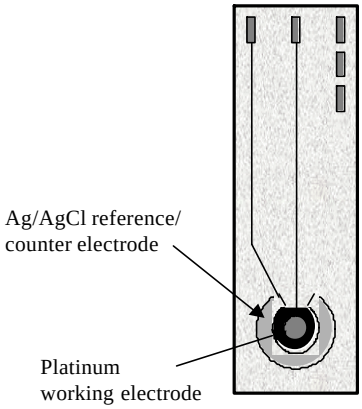

Figure 4.19: Schematic drawing of the platinum based thick-film transducer

The properties of the GDH-modified TFE were tested first in the batch system. For this characterization Dop and 4AP were used as model analytes.

4.1.5.1 Optimization of the electrodes and the measuring system

The GDH was mixed with polyurethane and this mixture was immobilized on the working electrode. At the day of use the GDH-biosensor was mounted into the measuring cell and a constant potential was applied.

The modified electrodes showed a stable baseline in glucose free buffer solution after 10 to 30 min, depending on the thickness of the polymeric layer. The equilibration of the system occurred because of swelling of the polymer layer and rinsing of loosely bound enzyme and PQQ. This stabilization time decreased to approximately 5 min after several days of use of the sensor. This short equilibration time was a substantial progress in contrast to the equilibration times needed for the CPE described in the previous sections. Particularly with regard to final application in the laboratory or even on-site measurements these short times are essential for the customer.

After a stable baseline was reached, 10 µL of a 100-fold concentrated Dop solution was inserted into the cell with 990 µL of the buffer. Intensive stirring led to fast mixing and rapid dilution to the final concentration. A concentration of 250 nmol/L Dop in the cell resulted in immediate response and the steady state current was reached within less than 30 s.

After intensive washing of the system 10 mmol/L glucose were added and an increased steady state was reached within less than 5 min. This higher background can be explained by glucose oxidation in presence of the PQQ. Wen et al. demonstrated that PQQ could act as mediator between GDH an electrode surface (Wen, Wollenberger et al. 1998). The glucose-amplified measurements were performed when the stable background in presence of glucose was reached. This two-step procedure was applied only for describing the equilibration behavior of the sensor. In the usual procedure, the measuring cell was directly flushed and filled with the working buffer containing 10 mmol/L glucose. Thus the second equilibration step was eliminated. In this case the analyte injection resulted in steady state response within less than 90 s.

4.1.5.1.1 Influence of enzyme immobilization

The concentration of the polymer was varied while the amount of GDH used for membrane preparation was kept constant. The influence of these parameters on Dop determination was studied in the batch as well as in the flow mode. The peak shape and height was depending on the polymer concentration used for immobilization (**Tab. 4.7**).

Table 4.7: *Sensor characteristics in dependence of polymer/enzyme ratio for injections of Dop*

Polymer/ Enzyme dilution	Immobilized Volume [µL]	Response time [s]		Sensitivity [nA·L/µmol]	
		Flow [0.5 mL/min]	Batch [V = 1 mL]	Flow [0.5 mL/min]	Batch [V = 1 mL]
a.) 1:1	4	90	55	20	45
b.) 1:5	4	12	10	50	85
c.) 1:5	2	30	30	30	55
d.) 1:10	4	15	20	35	70

Using the polymer solution with the highest concentration, lowest sensitivity for Dop was obtained. Additionally, a peak broadening was observed. The diffusional resistance mainly caused such poor response of the electrode. Reducing the polyurethane content led to a thinner polymer layer (type b) with the same enzyme loading per cm^2. The response time decreased and the sensitivity was enhanced. In this case, the higher permeability leads to faster recycling of the redox-active analyte and therefore to a higher efficiency of the amplification process.

Peak broadening was acceptably small for this type of modified electrodes. Decreasing the immobilized volume (**Tab. 4.7**) of the identical polymer/enzyme mixture used in type b led to lower sensitivity. This can be explained by the smaller amount of the enzyme. The same effect was observed with more diluted polyurethane solution before immobilizing on the thick-film electrode. This also resulted in lower sensitivity.

The influence of the PQQ during enzyme immobilization was investigated using types a, b, and c as mentioned in **Tab. 4.7**. Electrodes prepared in the presence of PQQ during embedding of the enzyme showed slightly higher sensitivity.

Sensor b prepared with PQQ produced the best performance with respect to response time and sensitivity towards Dop for both measuring devices and was therefore chosen for further investigation.

4.1.5.1.2 Optimization of the buffer system

For the optimization HEPES, TRIS, MOPS, Davis, and phosphate buffer were used in a pH range between 5.5 and 8.5. The results for the response towards Dop are presented in **Fig. 4.20**. Highest sensitivity was obtained in HEPES (pH 7,5) and Davis (pH 8,0) buffer. In Davis as well as in phosphate buffer calcium precipitation occurred. Since the binding of PQQ to GDH is improved in the presence of calcium ions, its precipitation can possibly lead to a loss of long term working stability.

Therefore the HEPES buffer of pH 7,5 was chosen for further characterization of the sensor system. In **Fig. 4.20** the buffer and KCl concentration was varied. Maximum response was obtained when using a 20 mM HEPES solution containing 20 mM potassium chloride. A sensitivity decrease of about 50 % was observed at a concentration of 200 mM of each compound.

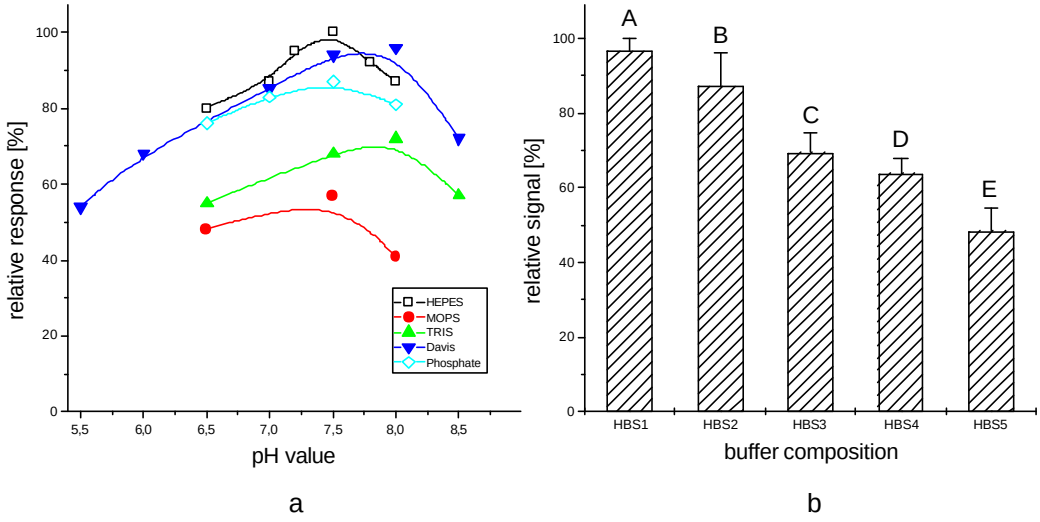

Figure 4.20: pH dependence of the GDH/PQQ modified electrodes in different buffer systems (a) and influence of the HEPES buffer composition (b) for 100 mmol/L Dop. The differences in the HEPES buffer were the following: A-C 20 mM HEPES with 20, 100 or 200 mmol/L KCl, D 100 mmol/L HEPES/KCl and E 200 mmol/L HEPES/KCl. All buffer solutions contained 1 mmol/L $CaCl_2$ and 10 mmol/L glucose

For further investigations 20 mmol/L HEPES buffer pH 7.5 containing 20 mmol/L potassium chloride, 1 mmol/L calcium chloride, from now on referred as HBS20, and 10 mmol/L glucose was chosen.

4.1.5.1.3 Flow rate and injection volume

Fig. 4.21 shows the influence of the flow rate on the sensor response in case of the Dop concentration of 100 nmol/L. For these experiments a defined volume was injected using a loop of 125 µL.

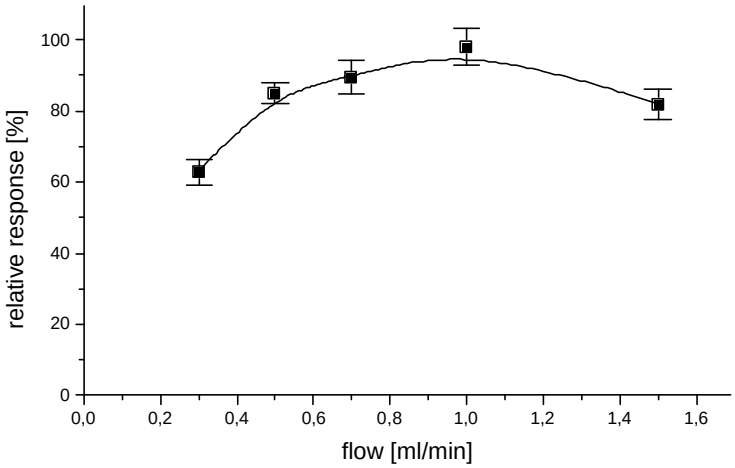

Figure 4.21: Influence of the flow rate for repeated injections of 100 nmol/L Dop using a defined injection loop of 125 µL, HBS20 with 10 mmol/L glucose as the carrier, and an applied voltage of 400 mV. The signal at a flow of 1 mL/min was set to 100 %

At small flow rates the peaks showed pronounced tailing. Increasing the flow rate led to a higher signal and sharper peak profiles. The relative response vs. the flow rate flattened out at values above 0.5 mL/min while further enhancement of the flow rate leads to a lower repeatability.

The coefficient of variation at 0.5 mL/min is 2.86 % (n = 5), while it is 4.8 and 5.3 % at flows of 0.7 and 1 mL/min respectively. At 1.5 mL/min the steady state current and the maximum peak height cannot be reached without increasing the injection volume to achieve a longer contact time at the electrode. A flow rate of 0.5 mL/min was chosen as a compromise between fast response time and narrow peak shape on the one hand and the repeatability of the signal on the other.

Using this flow rate and taking into account a response time of 12 s an injection volume of 100 µL was assumed to be sufficient for reaching the maximum response. A volume of 50 µL gives a signal of about 87 % of the maximum. The steady state is reached for a volume of 100 µL during one injection of 100 nmol/L Dop. Increasing the volume up to 500 µL did not further improve the sensitivity. For the time-controlled injections the valve was switched to "inject" position for 15 s. At a flow rate of 0.5 mL/min this results in a volume of 125 µL. This gives a safety margin of 25 µL. In this way a steady-state current is obtained over the whole dynamic range of the sensor.

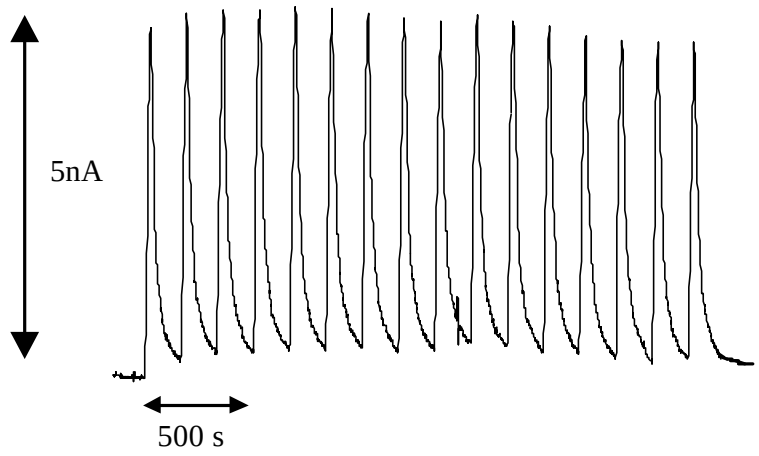

Figure 4.22: Flow injection measurements on GDH/PQQ modified thick-film electrodes of 100 nmol/L Dop in flow-through set-up using a flow of 0.5 mL/min with time dependent injection using Eppendorf EVA-injector. Injection time is 15 s. For other experimental conditions refer to **Fig. 4.21**.

Fig 4.22 shows the sensor response for Dop concentration of 100 nmol/L using the optimized flow system with automatic time based injection. One measurement is performed in 150 s and thus up to 24 injections per hour could be realized. Using a flow rate of 0.5 mL/min and an injection volume of 125 µL the repeatability was calculated using either peak height or area. Taking the 16 injections from figure 5 the coefficients of variation with 3.34 % for the peak height and 3.95 % for the area were calculated, while no obvious decrease of the peak height was observed.

4.1.5.2 Results obtained with GDH-TFE under optimized conditions

4.1.5.2.1 Operational stability

The stability of the electrodes was tested with repetitive injections of Dop. Over a period of 8-10 hours 100 nmol/L Dop could be measured without any loss of sensitivity at the third day of use (**Fig. 4.23**).

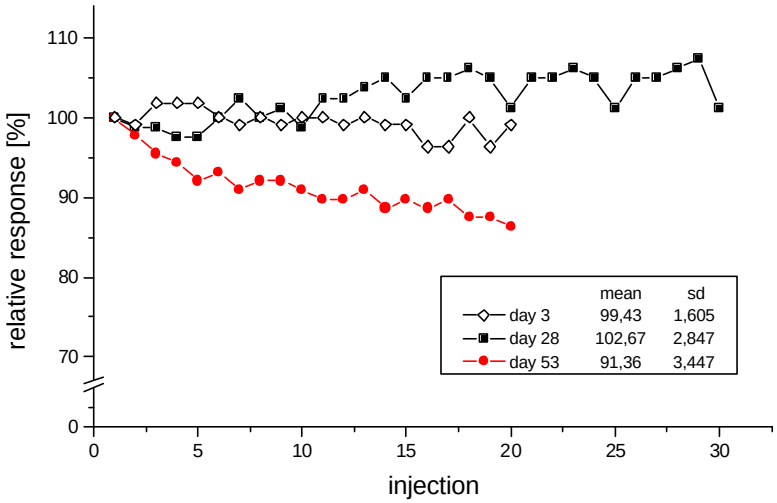

Figure 4.23: Comparison of the repeatability for thick-film electrode type b.) at different lifetimes. Repeated injections of 100 nmol/L Dop were performed in flow-through set-up. For experimental conditions refer to **Fig. 4.22.**

After 4 weeks still no change was visible and the electrode was used over a period of 8 h without any loss of sensitivity. Sensitivity slightly changed when measuring at the end of the sensor's lifetime. For example on day 53 a decrease to 86 % after 20 injections performed within 5 h was visible. The long-term stability was found to be up to 60 d (**Fig. 4.24**). During operation the sensors were kept at room temperature, while over night the electrodes were stored at 4°C in the refrigerator. For storage, the glucose in the buffer solution was replaced by 100 nmol/L PQQ for enzyme stabilization. Wrapped electrodes can be kept in a fridge for more than half a year without recognizable loss in sensitivity or changes in other characteristical parameters.

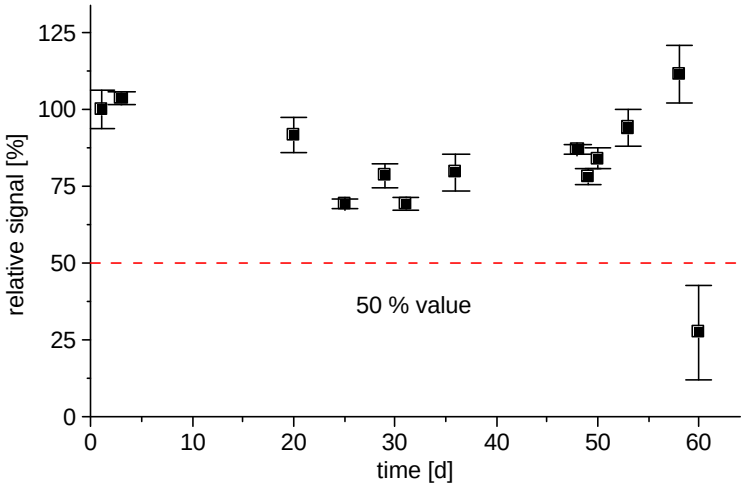

Figure 4.24: Operational stability of GDH/PQQ modified thick-film electrode type b.) Relative signal towards 100 nmol/L Dop obtained in flow-through set-up. For experimental conditions refer to **Fig. 4.22.**

Table 4.8: *Comparison of the stability with biosensor systems for phenolic compounds found in literature*

Biosensor system	Stability [d]	LLD [nmol/L]	Reference
GDH-TFE	> 60	1.3 (Dop)	(Rose, Pfeiffer et al. 2001)
Laccase SPE GDH SPE	14 24	50 (Dop) 2 (Dop)	(Lisdat, Ho et al. 1998)
Laccase/GDH membrane	4	0.2 (adrenaline)	(Szeponik, Möller et al. 1997)
Tyr/GDH membrane	7	0.6 (catechol)	(Makower, Eremenko et al. 1996)
GDH glassy carbon GDH microelectrodes	14-18 17	50 (Dop) 1 (Dop)	(Lisdat, Wollenberger et al. 1998)

As outlined by the data in **Tab. 4.8** the GDH-TFE biosensor offers a much higher operational stability compared with other systems containing GDH as biorecognition element, while the sensitivity and LLD are in the same range as found in literature.

4.1.5.2.2 Substrate spectra of the GDH-TFE

GDH is known for its sensitivity to a broad range of electron acceptors. The electrodes were tested on various phenolic substances which are either themselves analytes of interest or are generated in enzymatic indicator reactions for example in an immunoassay.

In **Tab. 4.9** the sensitivities for different phenolic compounds are listed.

Table 4.9: *Sensitivity and detection limits for phenolic compounds obtained in optimized flow through set-up. For experimental conditions refer to Fig. 4.22.*

Substrate	Sensitivity [nA·L/µmol]	Detection limit [nmol/L]	Substrate	Sensitivity [nA·L/µmol]	Detection limit [nmol/L]
***4*-aminophenol**	90	0.7	**Methylcatechol**	3.5	30
Dop	48	1.3	**Nitrocatechol**	2	45
Hydroquinone	40	2.5	***2,5*-dihydroxy-phenyl-acetic acid**	1.5	n.d
Benzoquinone	40	2.5	***3,4*-dihydroxy-phenyl-acetic acid**	0.9	n.d.
Catechol	15	7			

n.d. not determined

The highest response was observed for *4*-aminophenol, which is about two times higher than for Dop. This is in agreement with data obtained from previous work regarding both GDH-based bienzymatic and bioelectrocatalytic systems. Comparing the results for *4*-benzoquinone and hydroquinone no influence from the oxidation state is observed. This means that for the described sensor assembly the catalytic cycle can start with the enzymatic reduction of *4*-benzoquinone as well as with the electrochemical oxidation of hydroquinone at the surface of the electrode. The sensitivity for catechol (*1,2*-bezene-diol) is smaller than that for hydroquinone (*1,4*-benzene-diol) demonstrating that the position of the substitution influences the enzymatic conversion of the compound and therefore its electrochemical detection. This is also observed when comparing *2,5*- and *3,4*-dihydroxy-phenyl-acetic acid. The analyte with the two hydroxy groups arranged in *para* position shows almost twice the response intensity.

The carboxylic group in the side chain results in a drastic loss of sensitivity compared with Dop, which has a free amino group. This may be mainly due to its impaired ability to permeate the polymer layer.

One point confirming this assumption is the shape of the peaks, which shows pronounced broadening. But also the specificity of the enzyme and the differences in the electrochemical behavior should be taken into account. Examining the results of three catechols the influence of different substituents can also be seen, whereas *4*-nitrocatechol is measured with the lowest sensitivity followed by *4*-methyl- and unsubstituted catechol.

In **Fig. 4.25** four different substrates were compared showing all a linear range in the response between 10 nmol/L and 1 µmol/L (500 nM for 4AP) while the differences in sensitivity are obvious. These results are comparable with lower limits of detection found in the literature using bioelectrocatalytic or bienzymatic amplification. Bioelectrocatalytic amplification in stirred cells yielded detection limits for hydroquinone and *4*-aminophenol in the low and subnanomolar range. Since the biosensor developed in this work is optimized for Dop detection a closer look to the literature regarding the detection of this analyte is opportune.

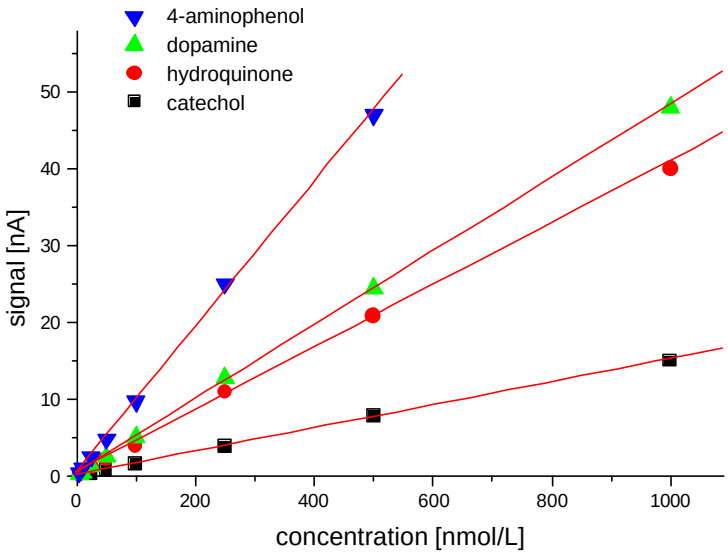

Figure 4.25: Concentration dependence on GDH-TFE-biosensor. For experimental conditions refer to **Fig. 4.22.**

Lisdat et al. reported a LLD of 1 nmol/L Dop using GDH on platinized microelectrodes, while Lindgren et al. obtained a LLD of 2.5 nmol/L Dop in flow systems with cellobiose dehydrogenase modified solid graphite electrodes (Lindgren, Stoica et al. 1999; Lisdat, Wollenberger et al. 1998). Integrating GDH in carbon paste electrodes leads to a LLD for Dop of 5 nmol/L in a stirred measuring device (Wollenberger and Neumann 1997). Using tyrosinase modified electrodes detection limits in the low nanomolar range for catechol were reported (Nistor, Emnéus et al. 1999; Önnerfjord, Emnéus et al. 1995). For bienzymatic systems using GDH in combination with tyrosinase or laccase, the lower detection limits are in the subnanomolar concentration range (Bauer, Eremenko et al. 1998; Ghindilis, Makower et al. 1995; Makower, Eremenko et al. 1996). Other biosensor systems are listed in **Tab. 4.10.**

Table 4.10: *Biosensors for determination of phenolic compounds*

Enzyme/Sensor	LLD [nM]	Cycle/response time [s]	Flow – batch	Reference
GDH/TFE	1.3 Dop	15 (r.t.)/150 (c.t.)	Flow	(Rose, Pfeiffer et al. 2001)
Tyr/SPCE	0.5 Dop	60 (r.t.)	Batch	(Yi-Feng and Hong-Yuan 2002)
Tyr/SPCE	25 cat	60 (c.t.)	Flow	(Cummings, Linquette-Mailley et al. 2001)
MT-Tyr/GDH PVA membrane	25 Dop/ 0.6 cat	120 (r.t.)	Batch	(Streffer, Vijgenboom et al. 2000)
SA-Tyr/GDH PVA membrane	15 Dop 10 catechol	120 (r.t.)	Batch	
Thermostable phenol hydroxylase/SGCE	4000 cat	10 (r.t.)	Batch	(Metzger, Reiss et al. 1998)
Coconut plant tissue/GC	2000 cat	60 (c.t.)	Flow	(Lima, Nascimento et al. 1997)
Lac/GDH PVA membrane	0.2 adr	300 (c.t.)/120 (r.t.) 1200 (c.t.)	Flow Batch	(Szeponik, Möller et al. 1997)
Tyr/GC	2400 Dop 4100 cat	90 (r.t.)	Batch	(Rodriguez and Rovas 2002)
Lac/GC	10 Dop	110 (r.t.)	Batch	(Lisdat, Wollenberger et al. 1997)
GDH/GC	1 nor		Batch	
Tyr/GDH	25 Dop	100 (r.t.)	Batch/Flow	
Lac/GDH	n.k.	60 (r.t.) 300 (c.t.)	Batch/Flow	
GOD/GC	1 HQ	500	Batch	(Mizutani, Yabuki et al. 1991)
CDH/SGE	2.5 Dop	120	Flow	(Lindgren, Stoica et al. 1999)
Tyr/SGE	15 cat	100 (c.t.)	Flow	(Nistor, Emnéus et al. 1999)
Tyr/GDH	0.6 cat	240	Batch	(Makower, Eremenko et al. 1996)
Tyr-polymer thick film	0.25 phe	150	Batch	(Kotte, Gründig et al. 1995)
Lac/SPCE	50 nM Dop	10 (r.t.)	Batch	(Lisdat, Ho et al. 1998)
GDH/SPCE	2 nM Dop	15 (r.t.)	Batch	

r.t. response time; c.t. cycle time; GC: glassy carbon; SPCE: screen printed carbon electrode; SGE: solid graphite electrode; SGCE: Sol-gel Clark-type electrode; PVA: polyvinyl alcohol; Tyr: tyrosinase; HRP: horse radish peroxidases; Lac: laccase; CDH: cellobiose dehydrogenase; GOD: glucose oxidase; M: mushroom; SA: *streptomyces antibioticus*; adr: adrenaline; nor: noradrenaline; HQ: hydroquinone; phe: phenol; cat: catechol;

In **Tab. 4.10** the detection limits for various biosensor systems towards phenolic compounds are listed. Additionally, the response behavior and information of the system (flow or batch) are shown. The comparison with the GDH-biosensor developed in this thesis shows that very short analysis times were combined with excellent LLDs. In literature the more sensitive biosensors mainly work in batch systems and their response and/or cycle times are rather long. Their application in automated flow systems is difficult. Biosensors applied in flow-systems lack in sensitivity or the cycle times increased drastically in comparison with experiments in the batch mode. Our newly developed GDH-biosensor nicely combines both and additionally offers an excellent stability as shown before. This makes the sensor a promising tool for a wide range of analytical application.

A comparison between Dop, adrenaline, and noradrenaline is given in Tab. **4.11**. The measuring range shows linearity over 3 orders of magnitude. This agrees with data from literature where catecholamine detection was the main target. L-dopa shows a sensitivity of about 10 % leading to a LLD of 22 nmol/L and a decreased linear range.

Table 4.11: *Sensitivity for catecholamines obtained in flow through set-up. For experimental conditions refer to Fig. 4.22.*

Substrate	Relative Sensitivity [%]	Lower detection limit [nmol/L]	Measuring range [nmol/L]
Dop	100	1.3	1.3-2000
Noradrenaline	81.3	2.1	2.1-2000
L-adrenaline	91.7	1.6	1.6-2000
L-dopa	9.8	22	22-1000

4.1.5.2.3 Amplification for aminophenols and Dop in stirred device

The enzymatic amplification for *ortho*-, *meta*- and *para*-substituted aminophenol and Dop was examined more in details.

For these experiments in a stirred measuring cell the analytes were first tested with the GDH-biosensor in the absence of glucose and the sensitivity was calculated from the resulting current vs. concentration plots. The measurements were repeated in the presence of glucose and the amplification factors were calculated by dividing of the two values. The applied potential was set to 400 mV in all cases.

Table 4.12: *Sensitivity and amplification factors for Dop and the three isomers of aminophenol.*

	Sensitivity [nA·L/µmol]		Amplification factor
	in absence of glucose	in presence of glucose	
Dop	3.1	85	27.4
2AP	2.9	241	83.1
3AP	0.03	0.03	n.d.
4AP	2.9	340	117.4

n.d. not determined

The results obtained for the three isomers of aminophenol show that 4AP leads to the highest sensitivity and the best amplification factor. 3AP was not oxidized at the electrode with an applied potential of 400 mV. Thus, no amplification factor could be determined. 3AP is not suitable for further experiments. The results gained for 2AP shows a high amplification, which however is still significantly smaller than that for 4AP. 4AP will be chosen as GDH substrate when using the sensor as label detector in flow immunoassays.

Dop was amplified worst leading to the lowest sensitivity in presence of glucose. This emphasizes that 2AP and 4AP are better substrates for the GDH than Dop.

4.1.5.2.4 Precision

The screen-printing for the preparation of basic transducers is well established for mass production. This technique allows the preparation of basic transducers without big parameter fluctuations. The immobilization of the enzyme is the crucial step in the biosensor fabrication. In **Fig. 4.25a** the response of three different sensors of one batch towards Dop is illustrated.

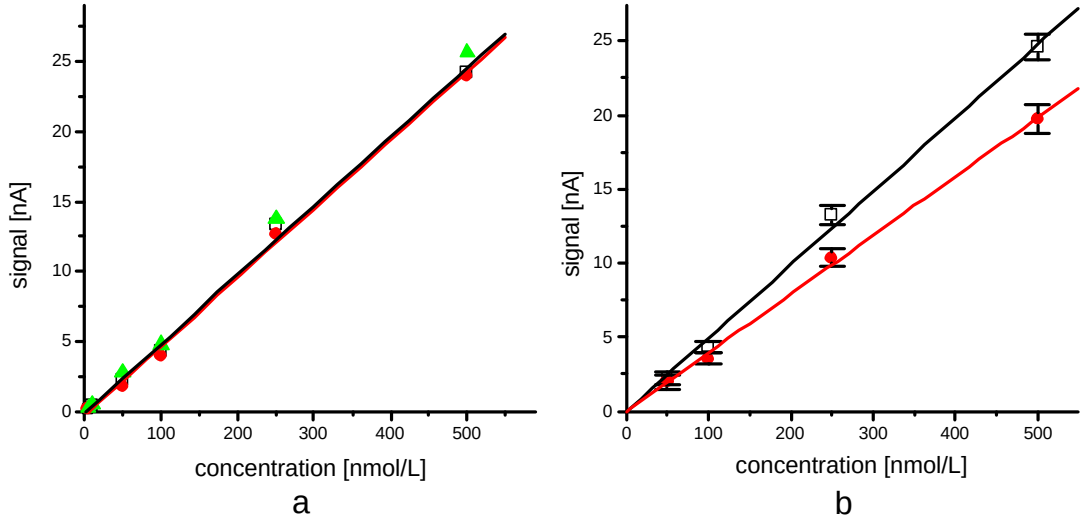

Figure 4.25: Comparison of oxidation currents obtained for Dop on GDH-TFE-biosensors. a.) Three different biosensors of the same batch (same enzyme /PU solution. produced at the same day) and b.) Two different batches (each with three electrodes produced the same day) were compared. The second batch was produced five month later than the first one. For experimental conditions refer to **Fig. 4.22**.

The sensors of the same batch were prepared the same day using one GDH-polyurethane mixture. In the concentration range for Dop between 10 nmol/L and 500 nmol/L the electrodes differ only slightly. Fitting the data with linear regression leads to sensitivities of 49.03, 50.71, and 52.5 nA·L/µmol Dop. The errors in the sensitivity are between 0.96 and 1.42 nA·L/µmol for the different sensors. The standard deviation of the fit showing the differences between the calculated Y-value and the measured Y-value over the range of the fit is between 0.4 and 0.6 nA.

The working linear range is equal and the differences in sensitivity and the limit of detection are remarkable small. Sensors of two different batches (type b) were compared in **Fig. 4.25b**. For each batch 3 sensors were taken for comparison. Means for various concentrations (50-500 nmol/L Dop) and their standard deviation were plotted and a linear regression was calculated leading to sensitivities of 50.66 ± 2.25 and 40.53 ± 1.74 nA·L/µmol.

The standard deviation of the fit is 1.33 nA and 0.79 nA respectively, showing a good correlation between the calculated values and the measured currents. Good linearity, high sensitivity and very small changes in the sensor parameters (e.g. response behavior, stability) were observed for both batches.

4.1.5.3 Summary of results obtained during GDH-TFE-biosensor development

GDH was successfully embedded into the polyurethane network on top of the platinum based TFE. It was shown that this is a simple and very reproducible manufacturing process to obtain a large number of biosensors with excellent characteristics. The experimental know-how gained during the immobilization of GDH on CPE facilitated the composition of the polyurethane solution. This resulted in an excellent long term and working stability of the GDH-TFE. Additionally a short equilibration time before the first measurement was achieved. This represents a great improvement compared with other immobilization techniques.

Furthermore the optimization of the polymer layer led to fast responding sensors applicable for the use in flow injection analysis. In the optimized semi-automated flow system up to 200 samples per day-shift can be analyzed.

The sensitivity towards various phenolic compounds was extremely good. Detection limits in the low nanomolar and subnanomolar range (for 4AP) combined with an extended linear range (three orders of magnitude for catecholamines) were obtained.

In summary, the properties of the GDH-TFE-biosensors reflect the very successful attempt to develop a fast and reliable detection system for phenolic compounds of various origins. Applications in automated flow-systems as well as for screening purposes in on-site analysis are conceivable. Moreover, the high sensitivity towards 4AP makes the GDH-TFE a promising tool as a detector in enzyme-labeled immunoassays.

The applicability of these electrodes was investigated and is presented in the following chapters.

4.1.5.4 Application of GDH-TFE-biosensor

4.1.5.4.1 Analysis of phenol mixtures

Enzyme biosensors only provide limited information about the analyzed sample. The concentration is related to one standard compound (i.e. equivalents of the calibration standard) and no information about single components is usually obtained.

Table 4.13: *Concentration of the different solutions tested*

	Phenol [mg/L]	***4*-CP [mg/L]**	***4*-Cresol [mg/L]**	**Catechol [mg/L]**		**Phenol [mg/L]**	***4*-CP [mg/L]**	***4*-Cresol [mg/L]**	**Catechol [mg/L]**
S1	3.5	0.525	0.7	0.875	**S6**	3.5	0.525	0.7	0.875
1	7	0.6	1	0	**26**	5	0.45	1.2	0.5
2	4	0.3	0.8	0.5	**27**	0	0.75	1.2	1
3	7	0.45	0.4	0.75	**28**	5	0.15	1.4	1.25
4	2	0.15	1.4	1.75	**29**	0	0.9	0.2	1.5
5	1	0	0	1.5	**30**	3	0.75	0.6	0.25
S2	3.5	0.525	0.7	0.875	**S7**	3.5	0.525	0.7	0.875
6	7	0.75	0	0.5	**31**	5	0.45	1	0.25
7	0	0.45	1.2	0.75	**32**	6	0.75	1.2	1
8	4	1.05	1.2	025	**33**	1	0.9	0.2	1.5
9	5	0.3	0,8	1.5	**34**	0	0.15	0.6	0
10	1	0.3	1.4	0	**35**	2	1.05	0.4	1.25
S3	3.5	0.525	0.7	0.875	**S8**	3.5	0.525	0.7	0.875
11	3	0.3	0.2	1.75	**36**	3	0	1	0
12	4	0.15	0.8	0.5	**37**	6	1.05	0.2	1.75
13	1	0.6	0.4	1	**38**	6	0.6	0.6	0.25
14	2	1.05	0.6	1.25	**39**	0	0	1	0
15	2	1.05	0.4	0	**40**	7	0.3	1.2	1
S4	3.5	0.525	0.7	0.875	**S9**	3.5	0.525	0.7	0.875
16	5	0.9	1	1.75	**41**	7	0.6	0.6	0.5
17	0	0	1.4	1.25	**42**	1	1.05	0.2	1.5
18	6	0.6	0.6	0.5	**43**	6	0.6	0.8	0.25
19	3	0.9	0.2	1	**44**	3	0.75	0.4	1.25
20	4	0	0	1.75	**45**	4	0	1.4	1.5
S5	3.5	0.525	0.7	0.875	**S10**	3.5	0.525	0.7	0.875
21	3	0.9	0	1.25	**46**	4	0.15	0.4	0.75
22	5	0.75	0	1.75	**47**	2	0.15	0.8	0.75
23	6	0.3	1	0.75	**48**	7	0.9	0.8	0.75
24	2	0.45	1.4	0.25	**S11**	3.5	0.525	0.7	0.875
25	1	0.45	0	1					

S1-11: Injection of the solution used for stability testing of the GDH-biosensor

This approach was based on the idea to determine the composition of an unknown sample based on additional analysis of the peak shape. The GDH-biosensor was tested using a mixture of four phenolic compounds of environmental interest, phenol, *p*-chlorophenol, cresol, and catechol. A comparison with similar measurement using different enzymes for biorecognition is the first step towards the design of a sensor array, which could finally lead to a chemometric approach.

For stability testing throughout the experiment one solution was prepared. The concentrations were 3.5 mg/L phenol, 0.525 mg/L *4*-chlorophenol, 0.7 mg/L *4*-cresol, and 0.875 mg/L catechol. Injections of this solution were performed before and after the experiment as well as after each 5th sample (S1-11, **Tab. 4.13**).

To study the response of the GDH-biosensor towards different compositions, 48 mixtures with various concentrations based on four phenolic stock solutions were injected (T**ab. 4.13)**.

A fixed volume of 50 µL was injected into the system and oxidation peaks were obtained for all samples using a potential of 300 mV vs. Ag/AgCl. Due to the high concentration in the micromolar range, the peaks were rather broad. Therefore, an extended washing period of 3 min was employed. All samples were injected as triplicates, leading to a total analysis time of 11.2 min for each mixture. In total, 59 solutions, i.e. 48 different mixtures and 11 times the mixture used for stability testing, were analyzed. Thus, the time for the whole experiment was 11 hours.

The stability of the sensor was excellent. Over the whole period of 11 h the baseline was stable and there was no significant change in the peak shape for the injections of the stability solution (**Fig. 4.26**).

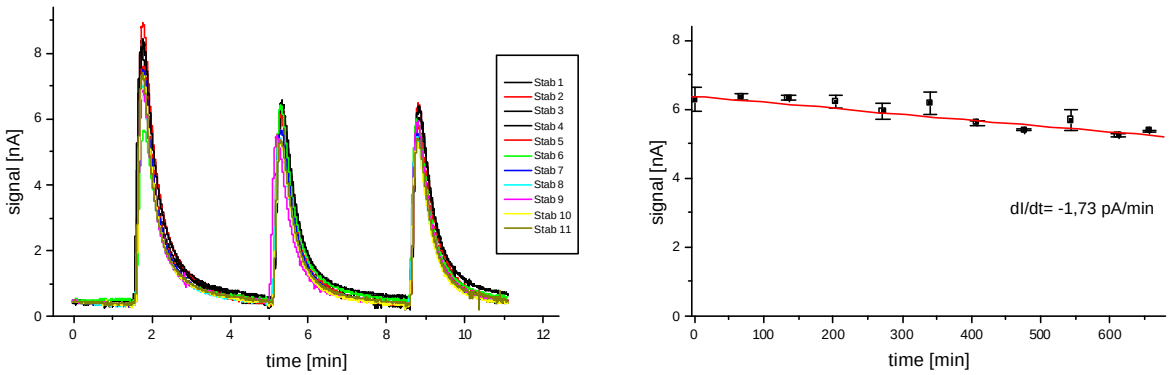

Figure 4.26: The signal vs. time plot for the injections of the mixture used for the stability studies is shown in the left graph. The changes in peak height over the whole time period have also been plotted (right graph). The mean was calculated using the 2nd and 3rd peaks only. Experimental conditions: Injection volume 50 µL, HBS20 with 10 mmol/L glucose as the carrier with a flow rate of 0.5 mL/min and an applied voltage of 300 mV

The statistical evaluation of the peak height for these injections emphasized the remarkable stability of the GDH-biosensor. The mean peak height decreased only by 0.91 nA in 11 h. From the regression a decrease of 0.103 nA/h was calculated which corresponds to a loss of 1.64 %/h. This is an excellent result for the stability of a biosensor, especially when taking into an account the high number of analyzed phenol mixtures and their high concentrations. Unfortunately the peak shape did not change remarkably for the different compositions. Based on these results no chemometric evaluation was successful. Nevertheless, the experiment underlined the excellent stability of the GDH-TFE-biosensor.

4.1.5.4.2 Implementation of the GDH-biosensor into the portable device

As demonstrated in the previous chapter the GDH-biosensors showed excellent applicability in the laboratory using the automated flow system with a continuous buffer stream in the measuring cell. Since the final goal was the on-site utilization of these sensors, a combination with a portable device had to be realized.

The liquid handling system was based on previous developments from BST and consisted of an injection valve and a manually driven pump, which did not allow a continuous flow of the working buffer (**Fig. 4.27**).

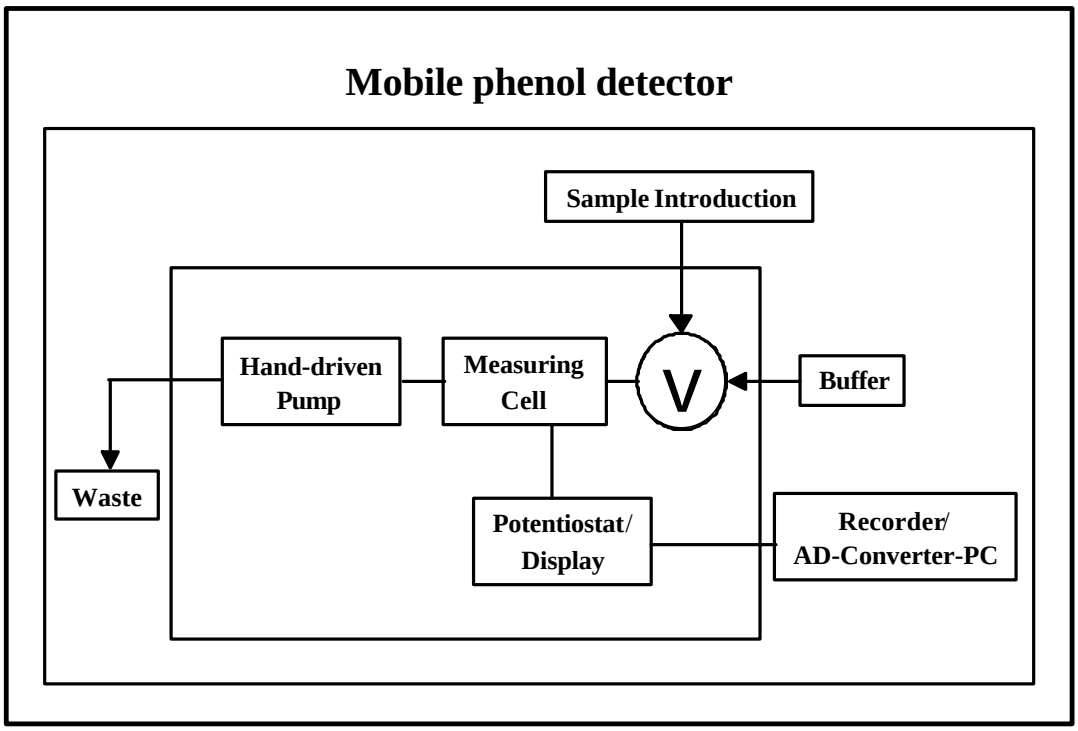

Figure 4.27: Schematic drawing of the portable measuring device for on-site analysis of phenolic compounds. The valve allows the flow of carrier buffer in "flow" position or the injection of sample in "inject" position.

Therefore, the next experiments towards the application of the GDH-biosensor in this device focused on the change from continuous measurements to stop flow experiments. Dop was chosen as the model analyte for all following experiments.

4.1.5.4.2.1 Stop flow experiments

The response of the GDH-biosensor towards Dop was investigated under stop flow conditions in the laboratory flow system **(**see **Fig. 2.5).** After the injection of the analyte for 20 s (167 µL), the pump was stopped for 3 min and the signal was recorded. Within this injection time the Dop signal reached a steady state value. The blank signal was recorded by injecting buffer.

4.1.5.4.2.1.1 Blank signal in stop flow mode

After the pump was stopped the baseline current decreased to a stable value during 30 to 40 s. This value was 1.5 nA below the baseline obtained by continuously passing the buffer through the cell. The current increased back to the baseline value in flow within 10 to 15 s (**Fig. 4.28** (trace B)).

4.1.5.4.2.1.2 Sample injection in stop flow mode

The injection of the sample resulted in a peak, after 20 s the steady state current was reached, and the flow was stopped in the cell. The peak current decreased as observed with the blank and a stable value was obtained. After restarting the pump, a second peak was registered. This was caused by the part of the sample that was stopped in the tube before it reached the measuring cell. Finally, the current reached the baseline value again (**Fig. 4.28**, trace A).

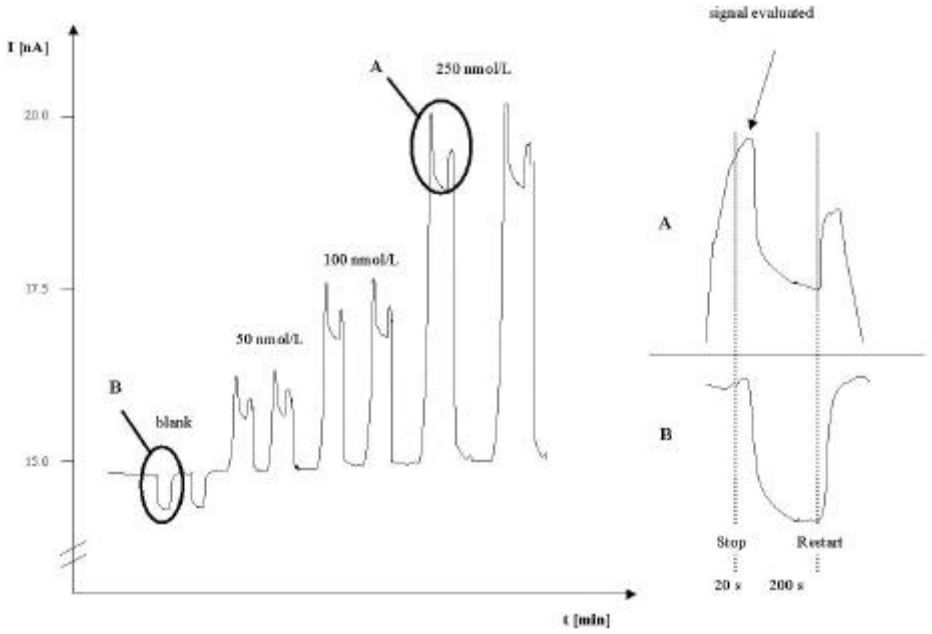

Figure 4.28: Signal vs. time obtained with the GDH-biosensors during stop-flow experiments in the automated system. Traces A and B were enlarged to explain the shape of the signal. The first peak was used for signal evaluation.

For data evaluation, the first peak current was taken. Using these settings, a linear concentration dependency was obtained for Dop between 50 and 1000 nmol/L. A sensitivity of 25.1 nA·L/µmol was calculated from the linear regression of the signal vs. concentration plot.

4.1.5.4.2.2 Portable device

The portable device was based on a flow system with an integrated flow cell. The pump was manually driven to prevent the high demand of electricity for automatic pumps, and thus a discontinuous buffer flow was realized. Measurements were performed in stop flow mode. The potentiostat and the data acquisition and storage unit were not integrated in the device.

The buffer reservoir was connected to the measuring cell via the injection valve. The pump was placed between the measuring cell and the waste container. The carrier buffer was sucked through the cell equipped with the GDH-biosensor when the pump wheel was slowly turned clockwise. A continuous flow was realized and resulted in stable baseline current. When the buffer flow was stopped, this background signal started to decrease by approximately 2 nA, but it returned to the original value within 5 s after turning the wheel again.

No changes in the background current were found due to fluctuations of the flow rate (faster or slower manual wheel turning). The injection valve has two possible positions **(Fig. 4.29)**: In position A the buffer can flow from the reservoir through the cell into the waste container. In position B this connection is disabled and sample can be injected.

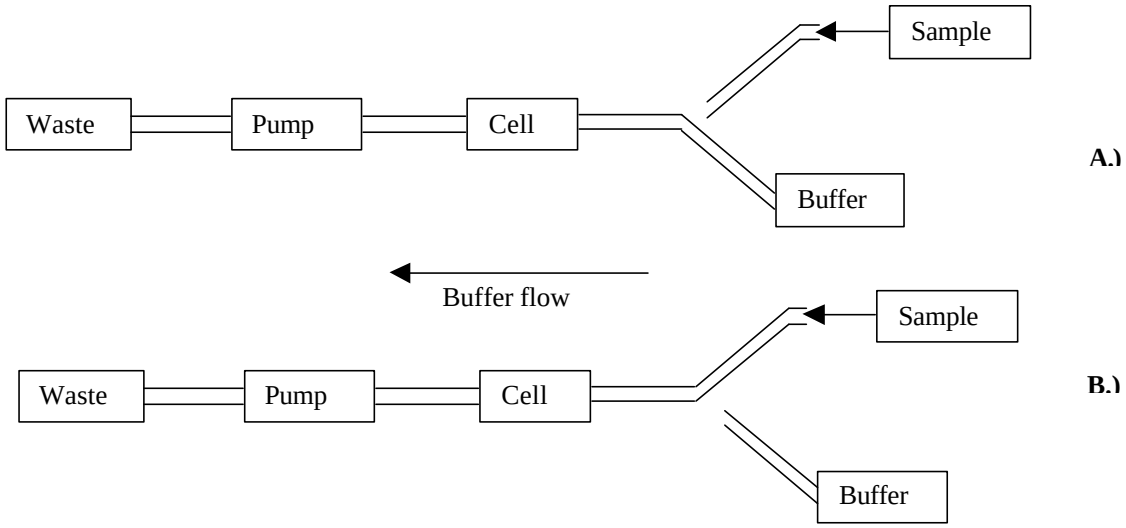

Figure 4.29: Buffer flow in the manual device for both positions of the injection valve. A.) This valve position enables the buffer flow from the reservoir through the cell. B.) This position allows the injection of the sample while the buffer stream is disconnected

The injection system was designed for end-to-end capillaries, which were kept in place by the aid of a holder. These capillaries were filled with the sample by capillary forces. After the filled capillary was placed into the injector, the sample was sucked into the system while the pump wheel was turned further clockwise.

The injection volume was about 5 µl (determined by turning the pump wheel for one quarter). To avoid dispersion, the sample plug was separated from the buffer using small air compartments before and after the sample. With the portable device, a linear concentration dependency for Dop was obtained between 50 and 1000 nmol/L. A sensitivity of 19.4 nA·L/µmol was calculated from the linear regression of the signal vs. concentration plot.

Table 4.14: *Sensitivity towards Dop using the different systems equipped with the same GDH-modified thick film electrode*

	Prototype	**Stop flow mode**	**Continuous flow system**
Sensitivity [nA·L/µmol]	19.4 ± 1.1	25.1 ± 0.3	28.9 ± 0.1

The sensitivity differed in all 3 set-ups. The highest sensitivity was obtained in the automated flow system using a continuous buffer and sample flux. The lower sensitivity in the stop flow mode was explained by depletion of analyte in the measuring cell.

Using the portable device with a manually driven pump, the sensitivity decreased to 19.4 nA·L/µmol. This can be explained by a much lower injection volume (5 µL instead of 167 µL in the stop flow experiments) and also by different flow characteristics. The measuring cell was not identical to that used in the automated system and an identical flow rate for each injection cannot be achieved by the user. Additionally, a higher background noise and a higher standard deviation for the measurements in the portable device were observed compared to the stationary system.

In summary, the portable device showed promising results for the quantification of phenolic compounds in cases where a laboratory based system is not applicable.

4.1.5.4.3 Application of the GDH-TFE for on-site real sample analysis

For the on-site monitoring of phenolic compounds in wastewater samples, the GDH-modified thick-film electrodes were integrated into the portable device from BST (described in the previous chapter). This system was used for real sample analyses during a field experiment (BIOSET EU Technical Meeting: "Biosensors for evaluation of the performance of wastewater treatment works") in Barcelona.

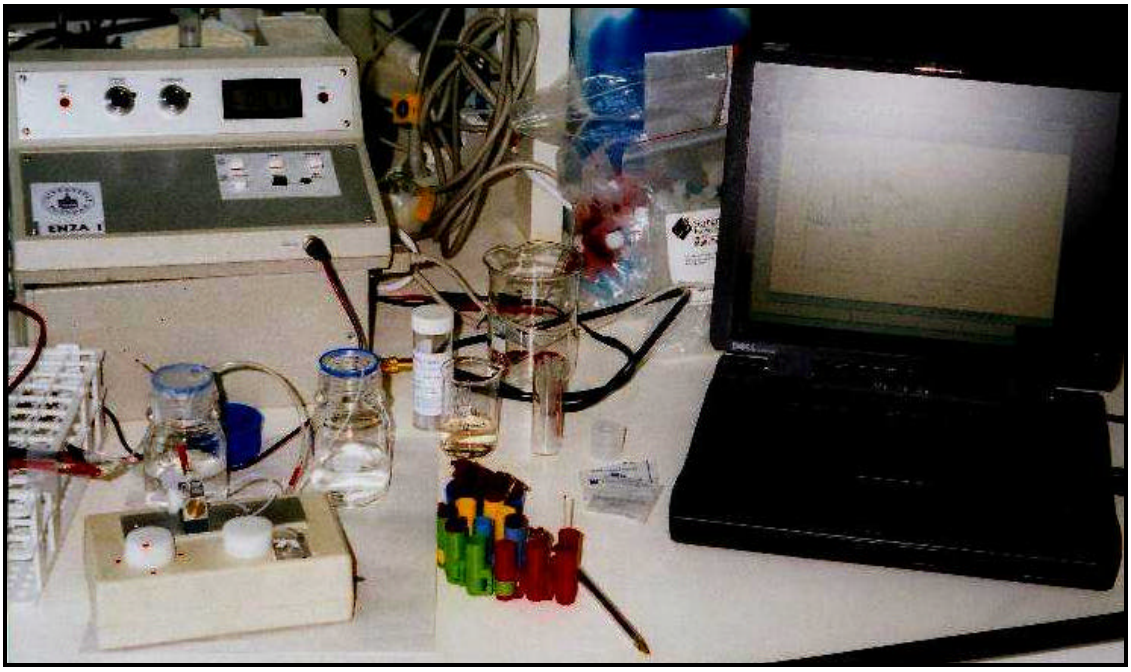

Figure 4.30: Experimental set-up during the BIOSET EU Technical Meeting in Barcelona

Among other phenol detecting biosensors, the GDH-biosensor was used to follow the content of phenolic compounds in the wastewater at different cleaning stages. The broad substrate spectra of GDH allowed the monitoring of this sum parameter without identification of the sample components.

All the experiments took place in the laboratory of the “La Llagosta” wastewater treatment plant. Samples from two different Catalan wastewater treatment plants (“La Llagosta” and “ Igulada ”) were analyzed. Water from the influent, effluent, and after a primary treatment step was examined as illustrated in **Fig. 4.31.**

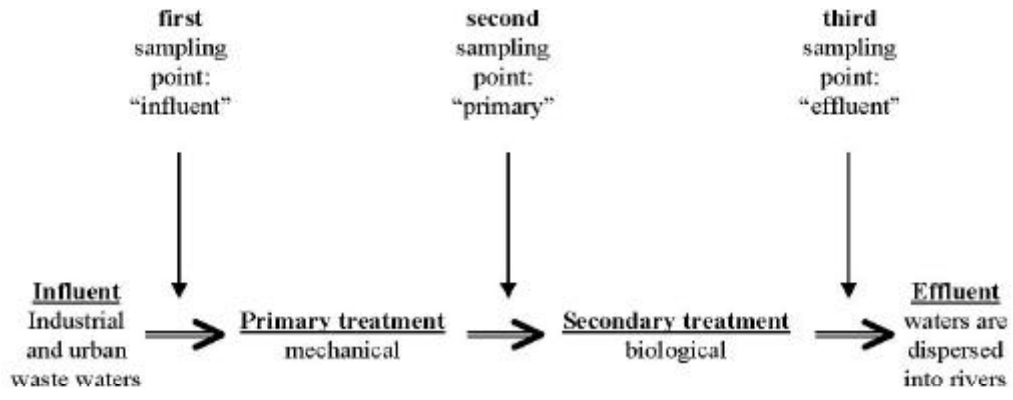

Figure 4.31: Sketch of the water-flow through the wastewater treatment plants including the investigated sampling points.

The sampling points were chosen to evaluate the cleaning efficiency of the wastewater treatment. The most polluted samples were expected for the raw influent. Here the first sampling took place ("influent"). The first cleaning step consisted of a mechanical treatment of the water.

The differences of phenol content in the water samples collected at sampling point one and two ("primary") will demonstrate the efficiency of the mechanical treatment step. The second sampling point is of great interest for the management of the plant since the water entering the second treatment (biological) should not harm the used organisms.

The third sampling point ("effluent") was placed at the effluent of the WWTP to demonstrate the efficiency of the biological treatment as well as to show that the released water matches the quality demanded in guidelines and policies.

The experiments were performed as shown in **Tab. 4.15**. First a calibration with catechol standards in plain buffer was performed, followed by the actual sample analysis using the standard addition method. Since a cleaning of the water was expected, first the less polluted effluent samples were analyzed. The probably most polluted influent samples were analyzed at the end to avoid the passivation of the sensor. After each water sample a calibration was performed.

Table 4.15: *Experiments performed during the field experiment in numerical order.*

No.	Experiment	No.	Experiment
C*1	Calibration in plain buffer	**R4**	Real sample analysis: Igualada after primary treatment
R*1	Real sample analysis: La Llagosta effluent	**C5**	Calibration in plain buffer
C2	Calibration in plain buffer	**R5**	Real sample analysis: La Llagosta influent
R2	Real sample analysis: Igualada effluent	**C6**	Calibration in plain buffer
C3	Calibration in plain buffer	**R6**	Real sample analysis: Igualada influent
R3	Real sample analysis: La Llagosta after primary treatment	**C7**	Calibration in plain buffer
C4	Calibration in plain buffer		

* C and R indicate calibration or real sample analysis

The GDH-biosensor has a broad substrate spectrum as shown during sensor evaluation. For these experiments, the signal was related to the response of the GDH-biosensor towards catechol. All results are therefore given as catechol equivalents. Sensor calibration was performed with aqueous catechol solutions of 10, 50, and 100 µg/L, respectively. The calibration plot was obtained with triplicate injections of these solutions into the working buffer. The obtained results are visualized in **Fig. 4.32**.

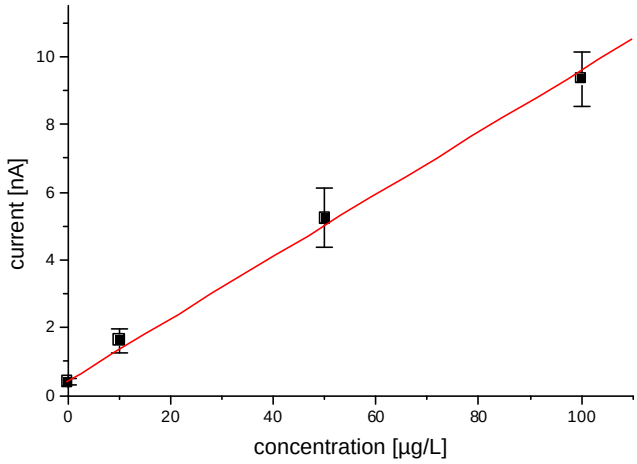

Figure 4.32: Calibration plot for catechol using a portable device equipped with the GDH-biosensor. Experiments were performed in the laboratory of "La Llagosta" treatment plant.

From this plot, a sensitivity of 0.092 nA/µg/L catechol and an LLD of 8.2 µg/L were determined.

For the analysis of real samples, the standard addition method was applied. To adjust the pH the samples were mixed 1:1 with double concentrated working buffer. This solution was injected into the manual device and the response was checked. If the response for the unspiked sample was not in the linear range of the GDH-biosensor a further dilution with buffer solution was performed. The diluted sample was spiked with catechol solutions as used for the calibration. **Fig. 4.33** shows a signal vs. time plot where the raw influent of the "Igualada" treatment plant was analyzed after dilution with buffer. Two injections were performed for each solution. The first two peaks show the response towards the sample without any addition of catechol. The higher peaks for the following injections are a result of the addition of the catechol standards.

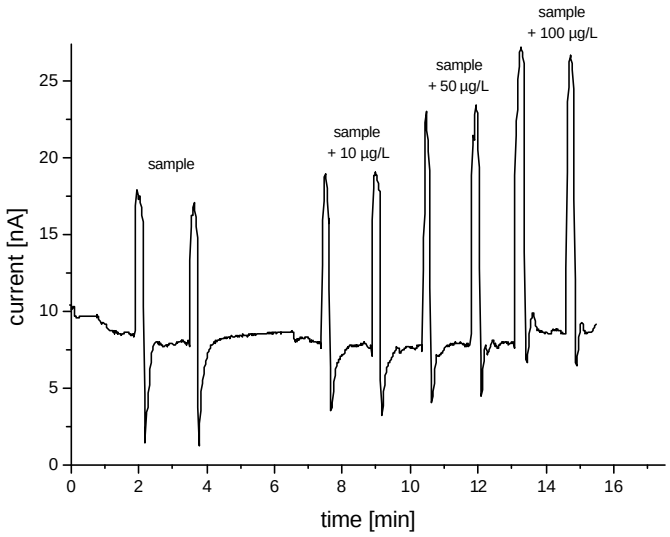

Figure 4.33: Signal vs. time plot obtained for diluted sample (1:10) from the Igulada treatment plant. Samples were spiked with catechol standard used for the calibration.

From these results the peak height vs. catechol concentration was plotted and the concentration of catechol equivalents in the unknown sample was determined as shown in the **Fig. 4.34**.

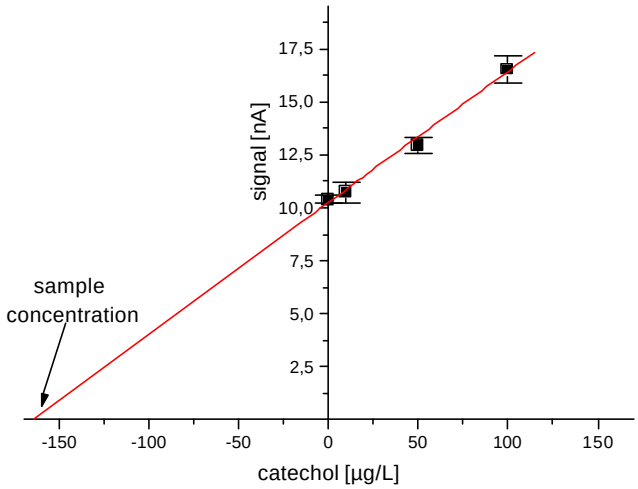

Figure 4.34: Graphic determination of the catechol equivalents concentration in an unknown sample shown for the raw influent of the Igualada treatment plant. The concentration is given by the extrapolated graph of the absolute catechol concentration for a signal of 0 nA.

The signal for the spiked samples were plotted vs. the catechol concentration and a linear fit was performed. From this plot the catechol concentration in the sample can be graphically deduced by extrapolation of the fitting to reach the X-value for a signal of 0 nA.

The plots for the real samples from the two wastewater treatment plants are shown in the **Fig. 4.35**.

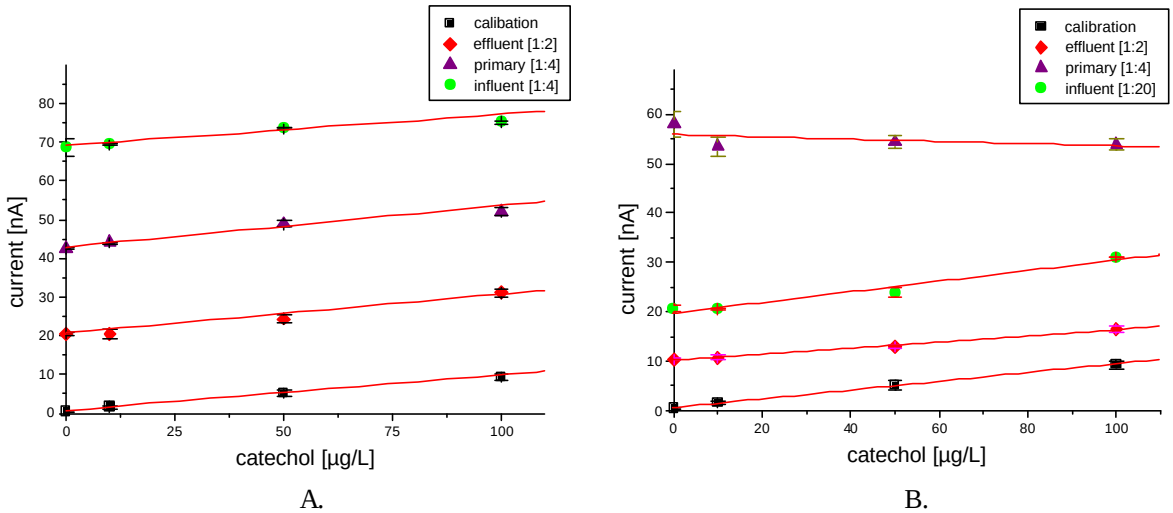

Figure 4.35: Samples obtained in the Lallagosta (A.) and Igualada (B.) treatment plant (Barcelona) and analyzed using the standard addition method. Dilution factors for the original samples are given in brackets. Experiments were performed using the GDH-biosensor equipped portable device. Final buffer composition was HBS20 with a concentration of 10 mmol/L glucose.

The catechol concentration was determined mathematically by the fitting equation as follows.

$$Y = a \cdot X + b$$
$$<=> \quad X = (Y-b) / a$$

The calculated results are given in **Tab. 4.16**.

Table 4.16: *Determination of the total amount of phenolic compounds. The phenol content is expressed as catechol equivalents; additionally, relative values are listed.*

Sample	Phenol content in undiluted sample	
	Catechol equivalents [µg/L]	Relative value [%]
La Llagosta influent	3416	100
La Llagosta after primary treatment	797	23.3
La Llagosta effluent	405	11.9
Igualada influent	3209	100
Igualada after primary treatment	n.d.*	n.d.*
Igualada effluent	320	10.0

n.d.*: not determined

As shown in **Tab. 4.16**, the concentration of phenolic compounds present in the samples was relatively high but decreased with advanced effluent treatment. The concentration of phenolic compounds in the sample, taken after the primary treatment in the "Igulada" plant, was not determined with the GDH-biosensor. The reason for this has been demonstrated in **Fig. 4.35**. The calculated fitting for this sample resulted in a negative slope. The GDH-biosensor was influenced drastically and did not allow the quantification of the spiked catechol. The results obtained with the GDH-biosensor were compared with two other phenol-detecting biosensors tested during the workshop.

A research group from Lund University, Sweden, applied cellobiose dehydrogenase as the phenol recognition element immobilized on a spectroscopic graphite rod. This was performed according to a previously published protocol (Lindgren, Stoica et al. 1999). A CDH-biosensor was placed as the working electrode in a wall-jet amperometric cell (Appelqvist, Marko-Varga et al. 1985). An Ag/AgCl (0.1 mol/L KCl) electrode was used as reference and a platinum wire as the auxiliary electrode. A potential of +300 mV was applied and the oxidation current was recorded on a chart recorder.

Researchers from the University of Alcalá, Spain, utilized tyrosinase immobilized on screen-printed carbon electrodes (Tyr-SPCE). These electrodes were mounted into the measuring cell of a FIA system developed by TRACE Biotech AG (Germany). Due to the mechanism of tyrosinase, a potential of – 100 mV was applied and the resulting reduction current was measured. The development and applications of the tyrosinase-biosensors were previously described (Lutz and Dominguez 1996; Ortega, Dominguez et al. 1994; Ortega, Dominguez et al. 1993; Parellada, Narvaez et al. 1998).

The results obtained with these two biosensors are shown in the **Tab. 4.17**.

The absolute values differed for all three biosensor. The concentrations determined by the GDH-biosensor are remarkably higher than the results found with the other two biosensors. The tyr-SPCE showed intermediate, the CDH-SGE low values (except for "La Llagosta" effluent).

Table 4.17: *Determination of the total amount of phenolic compounds in the wastewater samples using CDH- and tyrosinase-biosensor, respectively. The phenol content is expressed as catechol equivalents and additionally the relative value is listed.*

Sample	Phenol content in undiluted sample			
	CDH-SGE		Tyr-SPCE	
	c.e. [µg/L]	r.v. [%]	c.e. [µg/L]	r.v. [%]
La Llagosta influent	66.3	100	451	100
La Llagosta after primary treatment	54.9	63.5	308	68.3
La Llagosta effluent	15.2	22.9	3.7	0.8
Igualada influent	146.5	100	2300	100
Igualada after primary treatment	96.5	65.9	1200	52.2
Igualada effluent	12.4	8.5	30	1.3

c.e.: catechol equivalents; r.v.: relative value

This can be explained by the differences in the substrate spectra of the three enzymes and would indicate the highest specificity for the CDH. In contrast to tyrosinase, CDH can efficiently discriminate between mono-and diphenols (Lindgren, Stoica et al. 1999). The same is true for GDH, however the substrate spectra for the two enzyme differ strongly, thus the application of the GDH-biosensor leads to higher values. Nevertheless, taking the relative values all three biosensors used for the analysis of phenolic compounds showed comparable results.

The highest pollution was found for the raw influent but the treatment resulted in a reduction of approximately 90 % of phenolic contaminants during the cleaning process of the "Igualada" WWTP. This was the case for the GDH- and the CDH-biosensors. The tyr-SPCE even reflected a reduction to only 1.3 % of the initial phenol content. For the "La Llagosta" WWTP the CDH-biosensor showed a final contamination of 22.9 % while the value found by using GDH-biosensor corresponds to 11.9 % of the initial pollution. The tyrosinase-biosensor gave a value of 0.8 % after the cleaning process.

4.1.5.4.3.1 Stability of the GDH-biosensor during the field experiment

The stability of the GDH-biosensor was examined during the field-experiments by repeating the calibration with catechol in plain buffer after the analysis of each real wastewater sample (**Tab. 4.15**).

After approximately 5 h of experiments with the real samples interrupted by 15 h storage in a refrigerator, the calibration plots indicated only a loss of 15 % initial activity of the GDH-biosensor (**Fig. 4.36**).

The high stability is of particular interest, since an influence of unknown pollutants on the GDH-biosensor in the real samples should be expected. This can be seen by the differences in the slopes of the plots for the catechol addition to the real samples. Especially experiment No. 9 (the calibration in plain buffer performed after the analysis of water from sampling point 2 at the "Igualada" WWTP) showed that the influence of the real sample on the GDH-biosensor was reversible.

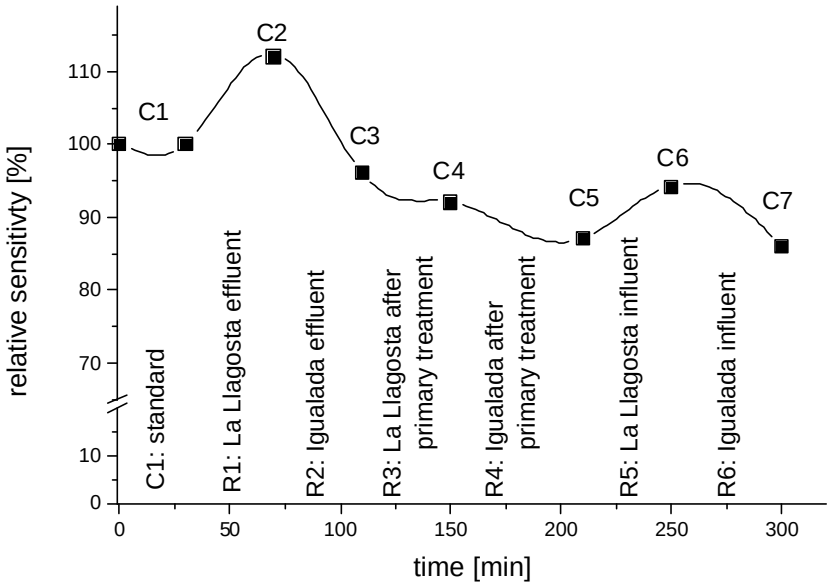

Figure 4.36: Stability of the GDH-biosensor during the field experiments in Barcelona, Spain. The sensitivity for catechol was determined in plain buffer after each real sample analysis. The ratio of these values and the initial value obtained before the first analysis of real wastewater sample was calculated and presented as the relative sensitivity. The order of experiments is explained in **Tab. 4.15**.

The GDH-biosensor has been shown to be applicable for the detection of phenolic compounds in real wastewater samples. The described effect of the real samples had only reversible effects on the catechol measurements and did not lead to destruction of the sensor.

4.1.5.4.3.2 Further interpretation of the standard addition experiments

As mentioned above, the phenol content at "Igualada; sampling point 2" was not determined with the GDH-biosensor, due to a negative slope of the fit. All other fits showed a positive slope as obtained for the calibration curve. Nevertheless, differences in the steepness of the plots are obvious. The parallel shift of the calibration plot showed the concentration of the analyte in the sample but no influence on the biosensor. Changes in the slope (the sensitivity towards catechol) are a result of enhanced or inhibited response of the sensor. A sensitivity value for catechol smaller than 100 % was found for both raw influent waters. The sample taken after primary treatment at the "Igualada" WWTP even gave a negative slope and thus a relative value could not be calculated.

Does this data provide additional information?

Lower sensitivity of the GDH-biosensor towards catechol (relative response below 100 %) means that the recognition of catechol is hindered. This can be due to diffusion limitation, i.e. the analyte cannot fully reach the electrode for oxidation, an effect caused by matrix components being electropolymerized by the applied potential. Since the samples were filtered in advance, a simple mechanical hindrance seems less likely. The other possibility is an inhibition of the GDH leading to a less sufficient amplification of the signal. Since the lowest sensitivities were found at the influent of the two WWTPs (most polluted samples), a reversible inhibition of the GDH by unknown sample components seems extremely probably. The results from the samples taken at "La Llagosta" WWTP showed that the relative response towards catechol was smallest at sampling point 1 ("influent"). After the primary treatment as well as in the effluent did not show any inhibition due to ongoing treatment.

For the "Igualada" samples, however, the signal vs. catechol concentration plots show the lowest sensitivity for catechol spiked into the water collected after primary treatment, which thus had higher inhibition effects than the influent water. The latter effect can be attributed to some of the organic pollutants, initially adsorbed on solid particles (e.g., sludge), being released into the water environment during the mechanical treatment performed trough-out the primary cleaning step. The biological treatment step was sufficient for both plants since the effluent water samples showed no inhibition of the enzyme.

A comparison with toxicity determination was performed. On-site toxicity testing was performed by G. Klöter from Merck, Germany, using a mobile ToxAlert® 10 instrument. This system determines toxicity via inhibition of luminescent bacteria (Vibrio fischerii; NRRLB-11177). The results showed that the influent water at "Igualada" was more toxic than the influent water at "La Llagosta". The toxicity test indicated more toxic samples after primary treatment in both plants.

Nevertheless, it is noticeable from the data in the **Tab. 4.18** that the final cleaning is efficient from the toxicity point of view (no toxicity was measured in the effluents). This corresponded to the results of the biosensor experiments, where a lower amount of phenols was recognized in the effluent waters.

Table 4.18: *Inhibition of the luminescence of bacteria using ToxAlert® 10 system. Samples from two WWTPs were taken on both days of the workshop and analyzed using two incubation times of 15 min and 30 min, respectively.*

Sampling point	**Inhibition [%] Day 1 incubation time**		**Inhibition [%] Day 2 incubation time**	
	15 min	**30 min**	**15 min**	**30 min**
La Llagosta influent	51	31	n.d.	n.d.
La Llagosta after primary treatment	67	50	46	19
La Llagosta effluent	0	0	0	0
Igualada influent	57	46	58	43
Igualada after primary treatment	86	72	89	80
Igualada effluent	0	0	0	0

n.d.: not detected

These results were pointed up by an Italian group using an ammonium nitrification analyzer (ANITA) for toxicity evaluation and measurements with the laboratory based ToxAlert® 100 instrument performed by a group from the IIQAB-CSIC, Barcelona, Spain.

4.1.5.4.3.3 Conventional chemical analysis

Identical wastewater samples were additionally analyzed by conventional chemical analysis using laboratory based SSPE-LC-MS and SPE-LC-MS systems and the results are shown in **Tab. 4.19**. These experiments were performed by M. Farré in the "Department of Environmental Chemistry, IIQAB-CSIC, Barcelona, Spain.

The chromatographic results for the raw influent water of "Igualada" WWTP showed the highest levels of different groups of compounds, such as phenolic compounds and non-ionic and anionic surfactants many of which are highly water-soluble. The higher toxicity found in the influent of this plant can be explained by this data. These results can be correlated with the fact that this WWTP receives a higher amount of industrial wastewaters (especially from the tannery industry) than the "La Llagosta" plant.

Although the majority of toxic compounds are efficiently removed during the wastewater treatment process, a fraction of them is still released in the effluent. This, however, led to no inhibition of the GDH-biosensor or the bacteria test. In addition, the concentration of some organic metabolites, e.g., nonylphenol and nonylphenol carboxylates is increased in the WWTPs effluents as seen in **Tab. 4.19.**

These compounds can be newly formed during the wastewater treatment by biodegradation of nonylphenol ethoxylates as described in literature (Ahel, Giger et al. 1994; Weinheimer and Varineau 1998).

Another likely explanation for higher concentrations of these pollutants after the primary treatment step is that they might be released from solid particles (such as sludge) during the mechanical treatment.

For all wastewater samples tested, the amount of phenolic compounds found by LC-MS analysis was lower than those found using the biosensors (see **Tab. 4.16, 4.17,** and **4.19**). The overestimation by the results obtained with the biosensors can be explained with the fact that only a limited number of monophenolic and no diphenolic compounds were monitored during the present chromatographic analysis.

Table 4.19: *Results of the chemical analysis performed by SPE-LC-MS and SSPE-LC-MS.*

Compound	WWTP Igualada			WWTP La Llagosta			Compound	WWTP Igualada			WWTP La Llagosta		
	Raw influent µg /L	Primary effluent µg/L	Final effluent µg/L	Raw influent µg/L	Primary effluent µg/L	Final effluent µg/L		Raw influent µg/L	Primary effluent µg/L	Final effluent µg/L	Raw influent µg/L	Primary effluent µg/L	Final effluent µg/L
PEG_x	3720	3200	352	1560	2835	290	Benzenesulfonate	n.q.	n.q.	n.q.	n.f.	n.f.	n.f.
$C_{10}EO_x$	110	37	n.f.	54	34	n.f.	4-methylbenzenesulfonate	40.1	56.3	11.6	39.9	141.2	0.8
$C_{12}EO_x$	83	54	n.f.	164	157	n.f.	4-chlorobenzenesulfonate	n.q.	n.q.	n.f.	n.f.	n.f.	n.f.
$C_{14}EO_x$	17	8	n.f.	43	29	n.f.	3-nitrobenzenesulfonate	4.9	0.2	n.q.	75.8	96.2	3.0
$C_{16}EO_x$	n.f.	n.f.	n.f.	n.f.	n.f.	n.f.	1-naphthalenesulfonate	167.8	128.4	49.3	50.7	54.9	1.5
$C_{18}EO_x$	n.f.	n.f.	n.f.	n.f.	n.f.	n.f.	2-naphthalenesulfonate	525.7	468.4	101.4	194.3	217.8	7.3
$NPEO_x$	570	160	8.4	171	148	13	2-amino-1-naphthalenesulfonate	1.4	1.1	n.q.	0.8	0.8	0.2
C_7DEA	14	7	n.f.	1.8	6.7	nf	1-amino-5-naphthalenesulfonate	0.6	0.5	0.4	n.f.	n.f.	n.f.
C_9DEA	49	29	n.f.	26	32	nf	1-hydroxy-6-aminonaphthalenesulfonate	28.2	21.3	1.3	n.f.	n.f.	n.f.
$C_{11}DEA$	274	65	1.3	87	66	0.3	3-amino-2,7-naphthalenedisulfonate	n.q.	2.6	81.5	n.f.	n.f.	n.f.
$C_{13}DEA$	6.4	1.3	n.f.	2.9	3.6	n.f.	estradiol	n.f.	n.f.	n.f.	n.f.	n.f.	n.f.
$C_{15}DEA$	1.1	0.8	n.f.	1.5	n.f.	n.f.	ethynyl estradiol	n.f.	n.f.	n.f.	n.f.	nf	n.f.
$C_{17}DEA$	n.f.	n.f.	n.f.	n.f.	n.f.	n.f.	Phenol	6	17	n.f.	n.f.	n.f.	n.f.
NPEC	0.8	5.8	80	n.f.	nf	13	2-Chlorophenol	n.f.	n.f.	20	6	20	n.f.
NP	1.5	2.3	6.6	n.f.	1.0	5.5	3-Chlorophenol	n.f.	nf	nf	15	16	n.f.
OP	n.f.	n.f.	1.1	n.f.	n.f.	1.6	4-Chlorophenol	n.f.	n.f.	n.f.	n.f.	n.f.	n.f.
BPA	7.1	2.9	n.f.	2.5	1.8	n.f.	2,4-dichlorophenol	83	23	16	n.f.	n.f.	n.f.
$C_{10}LAS$	79	56	9.4	99	67	0.6	2,4,6-Trichlorophenol	n.f.	n.f.	n.f.	17	n.f.	n.f.
$C_{11}LAS$	490	303	97	668	414	9.9	Pentachlorophenol	n.f.	n.f.	n.f.	n.f.	n.f.	n.f.
$C_{12}LAS$	192	126	21	309	139	5.6	Nitrophenol	11	21	n.f.	34	114	n.f.
$C_{13}LAS$	45	29	8	69	29	0.8	2,4-Dinitrophenol	n.f.	n.f.	n.f.	n.f.	n.f.	n.f.

Symbols: n.f. - not found; n.q. - not quantified;

4.1.5.4.3.4 Interference tests and validation

In order to verify the results above, experiments were performed to investigate the influence of interfering compounds on the response of the GDH-biosensor. The response for different concentrations of standard and mixture of standards was recorded. These results were related to the signal for the catechol standard and are presented in **Tab. 4.20**. The results obtained with the CDH-biosensor are given for comparison reasons.

Table 4.20: *Studies of potentially interfering compounds. The relative sensor responses were calculated as the ratio between the response for a certain concentration of the studied standard or mixture of standards tested and the catechol calibration in the working buffer. Concentration of standards used with the two biosensor: phenol - 1 mg/L (CDH) and 0.5 mg/L (GDH); carbaryl - 5 mg/L (CDH) and 0.5 mg/L (GDH); mixture of nonylphenol ethoxylates (NPEOs) - 50 µg/L + decylphenol ethoxylates (C10EOs) - 50 µg/L + dodecylphenol ethoxylates (C12EOs) - 50 µg/L ((CDH) and (GDH)); 2-chlorophenol - 5mg l-1 (CDH) and 0.5 mg l-1 (GDH); mixture of sulphonates - 5 mg/L (CDH) and 0.05 mg/L (GDH); mixture of linear alkylbenzene sulfonates (LAS) – 50 µg/L (CDH); mixture of nonylphenol (NP) – 50 µg/L and bisphenol A (BPA) - 50 µg/L ((CDH) and (GDH)); mixture of estradiol and ethinyl estradiol - 250 ng/L (CDH); atrazine - 5 mg/L (CDH) - 0.5 mg/L (GDH).*

Standard	Relative Response (%)	
	GDH-biosensor	CDH-biosensor
Catechol	100	100
Phenol	3,85	17,98
Carbaryl	3,94	0,61
NPEOs+C_{10}EOs+C_{12}EOs	8,24	0
2-Chlorophenol	4,23	0,98
Sulphonates, mixture	7,28	0
LAS, mixture	0 *	0
NP + BPA	9,48	0
Atrazine	4,93	0,32

** LAS mixture was analyzed afterwards in Potsdam using the laboratory based flow system and here no response was found.*

The GDH-based electrode seems to be less selective, recognizing all the tested compounds, except LAS, to some extent. This generally higher cross reactivity in comparison with the CDH-biosensor can explain the high catechol equivalent values obtained when real wastewater samples were analyzed.

Next, a certain concentration of each standard solution was spiked with catechol to estimate the inhibition or enhancement effects on the GDH-biosensors, as seen in **Fig. 4.37**. It can be seen that atrazine inhibited the response of the two biosensors by about 25%, but that all other compounds/compound mixtures tested had no significant influence on the sensors. Only in the presence of LAS the response of the GDH-biosensor towards catechol increased. As found by the analysis of the real sample by SPE-LC-MS and SSPE-LC-MS (**Tab. 4.19**) various LAS were present in samples and this might be another reason for the higher response of the GDH-biosensor compared with the others. Also many sulfonates (naphthalene- and benzenesufonates) were present in the examined water samples and these gave a response with the GDH-biosensor. The decrease in concentration of these compounds during the treatment would correlate with results of the GDH-biosensor.

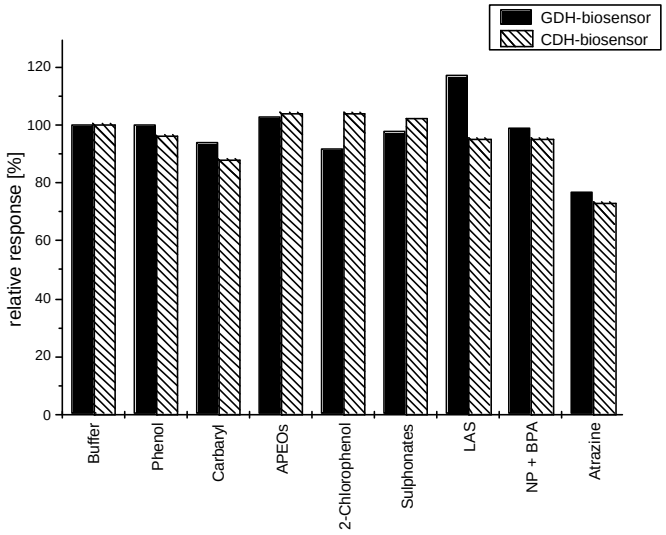

Figure 4.37: Influence of the different interfering compounds on the response of the two biosensors for catechol. The relative response was calculated as the ratio between the slopes of the catechol standard addition calibration effectuated in the working buffer with a certain concentration (as specified in **Tab. 4.20**) of standard compound or mixture of standards, and the slope of the standard catechol calibration.

As seen in **Tab. 4.19**, there are numerous other compounds present (however not tested as possible interfering compounds) in the real wastewater that could be responsible for the inhibiting effects on the two biosensors. Additionally it must be stated that the analysis performed by LC-MS or any other analytical method can only give an estimation of the pollution since the complexity of these samples allows only the analysis of selected compounds.

4.1.5.4.3.5 Summary of the on-site analysis using the GDH-TFE

The GDH-biosensor in combination with the portable measuring system was successfully used during the on-site workshop. Using the standard addition method we were able to indicate the reduction of phenolic compounds, estimated as catechol equivalents, during the on-going wastewater treatment. The highest pollution was found for the raw influent but the treatment resulted in a reduction of approximately 90 % of phenolic contaminants during the cleaning processes. Moreover, the comparison with a CDH-biosensor and a Tyr-SPCE underlined the usability of such devices for screening purposes in environmental analysis. Even the absolute values differed due to the substrate spectra of each enzyme the on-going treatment was observable and the results were comparable to chemical analysis and toxicity assessment. These facts make the GDH-biosensor a promising tool to be used for the evaluation of the two WWTPs.

4.1.5.5 Application of GDH-TFE-biosensor for ß-Gal detection

The GDH-biosensor showed very high sensitivity towards 4AP as shown in **section 4.1.5.2.2**. 4AP can be generated by enzymatic hydrolysis as schematically shown in **Fig. 4.38.**

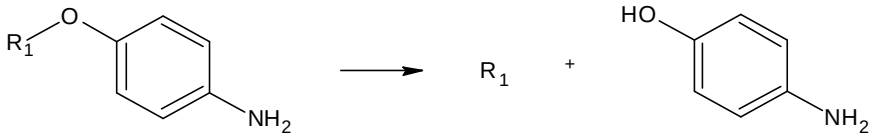

Figure 4.38: Generation of 4AP by enzymatic hydrolysis

Enzymes like ß-Gal or alkaline phosphatase can be used for the catalysis of this type of reaction. This offers the possibility to use the GDH-biosensor for the determination of their enzyme activity. ß-Gal has a pH optimum for the hydrolysis reaction around pH 7, while alkaline phosphatase has its optimum at around pH 9.

Since the GDH-biosensor works at an optimum pH-value of 7.5 as shown above (**Fig. 4.20**) the combination with ß-Gal seems preferable. The utilization of alkaline phosphatase would result in an additional working step for pH adjustment. *4*-aminophenyl-ß-D-galactopyranoside was used as substrate for the ß-Gal. We applied the GDH-biosensor for the quantification of the released 4AP.

4.1.5.5.1 Characterization of the GDH-FI system

First, the GDH-biosensor was calibrated in the flow system using 4AP solutions. Linearity was obtained between 10 and 500 nmol/L 4AP, resulting in a sensitivity of 50.3 nA·L/µmol in the absence of 4APG.

For the determination of ß-Gal 4APG was added to the working buffer solution and pumped continuously trough the measuring cell equipped with the GDH-biosensor.

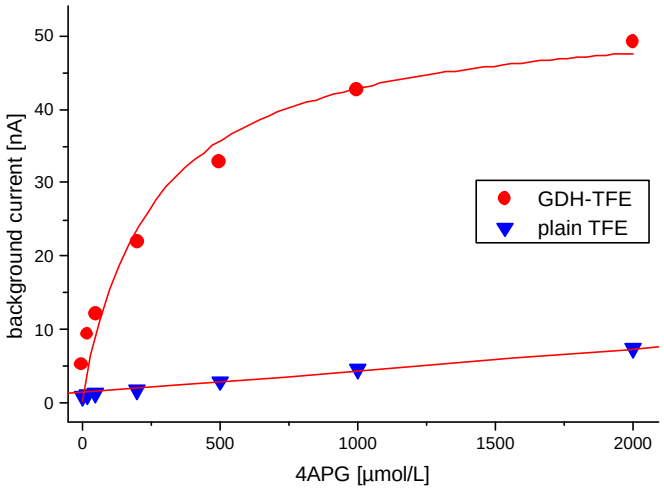

Figure 4.39: Background current for various 4APG concentrations on plain Pt-TFE and the GDH-biosensor, T = RT.

The presence of the 4APG resulted in an enormous but constant background current, which depended on the actual 4APG concentration in the buffer. The GDH-biosensor was tested in the presence of the 4APG at concentrations between 20 and 2000 µmol/L.

For comparison a plain Pt-TFE was mounted into the measuring cell and the same concentrations of 4APG were pumped through. The recorded background currents vs. the 4APG concentration are shown in **Fig. 4.39.**

The background current increased with higher concentration of the 4APG and it was much higher using the GDH-biosensor than it was using the plain TFE. The plain electrode showed a linear relation while the GDH-biosensor showed a leveling off Michaelis-Menten like dependence. This both indicate that GDH immobilized on the electrode's surface amplifies the signal.

Therefore, the catalytic reduction of 4IQ to 4AP by the GDH might be influenced by the 4APG present in the buffer. GDH-biosensor was tested for the quantification of the 4AP in the presence of the various 4APG concentrations. Measurements were performed with 4AP solutions (10-500 nmol/L) in the presence of various concentration of the 4APG (0-2000 µmol/L).

In **Fig. 4.40 b** the signal for 200 nmol/L 4AP in the presence of 4APG is shown using the GDH-biosensor. With increasing 4APG concentrations the signal decreased by 6 %. This indicates that the amplification becomes less sufficient at high 4APG concentrations.

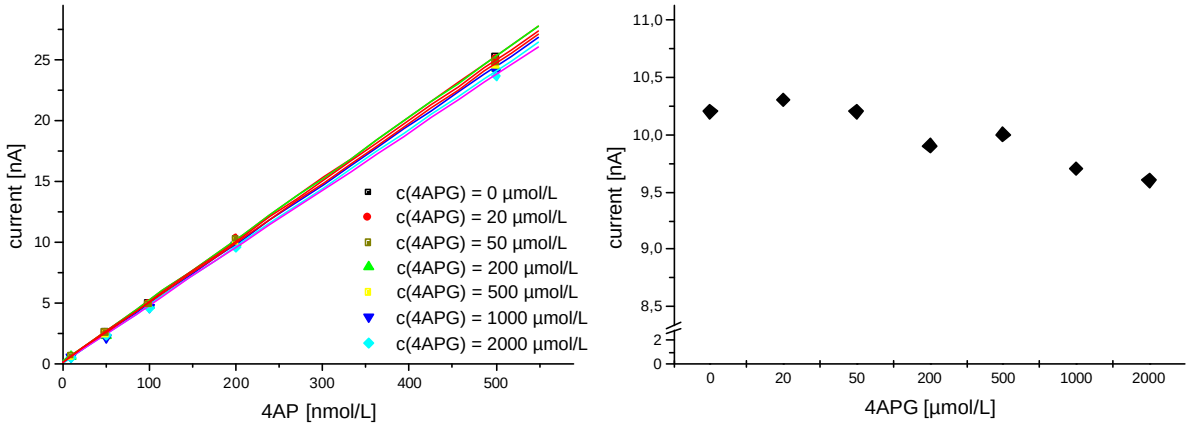

a **b**

Figure 4.40: Calibration plot for 4AP between 10 and 500 nmol/L using the GDH-biosensor at various 4APG concentrations (a). Signals were obtained for injections of 200 nmol/L 4AP at various substrate concentrations (b).

The sensitivity towards 4AP was calculated by linear regression of the calibration plots. It decreased from 50.3 nA·L/µmol in the absence of 4APG to 47.3 nA·L/µmol in the presence of 2 mmol/L 4APG. This reflects a decrease of 6 %. Nevertheless, a sensitive quantification of 4AP at concentration in the nanomolar range can be assured with the GDH-biosensor in the presence of 4APG in the buffer.

The same type of experiments was performed with an unmodified Pt-TFE. Much higher concentrations of 4AP were needed for the calibration plots. The sensitivity was 0.9 ± 0.04 nA·L/µmol for all plots and this reflects a deviation of 4.4 % but no significant decrease in sensitivity with increased 4APG concentration in the buffer.

4.1.5.5.2 ß-Gal determination

To determine ß-Gal this enzyme was mixed with the 4APG for a fixed time to allow the hydrolysis. This was performed by injection of the enzyme into the carrier buffer, which was downstream mixed with the substrate. The reaction took place while this mixture was transported through the mixing coil to the measuring cell. Here an oxidation current occurred when 4AP as the product of the hydrolysis reached the sensor. The height of the obtained

oxidation peaks corresponded directly to the 4AP concentration, which was calculated from the calibration plots. The constant flow rate determined the constant reaction time for all injections. The generated 4AP concentration depended on the ß-Gal activity present in the sample and the 4APG concentration in the buffer.

If the 4AP concentration generated during the hydrolysis exceeded the linear range of the sensor the measurement was repeated with diluted sample. These experiment were carried out at 6 different concentrations of 4APG. The exact data is given in **Tab. 4.21**.

Table 4.21: *Injected ß-Gal concentrations at the various 4APG concentrations in the buffer. The GDH-biosensor was used for quantification of the produced 4AP.*

4APG concentration [µmol/L]	**ß-Gal concentration [µg/L]**		
20	11.25	45	112.5
50	11.25	45	112.5
200	11.25	45	112.5
500	11.25	45	112.5
1000	2.25	5.63	11.25
2000	2.25	5.63	11.25

The resulting peak current was recorded and plotted in relation to the injected amount of ß-Gal. From this plot the sensitivity of the sensor towards ß-Gal was calculated using linear regression. The calculated values were plotted in dependence of the 4APG concentration in the buffer.

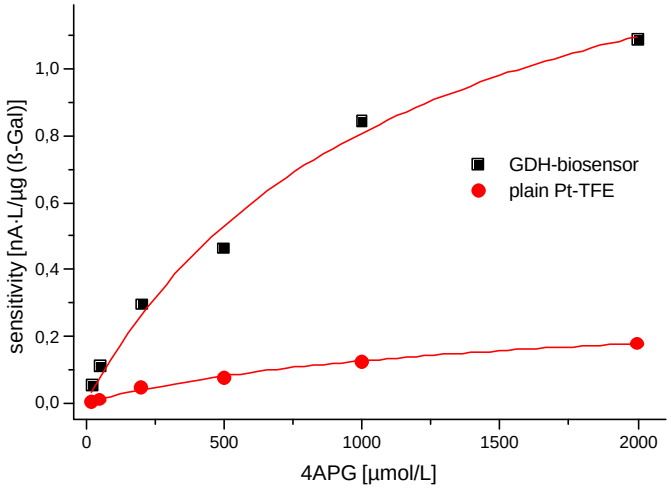

Figure 4.41: Sensitivity for ß-Gal at various 4APG concentrations obtained using the GDH-biosensor compared with a plain Pt-TFE.

As shown in **Fig. 4.41** the sensitivity of the GDH-biosensor for ß-Gal is much higher than compared with the Pt-TFE and it increases with higher 4APG concentration. This is according to the theorie of enzyme catalysis. At low substrate concentrations the turnover is limited. Taking a concentration of 4APG of 2mmol/L the sensitivity using the GDH-biosensor is 1.09 nA/µg/L ß-Gal and 0.18 nA/µg/L ß-Gal using an unmodified Pt-TFE. This equals a factor of 6.06. The better sensitivity allows discriminating small changes in the ß-Gal concentration.

In addition to the sensitivity the LLD can be calculated from the current vs. the ß-Gal concentration plots. The LLD is the ß-Gal concentration that gives a peak current 3 times higher than the noise threshold. The LLD vs. the concentration of 4APG is shown in **Fig. 4.42**. The LLD decreases with increasing 4APG concentration for both the GDH-biosensor and the Pt-TFE. For a 4APG concentration of 2 mmol/L the LLD decreases from 3.42 µg/L ß-Gal using the plain Pt-TFE down to 0.19 µg/L using the GDH-biosensor. This equals a factor of 18.

Since the molecular weight of ß-Gal is 540000 g/mol 0.19 µg/L ß-Gal equals a concentration of 352 fmol/L.

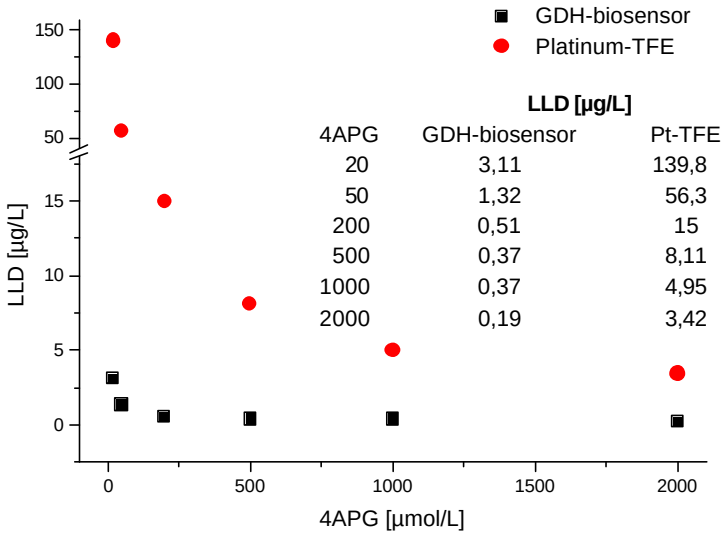

Figure 4.42: LLD for ß-Gal at various 4APG concentrations using the GDH-biosensor and a plain Pt-TFE.

The influence of the temperature was tested for the two sensors. Therefore the mixing coil was tempered using a water bath at 22°C (RT) and 45°C, respectively. Before the buffer reached the electrode it was cooled down to RT using a second water bath.

The results of these experiments are shown in **Tab. 4.22**.

Table 4.22: *Sensitivity for ß-Gal at two temperatures using a GDH-biosensor and a Pt-TFE*

4APG [µmol/L]	Sensitivity [nA·L/µg ß-Gal] GDH-biosensor 22°C	GDH-biosensor 45°C	Pt-TFE 22°C	Pt-TFE 45°C
20	0.05	0.16	< 0.01	0.01
50	0.11	0.35	< 0.01	0.04
200	0.29	0.68	0.04	0.14
500	0.46	1.36	0.07	0.34
1000	0.84	2.13	0.12	0.57
2000	1.09	3.49	0.18	0.92

Using a temperature of 45°C the enzymatic hydrolysis of 4APG is speeded up. This leads to higher sensitivity and lower LLD. For the GDH-biosensor the sensitivity increased by a factor of 3.2 and for the plain Pt-TFE by the factor of 5.1 when using a substrate concentration of 2 mmol/L 4APG.

The LLD decreases from 0.19 to 0.03 µg/L ß-Gal when the GDH-biosensor is applied as detection unit, which results in a factor of 6.3. For the plain Pt-TFE this factor is only 1.3. Both results are given for 2 mmol/L 4APG.

Table 4.23: *LLD for ß-Gal at two temperatures using a GDH-biosensor and a Pt-TFE*

4APG [µmol/L]	LLD[µg/L ß-Gal] GDH-biosensor 22°C	GDH-biosensor 45°C	Pt-TFE 22°C	Pt-TFE 45°C
20	3.11	0.59	139.8	73.4
50	1.32	0.26	56.3	25.2
200	0.51	0.13	15	8.81
500	0.37	0.09	8.11	5.34
1000	0.37	0.06	4.95	4.23
2000	0.19	0.03	3.42	2.65

The lowest concentration of ß-Gal that can be detected is thus 55.6 fmol/L using the GDH-biosensor at a temperature of 45°C.

4.1.5.5.3 Summary of ß-Gal detection using the GDH-TFE-biosensor

The GDH-biosensor was successfully applied for activity measurements of ß-Gal in an automated flow system. This is of special interest since the ß-Gal is an often-used enzyme label in immunoassay technology. The adoption for activity measurements of synthesized ß-Gal tracer will be shown later and there it will be compared with optical determination methods.

We showed that the GDH-biosensor is able to determine 4AP sensitively in the presence of the ß-Gal substrate 4APG. An increased background current was obtained when adding the 4APG to the carrier buffer. Nevertheless, we demonstrated that the extended linear range of the GDH-biosensor made it possible to use up to 2 mmol/L APG. The sensitivity decreased only by 6 % compared to buffer without addition of 4APG.

The GDH-biosensor was able to determine 0.19µg/mL ß-Gal at RT and a 4APG concentration of 2 mmol/L. This was a 18-fold improvement compared with an unmodified electrode. The sensitivity increased by more than 6 times. This allows discriminating very small amounts of the ß-Gal. These data showed that the GDH-biosensor is a very promising tool for label detection in immunoassays. Performing the experiments at a temperature of 45°C would further increase the sensitivity and lower the LLD, but more sophisticated equipment would be needed. Therefore, all experiments during immunoassay development were carried out at RT.

The results suggested that the GDH-biosensor might be used for the determination of *E. coli* according to the method described by Nistor et al. (Nistor, Osvik et al. 2002). In that paper 4AP produced by bacterial ß-Gal was monitored by with a CDH-biosensor and compared with chemiluminometric measurements. It was shown that with better LLD the time for initial *E. coli* detection decreased. A comparison of our GDH-biosensor with the CDH-biosensor showed the potential for improving results. The LLD for ß-Gal was 20-fold lower with the GDH biosensor. This would allow *E. coli* detection in samples with very low bacterial numbers, e.g. in drinking waters.

4.2 Heterogeneous immunoassay for *4*-nitrophenol ($4NO_2P$)

An immunoassay format with a labeled *4*-nitrophenol derivative was employed. The HOM was conjugated to the enzyme label (ß-Gal) using two different coupling procedures. The initial molar ratio of HOM to ß-Gal was varied during the synthesis. The tracer was characterized in terms of protein content, enzyme activity, and final HOM-ß-Gal ratio after the synthesis. The apparent affinity constants for the analyte and the tracer were determined using a microtiter plate ELISA and a flow immunoassay. In this format the HOM-ß-Gal tracer competes with the analyte present in the sample for a limited amount of antibody binding sites. The separation between the antibody-bound fraction and the free analyte and tracer molecules was realized using a column with immobilized protein G. The ß-Gal hydrolyzed the substrate *4*-aminophenylgalactoside. The generated 4AP enters into the bioelectrocatalytic amplification cycle at the glucose dehydrogenase biosensor. This immunoassay was applied for determination of *4*-nitrophenol, and the potential and the limitations of such a system are discussed.

4.2.1 Synthesis of the HOM-ß-Gal tracer

The conjugation of the HOM to ß-Gal was performed in a 3-step process.

1) *activation of the HOM*
2) *coupling to the enzyme*
3) *purification of the conjugate*

Two different activation methods were carried out during this synthesis. In the first activation method (I) N-hydroxysuccinimide and dicyclohexyl-carbodiimide were applied to obtain the activated ester function at the hapten. The second synthesis (II) used *2*-(*5*-norbornene-*2,3*-dicarboximido)-*1,1,3,3*-tetramethyl-uronium tetrafluoroborate (TNTU) and N-methylmorpholin (NMM) to obtain the activated ester function.

The coupling with the enzyme was based on the reaction of the activated ester function with the amino function of lysine side chains on the outer surface of the protein structure of ß-Gal. To obtain tracers with various characteristics 4 different dilutions of the activated HOM were mixed with enzyme solution. In this way 8 different tracers were synthesized. The final purification of the tracer was realized by dialysis with a molecular weight cut-off of 10 KDa. Free HOM with a molecular weight below 1 KDa was easily removed and the tracer with a molecular weight above 500 KDa was trapped.

4.2.2 Characterization of HOM-ß-Gal conjugates (ß-Gal tracers)

The purified tracer was stored in an amber vial at 4°C and aliquots were diluted for the experiments each day. The tracer was characterized in terms of enzyme activity, protein content, and final HOM-ß-Gal ratio.

Fig. 4.43 shows the relative specific activity of the ß-Gal tracers, as well as the determined real molar HOM/ß-Gal ratio *vs*. the initial molar ratio HOM/ß-Gal, for both procedures used for tracer synthesis (*i.e.*, I and II, see section **3.5.1**). The HOM concentration was determined spectrophotometrically at 420 nm and the ß-Gal concentration was determined using the Bradford method. From these two values the calculated ratio HOM to ß-Gal after synthesis was calculated and is shown in **Fig. 4.43**.

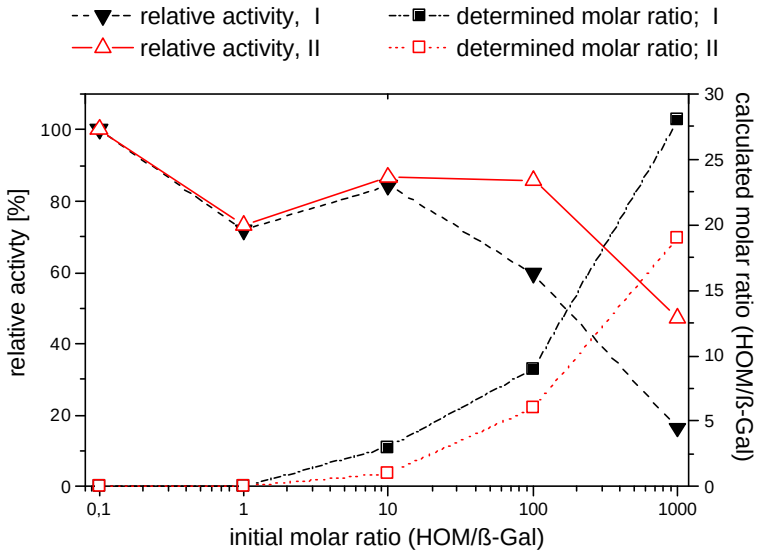

Figure 4.43: Relative *ß*-Gal specific activity in relation with the average number of HOM molecules conjugated to one protein molecule. Triangles present the specific activity of the tracers in relation to initial activity of *ß*-Gal used as reference. Squares show the calculated molar ratio between the hapten and enzyme label for each tracer. I (closed) and II (open) represent the different activation methods used during the tracer synthesis.

The relative activity of the synthesized HOM-*ß*-Gal conjugate decreased with the number of HOM molecules covalently bound to one enzyme molecule (except the initial ratio of 1:1). The initial ratio of 1000:1 led to the strongest loss in activity for both activation methods. Additionally, it can be seen that the activity of the tracer synthesized with activation procedure II was generally higher. In contrast, the coupling yield was higher using activation procedure I.

The decrease in the activity with the number of HOM molecules covalently bound to one enzyme molecule may be due to unfavorable conformational changes that take place when more HOM molecules are linked to the protein structure. Also the coupling of HOM molecule in close proximity of the active site o f the enzyme can be a reason for the decreased activity.

Activation procedure II (the TNTU-activated HOM) led to higher activity and this might be due to the conditions that were better suited for the *ß*-Gal molecules. These milder conditions of this procedure were emphasized by the fact that generally a lower coupling yield, *i.e.*, lower HOM/*ß*-Gal molar ratio, was found.

Table 4.24: *The effect of the HOM/ß-Gal molar ratio on the apparent affinity constants for the tracer and analyte. The K_{app} for $4NO_2P$ is 0.06 µmol/L.*

Activation Procedure	**HOM/ß-Gal initial molar ratio**	**K^*_{app} [µmol/L]**	**K^*_{app}/K_{app}**
I	10:1	10.9	180
I	100:1	25.0	407
I	1000:1	35.6	585
II	10:1	15.2	254
II	100:1	30.6	528
II	1000:1	41.4	704

In **Tab. 4.24** the apparent affinity constants for the ß-Gal tracers are listed. K^*_{app} is the apparent affinity for the antibody tracer interaction. K^*_{app}/K_{app} is the ratio between the apparent affinity for the tracer and $4NO_2P$, respectively.

It is obvious that the affinity of the antibody towards the tracer increased with the higher number of HOM molecules attached to one ß-Gal molecule.

4.2.2.1 EFIIA

The principle of the $4NO_2P$ determination was based on the separation of the antibody bound analyte and tracer fraction from the free fraction (unbound analyte and tracer). This was realized in a column using sepharose with immobilized protein G. This protein has a high affinity to the constant region of the antibodies. The antibodies were captured in the column while the unbound analyte and tracer molecules passed trough. The performance of the experiments is presented in **Tab. 4.25**.

Table 4.25: *Flow chart of the experiment performance using the flow system with GDH-biosensor detection*

Major steps	Single Steps	Description of the single steps	Trace in Fig. 4.44
Preparation of the Flow System	1	GDH-biosensor is mounted into the flow-through cell	
	2	HBS20 buffer is pumped through (stabilization)	
	3	4APG addition to the buffer (increasing background)	A
Separation, and Determination Of the Ab-bound Fraction	4	Off-line incubated sample mixture is injected	B
	5	Separation between Ab free and Ab bound fraction in the protein G column	
	6	The free fraction passes and results in a first peak	C (I)
	7	Buffer stream is stopped in the column and the measuring cell (background increases)	D
	8	Buffer stream is restarted (background decreases to original value in presence of 4APG)	E
	9	The aminophenol generated by the bound fraction is passes the GDH-biosensor and results in a peak	F (J)
Repetition	7a	For repetitive measurements the buffer stream in the column and the measuring cell is stopped again	D
of the Measurement	8a	Buffer stream is restarted (background decreases to original value in presence of 4APG)	E
	9a	The aminophenol generated by the bound fraction passes the GDH-biosensor and results in a peak	F´ (J´)
Regeneration	10	Disconnection of the protein G column for regeneration (removal of the bound fraction)	G
Repetition of the experiment	11	Injection of a new off-line incubated sample mixture (repetition of steps 4-9)	H

The response of the GDH-biosensor on the different steps of the experiment is plotted in **Fig. 4.44**. When the 4APG was introduced into the flow (at point A, **Fig. 4.44**), an increase in the background signal was observed. This was due to an impurity, which can be oxidized, present in the substrate. When the sample was injected (at point B), the

free tracer fraction (Ag*) passed through the protein G column and was detected by the GDH-biosensor (peak C). Since the hydrolysis of 4APG by the ß-Gal bound inside the column was relatively slow, there was no considerable change in the background current in the absence or presence of the As36-HOM-ß-Gal complex (AbAg*) trapped inside the protein G column (compare, for example, the current value before injection (trace B) and after trapping of the antibody bound tracer (before first trace D) in **Fig. 4.44**).

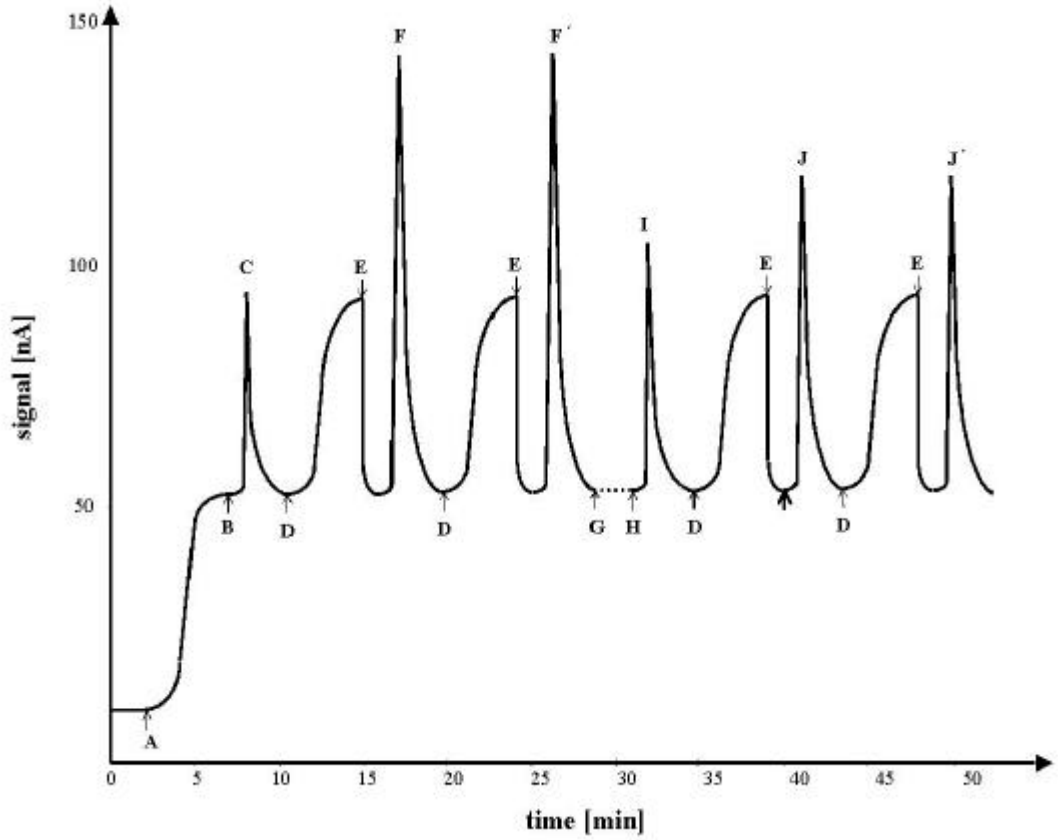

Figure 4.44: Flow-injection experiments. A: the substrate 4APG is introduced into the carrier flow, where the presence of an oxidizable impurity causes the increase in the background signal; B: the reference containing only the tracer and the antibody is injected (Ab-Ag*); C: signal given by the tracer fraction that is not bound to the antibody (Ag*); D: stopping the flow causes a new increase in the background current; E: when the flow is restarted, the background comes back to the baseline value; F: signal for the bound tracer fraction in the absence of the analyte (Ab-Ag*); G: regeneration of the protein G column; H: injection of the sample containing the analyte (Ag + Ab + Ag*); J: the peak given by measurement of bound tracer fraction in the presence of analyte (Ab-Ag* + Ab-Ag) is recorded. The measurement of the specific signals F and J were performed in duplicate.

After the complete elimination of the unbound sample fraction, the flow was stopped (at point D) for the incubation of the Ab-Ag* fraction, bound by the protein G column, with the ß-Gal substrate 4APG present in the carrier buffer. This caused an additional increase of the background current, due to the additional oxidation of the substrate impurity at the GDH-biosensor (signal between traces D and E).

When restarting the flow (at point E), the background current decreased back to its original value in presence of the 4APG. Shortly after the signal reached the baseline, the 4AP, generated during the incubation of the ß-Gal tracer fraction trapped inside the protein G column with 4APG, was detected by the GDH-biosensor (peak F). This signal was inversely correlated to the analyte concentration (compare, for example the peak J, obtained in the presence of the $4NO_2P$, with F, due to a sample containing only the antibody and tracer). The determination of the bound tracer

fraction was repeated by simply stopping the buffer stream again. This led to 4AP generation in the column again and a similar peak (compare F (J) and F´ (J´)) was obtained when restarting the buffer stream.

The Michaelis constant (K_m) for the conversion of 4APG under the action of ß-Gal and direct amperometric detection of 4AP in a flow system was found to be 180 µmol/L (Másson, Liu et al. 1995). The concentration of 4APG necessary for exploiting the maximum ß-Gal activity could not, however, be employed in the present assay. The concentration of substrate in the carrier flow was limited to only 50 µmol/L. The high sensitivity of the biosensor otherwise resulted in an enormous oxidation current background when higher substrate concentrations were used (see **Fig. 4.44**, between trace A and B). This reduced considerably the dynamic range for the biosensor measurements.

The limited concentration of 4APG reduced the velocity of the enzymatic formation of 4AP considerably. Therefore, the incubation time in the column was increased. Longer incubation would lead to more sensitive assays, but would reduce the number of analyzed samples. Finally, an enzyme-substrate incubation time of 5 min was sufficient and chosen as a compromise between the signal amplitude and analysis time. This short time is relevant for high numbers of analysis as demanded for screening purposes.

4.2.2.1.1 Antibody Dilution and Analyte Calibration

For the best assay sensitivity in competitive immunoassays the minimal possible tracer concentration has to be used. However, this decrease in concentration is limited by the deterioration in assay precision. The optimal tracer concentration was chosen in each case to be the one that gave a response about 120 times higher than the noise current, which was a signal considered sufficient for the development of an assay with a good precision. The tracers with initial HOM to ß-Gal molar ratios of 1:1 were not recognized even at very high antibody concentrations. Therefore they were not included in the following discussion. **Fig. 4.45a** and **4.45b** show the antibody dilution curves obtained for all the other tracers.

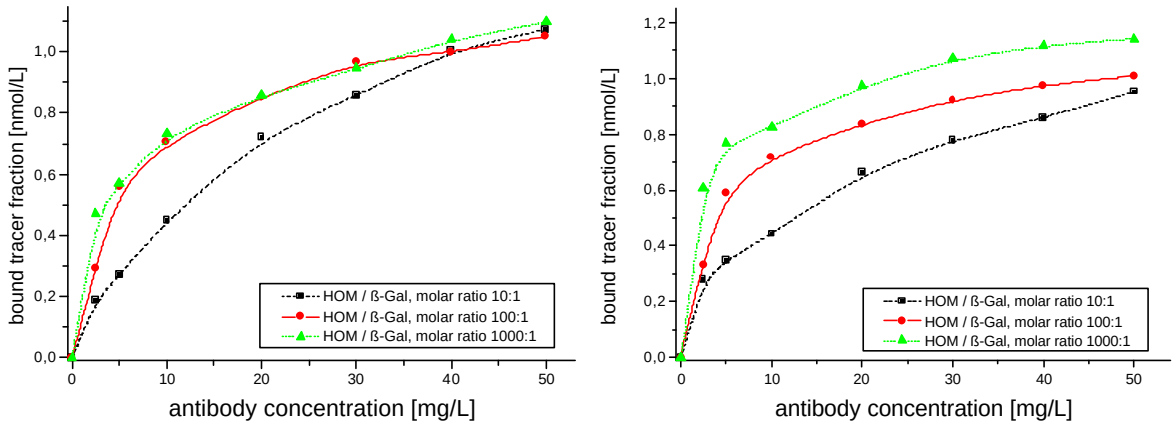

Figure 4.45: Antibody dilution curves for EFIA experiments. Tracer obtained by coupling procedure I (a) and II (b)

As expected, the tracers synthesized from the mixture containing the highest molar ratio - between hapten and enzyme label - were most easily recognized by the antibody, and the difference in affinity was more pronounced for the tracers synthesized by the activation procedure II.

Even though the same $4NO_2P$ derivative (HOM), coupled to keyhole limpet hemocyanin, was used for immunization of rabbits for production of antisera, the apparent affinity of the antibody-tracer interaction in the EFIA was however relatively low (i.e., around 10^7 mol/L, **Tab. 4.24**).

Moreover, the apparent affinity for the $4NO_2P$ was even lower (e.g., below 0.06 µmol/L), so that the developed assay led to high LLD values for $4NO_2P$ (i.e., in the µmol/L range, see **Fig. 4.46** and **Tab. 4.26**).

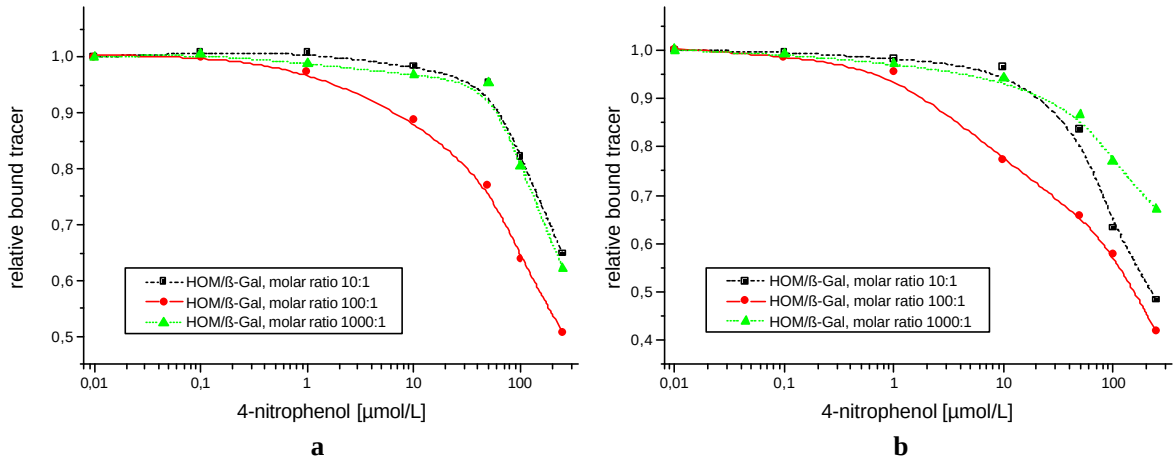

Figure 4.46: $4NO_2P$ calibration plots, flow experiments. Conditions: for concentration of tracers refer to **Tab. 4.24**; for As 36 concentrations for 50% tracer binding refer to **Tab. 4.26**. Tracers obtained by coupling procedure I (a) and II (b).

The best immunoassay performances (LLDs around 1.5 µmol/L) were obtained for the tracers with an intermediate molar ratio of hapten/*ß*-Gal. This was the ideal compromise between the two effects caused by the increase in the number of HOM groups coupled to the protein structure, the decrease in the *ß*-Gal activity (see **Fig. 4.44**), on the one hand, and the improvement of the tracer recognition by the antibody, on the other (see **Fig. 4.46** and **Tab. 4.24**).

Table 4.26: *EFIA characteristics. Symbols: $As36_{50}$ - Concentration of antibody that binds 50 % of the working tracer concentration; IC_{50} - analyte concentration that leads to 50 % inhibition of the signal in comparison with the zero dose. Other symbols, as given in Tab. 4.24. The LLD was calculated as the concentration of analyte that led to a change in signal equal to 3 times the standard deviation of signal at zero dose.*

Tracer			$As36_{50}$ [mg/L]	IC_{50} [µmol/L]	LLD [µmol/L]
A.P.	**HOM/ß-Gal, initial molar ratio**	***ß*-Gal concentration [nmol/L]**			
I	10:1	1.52	25.0	90 ± 6	19.1 ± 0.9
I	100:1	1.05	6.5	26 ± 2	1.7 ± 0.1
I	1000:1	0.94	4.5	352 ± 19	15.1 ± 0.9
II	10:1	1.30	17.3	76 ± 5	8.54 ± 0.5
II	100:1	0.80	32.5	24 ± 1	1.49 ± 0.07
II	1000:1	0.53	83.1	259 ± 12	7.0 ± 0.3

4.2.2.2 Microtiter Plate ELISA

The results obtained with the different tracers by microtiter plate ELISA are shown in **Tab. 4.27**.

Table 4.27: *ELISA characteristics. Symbols: IC_{50} - analyte concentration that leads to 50 % inhibition of the signal in comparison with the zero dose. The LLD was calculated as the concentration of analyte that led to a change in signal equal to 3 times the standard deviation of signal at zero dose.*

Tracer			IC_{50} [µmol/L]	LLD [µmol/L]
A.P.	**HOM/ß-Gal, initial molar ratio**	**ß-Gal concentration [nmol/L]**		
I	10:1	0.012	0.28 ± 0.04	0.058 ± 0.008
I	10:1	0.122	0.79 ± 0.09	0.66 ± 0.08
I	10:1	1.215	8.1 ± 0.8	1.2 ± 0.1
I	100:1	0.063	2.7 ± 0.4	0.12 ± 0.02
I	100:1	0.629	18 ± 2	1.1 ± 0.1
I	100:1	6.290	72 ± 8	24 ± 3
II	10:1	0.036	n.d.	n.d.
II	10:1	0.357	0.46 ± 0.06	0.055 ± 0.007
II	10:1	3.568	1.3 ± 0.2	0.08 ± 0.01
II	100:1	0.059	7.5 ± 0.9	0.040 ± 0.006
II	100:1	0.588	11 ± 2	0.60 ± 0.09
II	100:1	5.876	57 ± 5	9.4 ± 0.9

n.d. not determined

As seen, the best tracer in this ELISA was (A.P. II; 100:1) in its most diluted concentration, giving a LLD of 0.04 µmol/L $4NO_2P$.

A molar ratio HOM/ß-Gal (100:1), was the ideal compromise between the two effects caused by the increase in the number of HOM groups coupled to the protein structure. This corresponds to the results obtained with the EFIA. On the one hand, the ß-Gal activity decreased (**Fig. 4.44**), and on the other hand the tracer recognition by the antibody improved.

4.2.3 Discussion

The reason for the better performance of the ELISA is evidently that the substrate incubation time used was 20 h as compared to 5 min in the EFIA. A longer substrate incubation time allows the use of lower tracer concentrations, that in turn leads to lower antibody consumption. This results in a better LLD for the $4NO_2P$.

On the other hand, the higher the density of hapten derivatives on the enzyme, the higher the affinity of the antibody for the tracer is expected. The latter leads to lower antibody consumption, which is a factor that has to be taken into consideration in assay development when production of the antibodies is costly. In addition, depending on what the limitations are for a particular application, *i.e.* low LLD, broad dynamic range etc., and different tracers might prove to be useful for a particular need.

4.2.4 Summary

The possibility of combining an enzyme flow immunoassay (EFIA) for $4NO_2P$ with a PQQ dependent GDH-biosensor as the detector of the ß-Gal label was presented. The EFIA method has certain benefits, as high degree of automation and the additional amplification of the signal given by the amperometric biosensor. Some drawbacks were recognized, *i.e*. impossibility of using the optimal substrate concentration for the measurement of enzyme label activity (because of the impurity present in the commercial substrate). The EFIA developed in this work was compared with a microtiter plate ELISA, and the results obtained by the second technique are generally about 50 times better, but for a much longer (50 times) analysis time (24 min/sample for EFIA (repeat determination) compared with 20 h incubation for plate ELISA (96 samples including calibration and blank)). The results could be improved considerably by a supplementary purification of the ß-Gal substrate, which would allow higher substrate concentrations. An improvement in EFIA performance can also be expected by the increase of incubation time of the 4APG substrate and the ß-Gal fraction trapped inside the protein G-based column. Additionally the EFIA offers two possible detection strategies. First as shown here the bound fraction can be analyzed. Here, the sensitivity can be increased by longer incubation times. Secondly, the free fraction could be used for the quantification. This results in a loss of sensitivity and higher LLD, but allows shortening the time of analysis. The EFIA can be adapted according to the demanded specification of the analysis.

4.3 Heterogeneous Immunoassays for alkylphenols and alkylphenolethoxylates

A competitive immunoassay with labeled *4*-nonylphenol ethoxylate derivative was developed for alkylphenols and alkylphenol ethoxylates. The 4NPE derivative was conjugated to the enzyme label (ß-Gal) using the TNTU/NMM activation method. The conditions were chosen based on the results of the synthesis of the HOM-ß-Gal tracer. In this assay the ß-Gal tracer competed with the analyte present in the sample for a limited amount of antibody binding sites, immobilized in disposable PVC capillaries. The ß-Gal hydrolyzed its substrate 4APG. The generated *4*-aminophenol entered into the bioelectrocatalytic amplification cycle at the glucose dehydrogenase biosensor. This immunoassay was applied to the determination of 4NP, 4OP, 4NPE and 4OPE. The potential and the limitations of this system are discussed.

4.3.1 Synthesis of the HOM-ß-Gal tracer

The conjugation of the *4*-nonylphenol derivative to ß-Gal was performed in a 3-step process.

1. *activation of the 4-nonylphenol derivative*
2. *coupling to the enzyme*
3. *purification of the conjugate*

The activation of the 4NPE derivative was performed using 2-(5-norbornene-2,3-dicarboximido)-1,1,3,3-tetramethyl-uronium tetrafluoroborate and N-methylmorpholin to obtain the activated ester function. The coupling with the enzyme was based on the reaction of the activated ester function with the amino function of lysine side chains on the outer surface of the protein structure of ß-Gal.

4.3.2 Characterization of the ß-Gal tracers

Two methods were used for the determination of the activity of the free ß-Gal preparation and the ß-Gal tracer.

4.3.2.1 Optical activity measurements

First, a calibration with 4NP at concentrations between 10 and 90 µmol/L was performed, giving an extinction coefficient of 13250 L/mol/cm. The reference value was 18500 L/mol/cm (Roche-Industries 1999). The difference can be explained by variations in the buffer system. The experimentally determined value was used for all further calculations. Next, the initial activity of the free ß-Gal preparation was determined by measurement of the absorbance change due to formation of 4NP that correlated to the ß-Gal concentration present in the cuvette. Based on measurements of three ß-Gal dilutions (50, 100, 200 µg/L), the ß-Gal activity was found to be 311 ± 28 units/mg. This is comparable with the data provided by the supplier, which is 250-400 units/mg (Roche-Industries 1999).

The activity of the ß-Gal tracer was determined in the same way as above from the stock solution collected after the purification using the dilution factors 1:10000, 1:20000, and 1: 50000, respectively. The ß-Gal tracer activity in the stock solution was found to be 46.3 ± 2.1 units/mL.

4.3.2.2 Results obtained with the bioelectrochemical method using the GDH-FI system

The reaction of ß-Gal with its substrate 4APG results in increasing 4AP concentrations. Using consecutive injections the time dependence of this reaction was monitored with the GDH-FI system. By mixing ß-Gal with 2 mmol/L of 4APG, the reaction was started. During 10 min three successive injections of this solution into the GDH-FI-system were performed under strict time control. As soon as the enzymatically formed 4AP reached the GDH-biosensor, three oxidation peaks occurred.

This procedure was repeated for three free ß-Gal solutions containing 0.1, 0.2, and 0.5 µg/L, respectively. From the change in peak height with time, and thus the change in 4AP concentration with time, the free ß-Gal activity could be calculated and was found to be 268 ± 12 units/mg.

The ß-Gal tracer activity was determined in the same way as described for the free enzyme. The measurements were performed with the diluted tracer stock solution (1:500000, 1:1000000, and 1:2000000, respectively), and the calculations resulted in a ß-Gal tracer stock activity of 37.9 ± 0.7 units/mL.

Table 4.28: *Summarized characteristics of free ß-Gal and the synthesized tracer determined with the optical and bioelectrochemical method.*

Method	free ß-Gal		tracer	
	activity units/mL	concentrations µg/L	activity units/mL	dilutions
optical	311 ± 28	50, 100, 200	268 ± 12	1:10000, 1:20000, 1:50000
bioelectrochemical	46.3 ± 2.1	0.1, 0.2, 0.5	37.9 ± 0.7	1:500000, 1:1000000 1:2000000

The absolute activity values obtained by the optical and the electrochemical method differ, which is a result of the different substrates used. For comparison of the two methods the activity values for the tracer were divided by the values for the free ß-Gal. The obtained ratios were 0.149 (optical) and 0.141 (bioelectrochemical), which shows that the two methods compare very well. The advantage of the GDH-biosensor is the higher sensitivity. Less than 1 µg/L of the enzyme/tracer was needed for the measurement, while around 100 µg/L was needed for the optical method, with the incubation time being in the same range for both methods. The high detectability of the ß-Gal tracer in the GDH-FI system is especially interesting for immunoassay purposes. Secondly, the electrochemical measurements were performed in an automated flow system, reducing the manual working steps and thus decreasing the deviation between the measurements.

4.3.2.3 Tracer stability studies

The tracer stability was investigated over a period of two months by measuring the activity of the tracer stock and diluted tracer solutions using the GDH-FI system. The results are shown in **Fig. 4.47**. The stock solution shows a loss of around 25 % of the initial activity over a period of two month (a). On the other hand, the activity of the more diluted samples (1:1000) decreased rapidly within one week compared to the day of dilution. Two diluted samples were tested more frequently over a period of one week. Both solutions lost 75 % of their activity after 7 days. Additionally, three dilutions were prepared the same day and the activity was determined to exclude errors in the preparation. After 5 days of storage in the refrigerator the activity was measured and all three samples showed a decrease to approximately 30 % of the initial value. Based on these results the tracer was kept in the stock solution and the final dilution for experiments were prepared on the day of use.

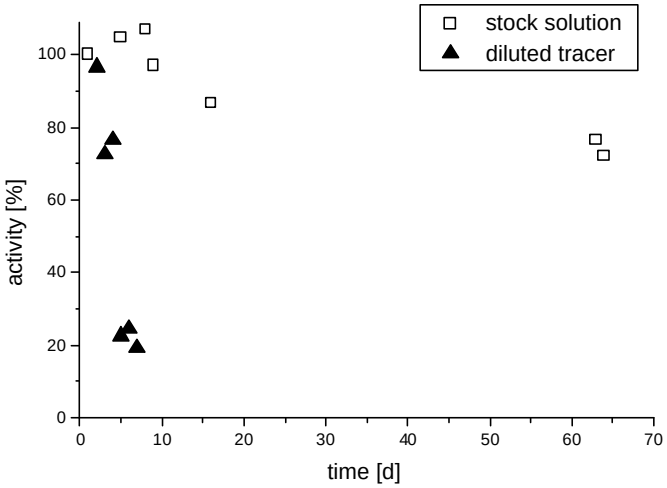

Figure 4.47: The stability of the ß-Gal tracer, stored at 4°C in HBS20, was tested bioelectrochemically in the GDH-FI system. Measurements were performed in the substrate buffer (HBS20 with 10 mmol/L glucose and 1 mmol/L 4APG) at a constant flow of 0.3 mL/min. The working potential was + 0.3 V vs. Ag/AgCl.

4.3.3 Microtiter plate ELISA

For ELISA experiments commercially available plates with an unknown amount of immobilized antibodies were used. The microtiter plate ELISA was performed to show the possibility to use the tracer in a competitive immunoassay, and also for comparison with the developed CIA.

Four analytes (NP, NPE, OP, OPE) were tested in the same concentration range as mentioned in the protocol for the commercial kit (Takeda-Industries 2000). The analyte calibration curves of the four different compounds are shown in **Fig. 4.48**.

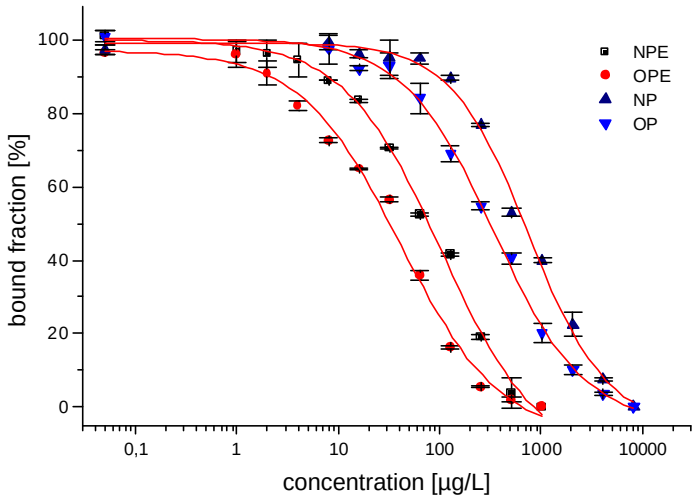

Figure 4.48: ELISA for APEs/APs. The ß-Gal tracer was diluted 1:20000 times. The blank was subtracted from the original data before calculating the relative signal.

These results were obtained after 200 min reaction of the antibody bound ß-Gal label with $4NO_2PG$ to produce the colored $4NO_2P$. The differences in the antibody affinity towards the various analytes are apparent. The IC_{50} values (at which 50 % of the initial tracer binding is observed) were obtained from the mid-point of the sigmoidal fit. For

the APEs the IC_{50} were 42 µg/L for OPE and 104 µg/L for NPE, thus allowing the quantification in the low µg/L range. The IC_{50} values for the AP were higher, i.e. 769 and 346 µg/L for NP and OP, respectively. The affinity of the antibody for APEs is much better than for the APs. The reason for this is most likely that the antigen used for immunization was based on an APE derivative and not on an AP. The other trend observed is the better recognition of the octyl derivatives compared to the nonyl derivatives. This is more surprising since the derivative used for immunization was a 4NPE derivative. Takeda Industries observed the same trend in the original ELISA developed. These ELISA experiments using the ß-Gal tracer showed similar results in terms of IC_{50} values as reported for the commercial kit from Takeda based on an HRP tracer, while the color development time is 200 min in contrast to 30 min for the commercial kit (Takeda-Industries, 2000).

4.3.4 Capillary immunoassay (CIA) with disposable separation units

A capillary immunoassay (CIA) based on electrochemical detection was developed using ß-Gal as the enzyme label. A GDH-biosensor was used to quantify the amount of the ß-Gal tracer based on determination of 4AP liberated by ß-Gal from its substrate 4APG.

The incubation of the analyte and tracer inside the antibody-coated capillaries and the washing steps were performed off-line whereas the determination of the bound tracer was performed using the GDH-FI system. The ß-Gal tracer activity bound inside the capillaries was determined by mounting the capillary into the loop of the injection valve of the GDH-FI system. The 4APG substrate solution was passed through the capillary where the contact time with the bound tracer was controlled by automatically switching the valve into "load" position (*i.e.* stop-flow in the capillary) after a fixed period, as described in the experimental section. A long stop-flow time in the capillary led to higher 4AP production and the observed current increased. As a compromise between short assay time and little tracer consumption the off-line incubation time in the capillaries was set to 150 s.

4.3.4.1 Methanol content in the buffer

Previously, a positive effect of methanol addition to the substrate buffer was reported (Takeda-Industries, 2000). Therefore the measurement of the antibody-bound tracer was performed in buffer solution containing different amounts of methanol. 4 sets of 3 similar capillaries were incubated for 20 min with diluted tracer (1:10000) in these experiments. No significant changes were observed in signal intensity when varying the MeOH content between 0 and 10 % (v/v) (results not shown). However, a significant influence on the reproducibility using different capillaries of the same batch was visible. The presence of MeOH showed a positive effect on the reproducibility when compared with methanol-free solution. 5 % MeOH reduced the differences to almost a quarter while 1 and 10 % MeOH gave slightly higher values. Therefore 5 % MeOH was present in the buffer during all the following experiments.

4.3.4.2 Optimization of the off-line incubation time

The next step was to optimize the off-line incubation time of the analyte and tracer in the capillaries. A short off line incubation of the tracer/sample mixture would be favorable since this would allow short assay times and thus the analysis of a higher number of samples, while longer incubation will cause more complete binding of tracer and analyte resulting in a higher signal. The influence of the incubation time is shown in **Fig. 4.49**. The equilibrium is reached after approximately 30 min and small differences in the incubation time will not lead to major changes of the amount of bound tracer and thus in the resulting signal.

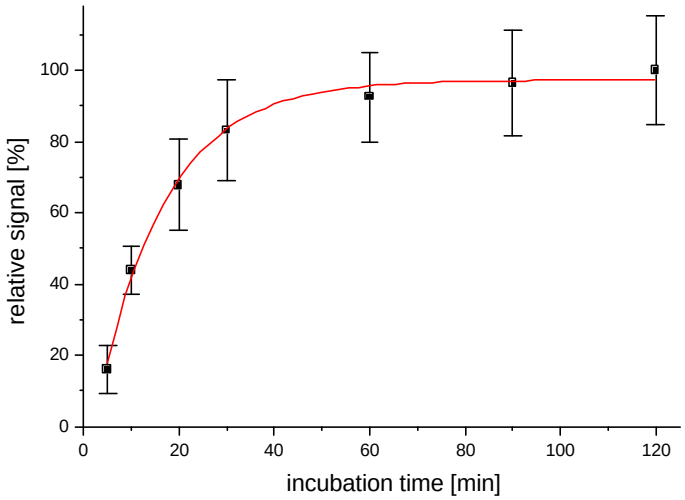

Figure 4.49: Influence of the off-line incubation time in the capillaries on the binding of tracer. Tracer dilution: 1:10000. The oxidation current obtained after 120 min was set to 100 % and all other values are given in relation. Measurements were performed in the substrate buffer (HBS20 with 5% methanol, 10 mmol/L glucose, and 2 mmol/L 4APG) at a constant flow of 0.3 mL/min. The working potential was + 0.3 V vs. Ag/AgCl.

The conditions chosen for the final assay were as follows: The substrate buffer was HBS20 containing 10 mmol/L glucose, 2 mmol/L 4APG, and 5 % methanol. The off-line incubation time for the tracer/analyte mixture in the antibody capillaries was 30 min. The contact time of ß-Gal with the substrate (4APG) was 150 s, while the valve was switched back to "load" position after 30 s. The tracer dilution in the final assay (**Fig. 4.50**) was set to 1:5000. This resulted in a signal of about 100 times the noise ratio in the absence of any analyte.

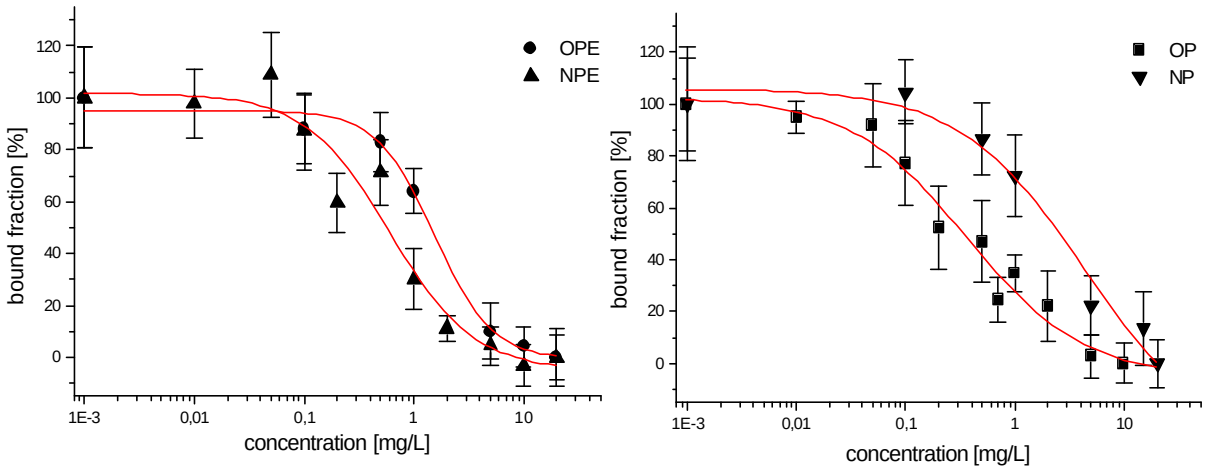

Figure 4.50: CIA measurements for AP and APEs using the GDH-FI system. The off-line incubation for the analyte-tracer mixture in the capillary was 30 min. The injection time was 30 s and the stop flow time was 150 s. Other conditions: as in **Fig. 4.49**.

In **Fig. 4.50**, the assays for four analytes are shown. For NPE and OPE the IC_{50} values were 378 and 605 µg/L, respectively. These numbers were lower compared to those of the APs, i.e., 1560 µg/L for OP and 4481 µg/L for NP. In comparison with the plate ELISA the IC_{50} values for all four analytes are higher using the capillaries, which most likely is due to the fact that the final quantification step was only 2.5 min in the CIA, while the development time in the plate ELISA was 200 min.

4.3.4.3 Cross reactivity studies

The effect of four possible cross reactants (*i.e*. phenol, 2,4,6-tricholorophenol, SDS and a technical LAS mixture) was tested. Phenol and *2,4,6*-tricholorophenol were chosen because of the structural relation to the main analytes as well as for their environmental relevance. SDS and LAS are anionic surfactants also present in many environmental samples. 50 mg/L of these compounds were used in the competitive assay format together with the APE tracer. Cross reactivity (CR) of the antibody with these compounds would result in an inhibition of the tracer signal at zero analyte doze. Only LAS showed a signal that was approximately 65 % of the initial (100 % tracer) signal, while none of the other compounds showed any significant CR (**Fig. 4.51**).

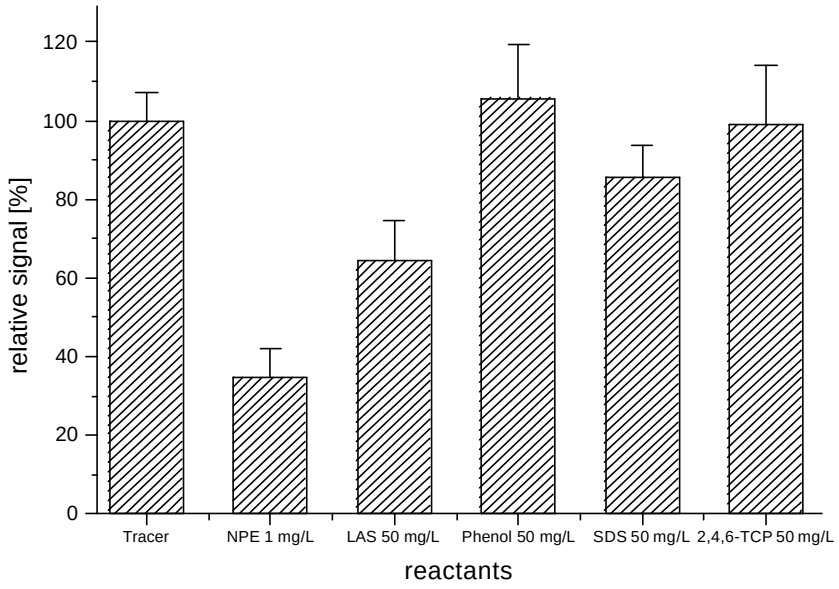

Figure 4.51: Influence of four possible cross reactants on the tracer signal at zero analyte doze. 50 mg/L of each compound were incubated for 30 min together with the APE tracer in the antibody-coated capillaries. The signals for the tracer at zero analyte doze and for 1 mg/L of NPE are plotted for comparison. Other conditions: as in **Fig. 4.49**.

To quantify the CR the signal for 50 mg/L of cross reactant was related to the concentration of the main analytes that showed the same diminution of the initial tracer signal. This corresponding analyte concentration was divided by 50 mg/L and the relative values in percentage are listed in **Tab. 4.29**.

Table 4.29: *Cross reactivity for four possible interfering compounds. The signals obtained for 50 mg/L of these cross reactants were divided with the concentration of the four main analytes that gave the same signal as with 50 mg/L cross reactant and expressed in percent.*

Cross reactants / Analytes	Linear alkylbenzene sulphonates	Sodium dodecyl sulphate	*2,4,6*-Trichlorophenol	Phenol
OPE	0.7	0.3	< 0.1	< 0.1
OP	1.9	0.8	< 0.1	< 0.1
NPE	0.3	0.1	< 0.1	< 0.1
NP	2.7	0.9	< 0.1	< 0.1

As shown there, the influence of all the selected cross reactants is below 1 % if compared to the ethoxylates. This is comparable with data reported in the operational manual of Takeda-Industries (Takeda-Industries 2000).

4.3.4.4 Unspecific binding of the tracer

For these experiments capillaries with immobilized BSA were used. The tracer was incubated in the capillaries for periods of 10 min up to 2 h, but no ß-Gal activity was observed in the GDH-FI system at incubation times less than one hour. The unspecific binding was recognized only after 2 h of incubation. Even after this long time-period the determined tracer amount was only 5 % of that found with antibody-coated capillaries after 30 min.

4.3.5 Summary of the capillary immunoassay for alkylphenols and alkylphenolethoxylates

We developed a capillary-based immunoassay (CIA) for APEs and AP, utilizing a GDH-biosensor for the label detection. ß-Gal was chosen as the enzyme label, which can be used at optimal pH conditions of the GDH-biosensor. This allows the quantification of the enzymatically-liberated 4AP downstream without changing the pH or the composition of the buffer system. The presence of the ß-Gal substrate in the buffer gives an increased background current, but nevertheless sensitive 4AP detection (47.3 nAL /µmol) in the presence of 4APG is possible using the GDH-biosensor.

The bioelectrochemical activity determination of ß-Gal, based on the determination of the enzymatically-liberated 4AP was compared with the more commonly performed optical measurements. Both approaches showed comparable results but the bioelectrochemical method reaches a much lower detection limit after shorter incubation times.

Figure 4.52: Final portable device for on-site analysis of phenolic compounds using a GDH-biosensor.

For the competitive immunoassays, an APE-derivative was labeled with ß-Gal. This tracer was mixed off-line with the sample. For competition this solution was filled into PVC capillaries coated with anti-APE antibodies. After the equilibrium was reached a manual-washing step followed. The amperometric GDH-biosensor placed in a flow system was utilized to quantify the antibody-bound tracer fraction and thus the analyte concentration in the sample within only a few minutes. The capillary immunoassay is very promising for future use as a screening tool in environmental applications.

Better assay performance may be obtained by optimization of the capillary pre-treatment and coating conditions. Up to now the amount of antibodies in the capillaries and different tracer synthesis were not further investigated. For a laboratory based-system an additional automation of the incubation and washing steps would be desirable. The main goal for the future development is the integration of the capillary immunoassay in the portable device for on-the-spot measurements (**Fig. 4.52**) where the capillaries can be used directly for the injection.

5 Conclusion and outlook

The development of fast and reliable biochemical tools for on-site screening in environmental analysis was the main target of the present work. Due to various hazardous effects such as endocrine disruption and toxicity phenolic compounds are key analytes in environmental analysis and thus were chosen as model analytes.

We developed a glucose dehydrogenase (GDH) biosensor, which could be used for the determination of phenolic compounds in the low nanomolar range. Moreover, this biosensor should be applicable in automated laboratory flow systems as well as in portable devices for on-site analysis. Additionally, the GDH-biosensor was used as label detector in enzyme-labeled flow-immunoassays. Therefore, a method in an automated flow system must be developed to determine the activity of the labeling enzyme.

To accomplish these goals GDH was immobilized on various electrode materials:

* *Carbon paste electrodes (CPE)*
* *Spectroscopic graphite electrodes (SGE)*
* *Screen-printed carbon electrodes (SPCE)*
* *Platinum based thick-film electrodes (Pt-TFE)*

Carbon paste electrodes

Based on previous work GDH-CPE were prepared with polyethylene imine (PEI) as polyelectrolyte. These electrodes were characterized both in a batch and a flow injection system to obtain information such as equilibration time before the first measurement, oxidation potential, pH dependency, response behavior to various analytes and reproducibility of sensor preparation. The electrodes offered high sensitivity with LLDs in the low nanomolar range in the batch system. Obvious drawbacks were found concerning long equilibration times and reproducibility of the manufacturing process. Additionally, the experiments in the flow system showed that the response of the GDH-PEI-CPE was very slow and thus not applicable. Therefore, modification of the carbon paste composition was tested. The application polystyrene sulfonic acid (PSSA; more negatively charged than PEI) shortened the equilibration time from 10 to 2 h and led to better reproducibility of sensor preparation. Also, the response behavior was improved for dopamine. The experiments showed dependence between the composition of the carbon paste, thus the charge of the electrode surface, and the response behavior for the analyte. For dopamine (a more hydrophilic analyte) the influence of the negatively charged PSSA was positive while for the determination of hydroquinone (more hydrophobic) the PEI-CPE showed faster response. This observation is of high interest during further immobilization experiments and sensor development.

The application of GDH-PSSA-CPE led to a sample throughput of 20 samples/h for 4-aminophenol (4AP) and 15 samples/h for dopamine (Dop). The LLD for the two analytes was 2 and 10 nmol/L, with a dynamic range up to 300 and 500 nmol/L.

Nevertheless, further optimization of the CPE composition and the flow system characteristics did not lead to an acceptable reproducibility of the GDH-CPE preparation. Too many manual steps are included here, and this makes it very difficult to obtain a consistently high quality biosensors.

Spectroscopic graphite electrodes

Immobilization of an enzyme by adsorption is a simple procedure for biosensor preparation. Unfortunately, our experiments showed that GDH could not be simply absorbed on a solid graphite rod using a procedure described in literature for cellobiose dehydrogenase. The GDH is either not adsorbed or easily removed from the surface of the electrode. Therefore, spectroscopic graphite was unsatisfactory as an immobilization support for GDH-biosensor development.

Screen-printed carbon electrodes

GDH was adsorbed on SPCE, and in contrast to spectroscopic graphite rods it was shown that this immobilization of the GDH led to an amplification of the oxidation current by enzymatic conversion of the oxidized analyte molecule. Higher sensitivity of the biosensor was obtained in presence of glucose than in its absence. All experiments with the GDH-SPCE were performed only in a batch system. The equilibration times were shorter than found with the carbon paste electrodes, but the LLDs for dopamine and 4AP were worse. The ease of preparation was an obvious advantage, but the sensor characteristics (LLD, sensitivity, stability, etc.) were not satisfactory.

Platinum based thick-film electrodes

GDH was successfully embedded into the polyurethane network on top of platinum based TFEs. This was a simple and very reproducible manufacturing process to obtain a large number of biosensors with excellent characteristics. The reproducibility within one batch of sensors was below 5 %. This immobilization technique led to an excellent long-term and working stability of the GDH-TFE that is superior to comparable systems described in literature. Additionally, a short equilibration time (less than 30 min in comparison with 2 h for optimized PSSA-CPE) before the first measurement was achieved. This represents a great benefit compared with the techniques used for GDH immobilization that were discussed above.

Furthermore, the optimization of the polymer layer led to fast responding sensors applicable for the use in flow injection analysis. In the optimized semi-automated flow system up to 24 samples/h can be analyzed. The sensitivity for various phenolic compounds was extremely good. Detection limits in the low nanomolar or subnanomolar range (0.7 nmol/L for 4AP) combined with an extended linear range (*e.g.*, three orders of magnitude for catecholamines) were obtained.

Summarizing, the properties of the GDH-TFE-biosensor reflect the very successful attempt to develop a fast and reliable detection system for phenolic compounds of various origins. Applications in automated flow-systems as well as for screening purposes in on-site analysis are conceivable. Moreover, the high sensitivity towards 4AP makes the GDH-TFE a promising tool as a detector in immunoassays using an enzyme. The GDH-TFE was tested for different applications.

Application for analysis phenol mixtures

Enzyme biosensors provide only limited information about the analyzed sample. The concentration is related to one standard compound (*i.e.* equivalents of the calibration standard) and information about single components is usually not obtained, only when a very specific enzyme is applied. Sensorarrays can be used to overcome this bootleneck. Therefore we favored an approach, where various phenol-converting enzymes are involved. The idea is to determine the composition of an unknown sample by analysis of the peak height and additionally by examination of the peak shape. Finally, the response pattern of the different enzymes could be chemometrically analyzed.

In this experiments the GDH-biosensor was tested using a mixture of four phenolic compounds of environmental interest. The final goal was to learn about the peak pattern obtained with the GDH-biosensor for the mixtures containing different concentrations of each compound. To exclude the influence of time a stability solution (one mixture with a fixed concentration of the four analytes) was injected at frequent intervals.

Unfortunately, the peak shape did not change remarkably for the different compositions. Based on these results no chemometric evaluation was successful. Nevertheless, the experiment emphasized the applicability of the GDH-biosensor in an automated flow-system and confirmed its excellent stability. Over the whole period of 11 h the baseline was stable and there was no significant change in the peak shape for the injections of the stability solution. The statistical evaluation of the peak height for these injections emphasized the remarkable characteristics of the GDH-biosensor. The mean peak height decreased by less than 1 nA in 11 h (*i.e.*, 1.64%/h). This is an extraordinary result for the stability of a biosensor, especially when taking into an account the high number of analyzed phenol mixtures and their high concentrations.

Implementation of the GDH-biosensor into the portable device and on-site application

For on-site analysis of phenolic compounds the GDH-biosensor was supposed to be integrated into a small portable device. Little reagent and electrical power consumption combined with ease of use were the edging demands of this development. Therefore, the GDH-biosensor was fitted as the detector into a portable device that was based on a flow system with an integrated flow cell. The pump was manually driven to prevent the high demand of electricity, and thus a discontinuous buffer flow was realized. The sensitivity decreased to 19.4 nA·L/µmol for dopamine using the portable device, when compared with 28.9 nA·L/µmol in the automated flow system. This can be explained by different flow characteristics. The measuring cell was not identical with the one used in the automated system and an identical flow rate for each injection cannot be achieved by the user. Additionally, higher background noise and higher standard deviation for the measurements was observed with the portable device.

Nevertheless, the device equipped with a GDH-biosensor was successfully applied for the evaluation studies of two wastewater treatment plants during a field experiment (BIOSET EU Technical Meeting: "Biosensors for evaluation of the performance of wastewater treatment works") in Barcelona.

Using the standard addition method we were able to indicate the reduction of phenolic compounds, estimated as catechol equivalents, during the wastewater treatment process. The highest pollution was found for the raw influent but the treatment resulted in a reduction of approximately 90 % of phenolic contaminants during the cleaning processes. Moreover, the comparison with a CDH-biosensor and a Tyr-SPCE underlined the usability of such devices for screening purposes in environmental analysis. Even the absolute values differed due to the differences in selectivity of the three enzymes, the on-going treatment was observable and the results were comparable to the ones obtained by chemical analysis and toxicity assessment. These facts made the GDH-biosensor a promising tool to use for the evaluation of the two WWTPs.

Application of GDH-biosensor for ß-Gal detection

The GDH-biosensor was applied for the detection of ß-Gal used as enzyme label in an immunoassay. Since the optimal pH value for the sensor response is around 7.5, which is approximately the same for the reaction catalyzed by ß-Gal, the GDH-biosensor allows the downstream quantification of the enzymatically-liberated 4AP without changing the pH or the composition of the buffer system.

The presence of the ß-Gal substrate (*4*-aminophenyl-ß-*D*-galactopyranoside; 4APG) in the buffer gives a high background current, but nevertheless sensitive 4AP detection (47.3 nA L/µmol) in the presence of 4APG is possible using the GDH-biosensor. The determination of ß-Gal activity with the GDH-biosensor was compared with the more commonly performed optical measurements. Both approaches showed comparable results, but the bioelectrochemical approach reached a much lower detection limit, and the automaton led to a better reproducibility of the results.

The GDH-biosensor was able to determine 0.19 µg/mL ß-Gal (ß-Gal activity 311 ± 28 units/mg) at room temperature and a 4APG concentration of 2 mmol/L. This was an 18-fold improvement compared with an unmodified electrode. The sensitivity increased by more than 6 times. This allows discriminating very small amounts of the ß-Gal. These results were compared with optical measurement of enzymatically-liberated *4*-nitrophenol. The bioelectrochemical method was superior in terms of sensitivity and reproducibility and it still offers further possibilities of automation.

These data showed that the GDH-biosensor is a very promising tool for label detection in immunoassays. Performing the experiments at a temperature of 45°C would further increase the sensitivity and lower the LLD, but a more sophisticated equipment would be needed. The results suggested that the GDH-biosensor might be used for the determination of *E coli* according to the method described by Nistor et al. (Nistor, C. 2002a). In that paper 4AP produced by bacterial ß-Gal was monitored with a CDH-biosensor and compared with chemiluminometric measurements. It was shown that with better LLD the time for initial *E. coli* detection decreased. A comparison of our GDH-biosensor with the CDH-biosensor showed the potential for improving the results for bacteria detection. The LLD for ß-Gal was 20-fold lower with the GDH-biosensor. This would allow *E. coli* detection in samples with very low bacterial numbers, *e.g.* in drinking waters.

Heterogeneous immunoassay for *4*-nitrophenol ($4NO_2P$)

The possibility of combining an enzyme flow immunoassay (EFIA) for $4NO_2P$ with a PQQ dependent GDH-biosensor as the detector of the ß-Gal label was presented. The EFIA method has certain benefits, as high degree of automation and the additional amplification of the signal given by the amperometric biosensor. Some drawbacks were also recognized, *i.e.* impossibility of using the optimal substrate concentration for the measurement of enzyme label activity (only 50 µmol/L 4APG were used because of the impurity present in the commercial substrate). The developed EFIA was compared with a microtiter plate ELISA, and the results obtained by the second technique were generally about 50 times better, but for a much longer (50 times) analysis time (24 min/sample for EFIA (double injection) compared with 20 h incubation for plate ELISA (96 samples including calibration and blank)). The results could be considerable improved by a supplementary purification of the ß-Gal substrate allowing higher substrate concentrations. An improvement in EFIA performances can be also expected by the increase of incubation time between the 4APG substrate and the ß-Gal fraction trapped inside the protein G-based column. Additionally the EFIA offers two possible detection strategies. First, as shown here, the bound fraction can be analyzed. Here, the sensitivity can be increased by longer incubation times. Secondly, the free fraction could be used for the quantification. This would result in a loss of sensitivity and higher LLD, but allows shortening the time of analysis. According to the intent of the analysis the EFIA can be adapted by measuring the free or bound fraction and by changing the stop-flow settings.

Heterogeneous Immunoassays for alkylphenols (AP) and alkylphenolethoxylates (APE)

For on-site analysis we developed a capillary immunoassay (CIA) for APE and AP, utilizing the GDH-biosensor for the label detection. This could be combined with the portable device described for the evaluation of the cleaning efficiency in wastewater treatment plants.

For the competitive immunoassays, an APE-derivative was labeled with ß-Gal. This tracer was successfully tested in a microtiter plate. Comparing the results obtained with the assay using ß-Gal-tracer and the ELISA, commercially available from Takeda Industries, we observed the same measuring range and the same allocation in the IC_{50} values (OPE<NPE<OP<NP). This underlines the applicability of the ß-Gal-tracer in the capillary immuno assay.

For the CIA, the tracer was mixed off-line with the sample. For competition, this solution was filled into PVC capillaries coated with anti-APE antibodies. The equilibrium was reached after 30 min and a manual-washing step followed. The final measurements were performed in an automated flow-system and the capillary was integrated as part of the injection-loop. The antibody bound tracer fraction was quantified by the amperometric GDH-biosensor placed in a flow system and thus the analyte concentration in the sample was determined. A set of measurement with triplicate injection for each capillary was completed in only 10 min. The IC_{50} values obtained with the CIA are about a decimal power above the results gained with the ELISA. The cross reactivity of structural related compounds and other surfactants was below 1% compared with the APE. This allows a good correlation of signals with the presence of AP and APE. Summarizing, the capillary immunoassay is very promising for future use as a screening tool in environmental applications, especially for a small number of samples.

Better assay performance may be obtained by optimization of the capillary pre-treatment and coating conditions. Up to now the amount of antibodies in the capillaries and different tracer synthesis were not further investigated. When working in a laboratory based-system an additional automation of the incubation and washing steps would be desirable. The main goal for the future development is the integration of the capillary immunoassay in the portable device for on-spot measurements where the capillaries can be used directly for the injection into a portable device.

The results of this thesis emphasize that GDH is a valuable biorecognition element and embedding this enzyme in an adapted environment leads to high stability and excellent biosensor characteristics. The use of screen-printed electrodes as basic transducers allows the preparation of a large number of amperometric biosensors with consistently high reproducibility. The GDH-biosensors can be introduced as screening tools in various analytical fields and the combination with immunoassay technology even widens its application area.

6 References

American Chemical Society (23.01.2002) Environmental Science and Technology: Biosensor Defined (http://pubs.acs.org/hotartc/est/96/nov/biosensor.html)

Ahel, M. and Giger, W. (1985); Analytical Chemistry **57**: 1577

Ahel, M., Giger, W. and Schaffner, C. (1994); Water Research **28**: 1143

Akerstrom, B. and Bjorck, L. (1986); J Biol Chem **261** (22): 10240

Anderson, P. G., Magan, A. J., Ligler, F. S. and King, K. D. (1997); Biosensors & Bioelectronics **12** (4): 329

APE research council, August 8, 2001; (http://www.aperc.org)

Appelqvist, R., Marko-Varga, G., Gorton, L., Torstensson, A. and Johansson, G. (1985); Analytica Chimica Acta **169**: 237

Aprea, C., Colosio, C., Mammone, T., Minoia, C. and Maroni, M. (2002); Journal of Chromatography B **769**: 191

Arce, L., Ríos, A. and Valcárcel, M. (1998); Journal of Chromatography A **827**: 113

Arrhenius, S. (1907); Immunochemie. Akademische Verlagsgesellschaft, Leipzig

Arthur, C. L., Potter, D. W., Buchholz, K. D., Motlagh, S. and Pawliszyn, J. (1992); LC-GC **10**: 656

Barman, T. E. (1969); Enzyme Handbook, vol. 1 and 2. Springer-Verlag, Berlin, Heidelberg, New York

Bartlett, P. N. and Cooper, J. M. (1993); Journal of Electroanalytical Chemistry **362**: 1

Bately, G. E. (1987); Journal of Chromatography A **389**: 208

Bauer, C. G., Eremenko, A. V., Förster-Ehrentreich, E., Bier, F. F., Makower, A., Halsall, B. H., Heineman, W. R. and Scheller, F. W. (1998); Analytical Chemistry **68** (15): 2453

Bauer, C. G., Eremenko, A. V., Kühn, A., Kürzinger, K., Makower, A. and Scheller, F. W. (1998); Analytical Chemistry **70**: 4624

Bennett, E. R. and Metcalfe, C. D. (1998); Environmental Toxicology and Chemistry **7**: 1230

Bennie, D. T., Sullivan, C. A., Lee, H.-B., Peart, T. E. and Maguire, R. J. (1997); The Science of the Total Environment **193**: 263

Berson, S. A. and Yalow, R. S. (1959); Nature (London) **256**: 495

Bier, F. F. (1998); Analytical Biochemistry, Potsdam University, Potsdam

Bier, F. F., Förster-Ehrentreich, E., Makower, A. and Scheller, F. W. (1996); Analytica Chimica Acta **328**: 27

Bilitewski, U. and Turner, A. P. (2000); Biosensors for environmental monitoring. Harwood Academic Publishers,

Bjorck, L. and Kronvall, G. (1984); J Immunol **133** (2): 969

Bjorck, L., Miorner, H., Kuhnemund, O., Kronvall, G. and Sundler, R. (1984); Scand J Immunol **20** (1): 69

Blackburn, M. A., Kirby, S. J. and Waldock, M. J. (1999); Marine Pollution Bulletin **38**: 109

Blake, C. and Gould, B. J. (1984); The Analyst: 109

Bolz, U., Körner, W. and Hagenmaier, H. (2000); Chemosphere **40**: 929

Boos, K. S., Walfort, A., Lubda, D. and Eisenbeiss, F. (1991); DE1 30 475 AL; Germany

Bradford, M. M. (1976); Anal Biochem **72**: 248

Brodfuehrer, J. I., Chapman, D. E., Wilke, T. J. and Powis, G. (1990); Drug Metab Dispos **18** (1): 20

Brouwer, E. R. and Brinkman, U. A. T. (1994); Journal of Chromatography A **678**: 223

Burestedt, E., Kjellström, S., Emnéus, J. and Marko-Varga, G. (2000); Analytical Biochemistry **279** (1): 46

Burestedt, E., Nistor, C., Schlagerlöf, U. and Emnéus, J. (2000); Analytical Chemistry **72** (17): 4171

Busto, O., Olucha, J. C. and Borrull, S. (1991); Chromatographia **32**: 423

Cardwell, T. J., Hamilton, I. C., McCormick, M. J. and Symons, R. K. (1986); International Journal of Environmental Analytical Chemistry **24**: 23

Cass, A. E. G. (1990); Biosensor . A practical approach. IRL Press, Oxford

Castillo, M., Alonso, M. C., Riu, J., Reinke, M., Klöter, G., Dizer, H., Fischer, B., Hansen, P. D. and Barceló, D. (2001); Analytica Chimica Acta **426**: 265

Castillo, M. and Barceló, D. (1997); Trends in Analytical Chemistry **16**: 574

Castillo, M., Riu, J., Ventura, F., Boleda, R., Scheding, R., Schroder, H. F., Nistor, C., Emnéus, J., Eichhorn, P., Knepper, T. P., Jonkers, C. C. A., de Voogt, P., Gonzalez-Mazo, E., Leon, V. M. and Barceló, D. (2000.); Journal of Chromatography A **889**: 195

Castillo, M., Ventura, F. and Barceló, D. (1999); Waste Management (Tucson, Arizona) **19**: 101

Chapin, R. E., Delaney, J., Wang, Y., Lanning, L., Davis, B., Collins, B., Mintz, N. and Wolfe, G. (1999); Toxicological Science **52**: 80

Christophersen, M. J. and Cardwell, T. J. (1996); Analytica Chimica Acta **323**: 39

Christopoulos, T. K. and Diamandis, E. P. (1992); Anal Chem **64** (4): 342

Clark, L. C. and Lyons, C. (1962); Ann. N. Y. Academic Science **102**: 29

Clark, M. F. and Adams, A. N. (1977); Journal of Gen. Urol. **34**: 475

Clement, R. E. and Wang, P. W. (1997); Analytical Chemistry **69**: 251R

Clement, R. E. and Wang, P. W. (1999); Analytical Chemistry **71**: 257R

Cosnier, S. (1999); Biosensors & Bioelectronics **14** (5): 443

Cowell, D. C., Dowman, A. A. and Ashcroft, T. (1995); Biosensors & Bioelectronics **10**: 509

Crisp, T. M., Clegg, E. D., Cooper, R. L., Wood, W. P., Anderson, D. G., Baetcke, K. P., Hoffmann, J. L., Morrow, M. S., Rodier, D. J., Schaeffer, J. E., Touart, L. W., Zeeman, M. G. and Patel, Y. M. (1998); Environ Health Perspect **106 Suppl 1**: 11

Cummings, E. A., Linquette-Mailley, S., Mailley, P., Cosnier, S., Eggins, B. R. and McAdams, E. T. (2001); Talanta 55: 1015

de Voogt, P., de Beer, K. and van der Wielen, F. (1997); Trends in Analytical Chemistry **10**: 584

Del Carlo, M., Lionti, I., Zaccini, M., Cagnini, A. and Mascini, M. (1997); Analytica Chimica Acta **342**: 189

Del Carlo, M. and Mascini, M. (1996); Analytica Chimica Acta **336**: 167

Diamandis, E. P. and Christopoulos, T. K. (1996); Immunoassay. Academic Press Inc., San Diego

Ding, Y., Zhou, L., Halsall, B. H. and Heineman, W. R. (1999); Journal of Pharmaceutical and Biomedical Analysis **19**: 153

Dreyhurst, G., Kadish, K. M., Scheller, F. W. and Renneberg, R. (1982); Biological Electrochemistry. Academic Press, New York

Du, X., Anzai, J., Osa, T. and Motohashi, R. (1996); Electroanalysis (New York) **8**: 813

Ekins, R. and Chu, F. (1997); J Int Fed Clin Chem **9** (3): 100

Ekins, R. and Edwards, P. (1997); Clin Chem **43** (10): 1824

Ekins, R. and Edwards, P. (1998); Clin Chem **44** (8 Pt 1): 1773

Ekins, R. P. (1960); Clinica Chimica Acta **5**: 453

Emr, S. A. and Yacynych, A. M. (1995); Electroanalysis (New York) **7**: 913

Engvall, E., Jonson, K. and Perlmann, P. (1971); Biochemica and Biophysica Acta **251**: 427

Engvall, E. and Perlmann, P. (1971); Immunochemistry **8**: 871

Engvall, E. and Perlmann, P. (1972); J Immunol **109** (1): 129

EPA-Method 625 (1984); Base / Neutrals and Acids: Environmental Protection Agency, Part VIII, 40, CFR Part 136, 26 October 1984, 153; Fed. Regist.; Washington DC

EPA-Method 604 (1984); Phenols, Environmental Protection Agency: Part VIII, 40, CFR Part 136, Fed. Regist., 26 October 1984, 58.; Fed. Regist.; Washington DC

EPA-Method 8041 (1995); Phenols by Gas Chromatography: Capillary Column Technique Environmental Protection Agency; Fed. Regist.; Washington DC

Eremenko, A., Bauer, C. G., Makower, A., Kanne, B., Baumgarten, H. and Scheller, F. W. (1998); Analytica Chimica Acta **358**: 5

Farré, M., García, M. J., Tirapu, L., Ginebreda, A. and Barceló, D. (2001); Analytica Chimica Acta **427**: 181

Farré, M., Pasini, O., Alonso, M. C., Castillo, M. and Barceló, D. (2001); Analytica Chimica Acta **426**: 155

Ferguson, P. L., Iden, C. R. and Brownawell, B. J. (2000); Analytical Chemistry **72**: 4322

Fernandez-Hernando, P. and Miller, J. N. (1991); J Pharm Biomed Anal **9** (10-12): 1121

Finklea, H. O. (1996). *in* Electroanalytical Chemistry (Bard, A. J. and Rubinstein, I.); Marcel Dekker, New York

Furtmann, K. (1994); Fresenius Journal of Analytical Chemistry **348**: 291

García-Viguera, C. and Bridle, P. (1995); Food Chemistry **54**: 349

Ghindilis, A. L., Makower, A., Bauer, C. G., Bier, F. F. and Scheller, F. W. (1995); Analytica Chimica Acta **304**: 25

Gonnord, M. F. and Collet, J. (1993); Chromatographia **645**: 327

Gunkel, G. (1994); Bioindikation in aquatischen Ökosystemen. Gustav Fischer Verlag, Jena

Hansen, P. D. (1992); Acta Hydrochim. Hydrobiol. **20** (2): 92

Hansen, P. D. (1995); The potential and limitations of new technical approaches to ecotoxicology monitoring. *in* Environmental toxicology assessment (Richardson, M.); Taylor and Francis, London

Hansen, P. D. and von Usedom, A. (1997); New biosensors for environmental analysis. *in* Frontiers in Biosensorics II: Practical Applications (Scheller, F. W., Schubert, F. and Fredowitz, J.); Birkhäuser, Basel

Harrison, R., Goodrow, M., Gree, S. and Hammock, B. (1991); Immunoassays for trace Chemical Analysis. American Chemical Society,

Hawrelak, M., Bennet, E. and Metcalfe, C. (1999.); Chemosphere **39**: 745

Heinig, K., Vogt, C. and Werner, G. (1996.); Journal of Chromatography A **745**: 281

Hennion, M. C., Pishon, V. and Barceló, D. (1994); Trends in Analytical Chemistry **13**: 361

Herrero-Martínez, J. M., Fernández-Martí, M., Simó-Alfonso, E. and Ramis-Ramos, G. (2001); Electrophoresis (Weinheim, Federal Republic of Germany) **3**: 526

Ho, W. O., Athey, D. and McNeil, C. J. (1995); Biosensors & Bioelectronics **10**: 683

Hock, B., Dankwardt, A., Kramer, K. and Marx, A. (1995); Analytica Chimica Acta **311**: 393

Hofstetter, O., Hofstetter, H., Schurig, V., Wilchek, M. and Green, B. S. (1999); Nature Biotechnology **17**: 371

Hofstetter, O., Hofstetter, H., Wilchek, M., Schurig, V. and Green, B. S. (1998); Journal of the American Chemical Society **120**: 3251

Ishikawa, E. (1987); Clin Biochem **20** (6): 375

Jackson, T. M. and Ekins, R. P. (1986); J Immunol Methods **87** (1): 13

Jahr, D. (1998); Chromatographia **47**: 49

Janata, J. (1990); Analytical Chemistry **62** (33R-44R)

Jáuregui, O., Moyano, E. and Galceran, M. T. (1997); Journal of Chromatography A **787**: 79

Jáuregui, O., Moyano, E. and Galceran, M. T. (2000); Journal of Chromatography A **896**: 125

Kalcher, K., Wang, J., Kauffmann, J. M., Svancara, I., Vytras, K., Neuhold, C. and Zhongping, Y. (1995); Electroanalysis (New York) **7**: 1

Karube, I. and Nomura, Y. (2000); Journal of Molecular Catalysis **10**: 177

Kibbey, T. C. G., Yavaraski, T. P. and Hayes, K. F. (1996); Journal of Chromatography A **752**: 155

Kiewiet, A. T. and de Voogt, P. (1996); Journal of Chromatography A **733**: 185

Kinoshita, K. (1988); Carbon - Electrochemical and physiochemical properties. Wiley, New York

Körner, W., Bolz, U., Süßmuth, W., Hiller, G., Schuller, W., Hanf, V. and Hagenmaier, H. (2000); Chemosphere **40**: 1131

Koryta, J., Dvorák, J. and Kavan, L. (1993); Principles of Electrochemistry. Wiley, Chichester

Kotte, H., Gründig, B., Vorlop, K. D., Strehlitz, B. and Stottmeister, U. (1995); Analytical Chemistry **67**: 65

Kreisselmeier, A. and Dürbeck, H. W. (1997); Journal of Chromatography A **775**: 187

Kreuzer, M. P., O'Sullivan, C. K. and Guilbault, G. G. (1999); Analytica Chimica Acta **393** (1-3): 95

Kronkvist, K., Lövgren, U., Edholm, L. E. and Johansson, G. (1993); Department of Analytical Chemistry, University of Lund, Lund

Labrousse, H. and Avrameas, S. (1987); J Immunol Methods **103** (1): 9

Lacorte, S., Fraisse, D. and Barceló, D. (1999); Journal of Chromatography A **857**: 97

Landsteiner, K. (1933); Die Spezifität der serologischen Reaktionen. Julius Springer Verlag, Berlin

Larsson, N. (2001); Analytical Chemistry, Lund University, Lund

Li, K., Woodward, L. A., Karu, A. E. and LI, Q. X. (2000); Analytica Chimica Acta **419**: 1

Lima, A. W. O., Nascimento, V. B., Predotti, J. J. and Angnes, L. (1997); Analytica Chimica Acta **354**: 325

Lindgren, A., Emnéus, J., Marko-Varga, G., Irth, H., Oosterkamp, A. J. and Eremin, S. (1998); Journal of Immunological Methods **211** (1-2): 33

Lindgren, A., Stoica, L., Ruzgas, T., Ciucu, A. and Gorton, L. (1999); Analyst **124**: 527

Lindstrom, K. and Nordin, J. (1976); Journal of Chromatography A **128**: 13

Lisdat, F., Ho, W. O., Wollenberger, U., Scheller, F. W., Richter, T. and Bilitewski, U. (1998); Electroanalysis (New York) **10**: 803

Lisdat, F., Wollenberger, U., Makower, A., Hörtnagl, H., Pfeiffer, D. and Scheller, F. W. (1997); Biosensors & Bioelectronics **12**: 1199

Lisdat, F., Wollenberger, U., Paeschke, M. and Scheller, F. W. (1998); Analytica Chimica Acta **368**: 233

Lopez-Avila, V. and Hill, H. H. (1997); Analytical Chemistry **69**: 289R

Lutz, E. S. M. and Dominguez, E. (1996); Electroanalysis (New York) **8**: 117

Maggio, E. R. (1980); Enzyme immunoassay. CRC Press, Cleveland

Maiolini, R., Ferrua, B. and Masseyeff, R. (1975); J Immunol Methods **6** (4): 355

Makower, A., Eremenko, A. V., Streffer, K., Wollenberger, U. and Scheller, F. W. (1996); Journal of Chemical Technology and Biotechnology **65**: 39

Marcheterre, L., Choundry, G. G. and Webster, G. R. B. (1988); Reviews in Environmental Contamination and Toxicology **103**: 61

Marcomini, A. and Giger, W. (1987); Analytical Chemistry **59**: 1709

Marcomini, A. and Zanette, M. (1996); Journal of Chromatography A **733**: 193

Markhem, D. A., McNett, D. A., Burk, J. H., Klecka, G. M., Bartels, M. J. and Staples, C. A. (1998); International Journal of Environmental Analytical Chemistry **69**: 83

Másson, M., Liu, Z., Haruyama, T., Kobatake, E., Ikariyama, Y. and Aizawa, M. (1995); Analytica Chimica Acta **304**: 353

McCreery, R. L. (1991). *in* Electroanalytical Chemistry (Bard, A. J.); Marcel Dekker, New York

Metzger, J., Reiss, M. and Hartmeier, W. (1998); Biosensor & Bioelectronics **13**: 1077

Mizutani, F., Yabuki, S. and Asai, M. (1991); Biosensors & Bioelectronics **6**: 305

Morales, E. and Cela, R. (2000); Journal of Chromatography A **896**: 95

Moseley, P. T. and Crocker, A. J. (1996); Sensor materials. IOP Publishing,

Murray, R. W. (1984). *in* Electroanalytical Cehmistry (Bard, A. J.); Marcel Dekker, New York

Naylor, C. G. (1995); Surfact. Wastewat. **27**: 29

Neilson, A. H., Ellard, A. S., Hynning, P. A. and Ramberger, M. (1991); Toxicological and Environmental Chemistry **3**: 3

Ng, L. K., Lafontaine, P. and Harnois, J. (2000); Journal of Chromatography A **873**: 29

Nistor, C. and Emnéus, J. (1998); Journal of Analytical Communication **35**: 417

Nistor, C. and Emnéus, J. (1999); Waste Management (Tucson, Arizona) **19**: 147

Nistor, C., Emnéus, J., Gorton, L. and Ciucu, A. (1999); Analytica Chimica Acta **387**: 309

Nistor, C., Osvik, A., Davidsson, R., Rose, A., Wollenberger, U., Pfeiffer, D., Emneus, J. and Fiksdal, L. (2002); Water Science and Technology **45** (4-5): 191

Nistor, C., Rose, A., Wollenberger, U., Pfeiffer, D. and Emnéus, J. (2002); The Analyst **127**: 1076

Niwa, O., Morita, M. and Tabei, H. (1991); Electroanalysis (New York) **3**: 163

Oellerich, M. (1984); J Clin Chem Clin Biochem **22** (12): 895

Ogan, K. and Katz, E. (1981); Analytical Chemistry **53**: 160

Önnerfjord, P., Emnéus, J., Marko-Varga, G. and Gorton, L. (1995); Biosensors & Bioelectronics **10**: 607

Önnerfjord, P., Eremin, S., Emnéus, J. and Marko-Varga, G. (1998); Journal of Chromatography A **800**: 219

Oosterkamp, A. J., Hock, B., Seifert, M. and Irth, H. (1997); Trends in Analytical Chemistry **10**: 544

Ortega, F., Dominguez, E., Burestedt, E., Emnéus, J., Gorton, L. and Marco-Varga, G. (1994); Journal of Chromatography A **675**: 65

Ortega, F., Dominguez, E., Jonson-Petterson, G. and Gorton, L. (1993); Journal of Biotechnology **31**: 289

Ortner, E. K. and Rower, E. R. (1999); Journal of Chromatography A **863**: 57

Palmer, D. A. and Miller, J. N. (1995); Analytica Chimica Acta **303**: 223

Palmisano, F., Zambonin, P. G. and Centonze, D. (2000); Fresenius Journal of Analytical Chemistry **366** (6/7): 586

Pardue, H. L. (1997); Clin Chem **43** (10): 1831

Piangerelli, V., Nerini, F. and Cavalli, S. (1993); Ann. Chim. **83**: 331

Pocurull, E., Marcé, R. M. and Borrull, F. (1996); Journal of Chromatography A(738): 1

Powley, M. W. and Carloson, G. P. (1999); Toxicology **139**: 207

Parellada, J., Narvaez, A., Lopez, M. A., Dominguez, E., Fernandez, J. J., Pavlov, V. and Katakis, I. (1998); Analytica Chimica Acta **362** (1): 47

Puig, D. and Barceló, D. (1995); Analytica Chimica Acta **311**: 63

Puig, D. and Barceló, D. (1997); Journal of Chromatography A **778**: 313

Realini, P. A. (1981); Journal of Chromatographic Science **19**: 124

Rivas, A., Olea, N. and Olea, S., F. (1997); Trends in Analytical Chemistry **16**: 613

Roche-Industries (1999); ß-galactosidase product information sheet

Rodriguez, M. C. and Rovas, G. A. (2002); Analytica Chimica Acta **459**: 43

Rogers, K. R. (1995); Biosensors & Bioelectronics **10**: 533

Rose, A., Pfeiffer, D., Scheller, F. W. and Wollenberger, U. (2001); Fresenius Journal of Analytical Chemistry **369** (2): 145

Rudel, R. A., Melly, S. J., Geno, P. W., Sun, G. and Brody, J. G. (1998); Environmental Science and Technology **32**: 861

Savies, C. (1994); Antibodies. *in* The immunoassay handbook (Wild, D.); Stockton Press, New York

Scheller, F. W., Bauer, C. G., Makower, A., Wollenberger, U., Warsinke, A. and Bier, F. F. (2001); Analytical Letters **34**: 1233

Scheller, F. W., Schubert, F., Neumann, B., Pfeiffer, D., Hintsche, R., Dransfeld, I., Wollenberger, U., Renneberg, R., Warsinke, A. and Johansson, G. (1991); Biosensors & Bioelectronics **6** (3): 245

Scheller, F. W., Wollenberger, U., Schubert, F., Pfeiffer, D. and Bogdanovskaya, V. A. (1987); GBF Monographs **10**: 39

Schmidt, H. L., Schuhmann, W., Scheller, F. W. and Schubert, F. (1992). *in* Sensors a comprehensive survey (Göpel, W., Hesse, J. and Zemel, J. N.); VCH, Weihnheim

Schneider, R. J., Weil, L. and Niessner, R. (1992); Fresenius Journal of Analytical Chemistry **343**: 145

Schubert, F., Kirstein, D., Schröder, K. L. and Scheller, F. W. (1985); Analytica Chimica Acta **169**: 391

Schuhmann, W. (1995); Mikrochimica Acta **121**: 1

Schumacher, J. T., Münch, I., Richter, T., Rohm, I. and Bilitewski, U. (1999); Journal of Molecular Catalysis **7**: 67

Scullion, S. D., Clench, M. R., Cooke, M. and Ashcroft, A. E. (1996); Journal of Chromatography A **733**: 207

Sharpe, R. and Skakkebaek, N. E. (1993); The Lancet **341**: 1392

Sittampalam, G. S. and Wilson, G. S. (1984); Trends in Analytical Chemistry **3**: 4

Soto, A. M., Justicia, H., Wray, J. W. and Sonnenschein, C. (1991); Environmental Health Perspectives **92**: 167

Stangl, G., Weller, M. G. and Niessner, R. (1995); Fresenius Journal of Analytical Chemistry **351**: 301

Starodub, N. F., Kanjuk, N. I., Kukla, A. L. and Shirshov, Y. M. (1999); Analytica Chimica Acta **385**: 461

Stöcklein, W. F. M., Rhode, M., Scharte, G., Behrsing, O., Warsinke, A., Micheel, B. and Scheller, F. W. (2000); Analytica Chimica Acta **405**: 255

Streffer, K., Vijgenboom, E., Tepper, A. W. J. W., Makower, A., Scheller, F. W., Canters, G. W. and Wollenberger, U. (2000); Analytica Chimica Acta

Szeponik, J., Möller, B., Pfeiffer, D., Lisdat, F., Wollenberger, U., Makower, A. and Scheller, F. W. (1997); Biosensors & Bioelectronics **12** (9-10): 947

Takeda-Industries (2000); Non-ionic surfactant APE ELISA KIT (Microplate) Operation Manual

Takino, M., Daishima, S. and Yamaguchi, K. (2000); Journal of Chromatography A **904**: 65

Talmage, S. S. (1994); Environmental and Human Safety of Major Surfactants, Alcohol Ethoxylates and Alkylphenol Ethoxylates (The Soap and Detergent Association). Lewis Publishers, Inc., Boca Raton

Tang, H., Lunte, C. E., Halsall, B. H. and Heineman, W. R. (1988); Analytica Chimica Acta **214**: 187

Thevenot, D. R., Toth, K., Durst, R. A. and Wilson, G. S. (1999); Pure and Applied Chemistry **71**: 2333

Thorpe, G. H. G., Kricka, L. J., Moseley, S. B. and Whitehead, T. P. (1985); Clinical Chemistry **31**: 1335

Traversa, E., Sadaoka, Y., Carotta, M. C. and Martinelli, G. (2000); Sensors and Actuators, B: Chemical Sensors and Materials **65**: 181

Turner, A. P., Karube, I. and Wilson, G. S. (1987); Biosensors, fundamentals and applications. Oxford University Press, Oxford

Valsecchi, S., Polesello, S. and Cavalli, S. (2001); Journal of Chromatography A **925**: 297

van Emon, J. M. (2001); Evolution of environmental immunochemistry. American Chemical Society 222nd ACS National Meeting, Chicago, IL

van Emon, J. M., Gerlach, C. L. and Brownman, K. (1998); Journal of Chromatography B **715**: 211

van Emon, J. M., Gerlach, C. L. and Sadik, O. A. (1997); Electrochemical immunosensors for pesticide detection. American Chemical Society 213th ACS National Meeting, San Francisco

Vinas, P., Lopez-Erroz, C., Marin-Hernández, J. J. and Hernández, C. (2000); Journal of Chromatography A **871**: 85

Vincent, G. (1991); Micro-Pollutants in the Aquatic Environment. Kluwer Academic Publishers, Dordrecht

Wallace, G. G. (1999); Trends in Analytical Chemistry **18** (4): 245

Wang, J., Nascimento, V. B., Kane, S. A., Rogers, K. R., Smyth, M. R. and Angnes, L. (1996); Talanta **43**: 1903

Wang, J., Pamidi, P. V. and Park, D. S. (1996); Analytical Chemistry **68**: 2705

Wang, J., Rivas, G., Cai, X., Palecek, E., Nielsen, P., Shiraishi, H., Dontha, N., Luo, D., Parrado, C., Chicharro, M., Farias, P. A. M., Grant, D. H., Ozsoz, M. and Flair, M. N. (1997); Analytica Chimica Acta **347**: 1

Wang, J., Tian, B., Nascimento, V. B. and Angnes, L. (1998); Electrochimica Acta **43** (23): 3459

Weinheimer, R. M. and Varineau, P. T. (1998); Polyoxyethylene Alkylphenols. *in* Nonionic Surfactants (van Os, N. M.); Marcel Dekker Inc., New York

Weller, M. G. (2000); Institute of Hydrochemistry, Technical University, Munich

Weller, M. G., Weil, L. and Niessner, R. (1996); Direct supression of cross-reactivity in immunoassays by pH-variation (poster)Analytica conference96, Munich

Wen, J., Wollenberger, U. and Scheller, F. W. (1998); Biol. Chem. **379**: 1207

White, R., Jobling, S., Hoare, S. A., Sumpter, J. P. and Parker, M. G. (1994); Endocrinology **135**: 175

Wijayawardhana, C. A., Purushothama, S., Cousino, M.-A., Halsall, B. H. and Heineman, W. R. (1999); Journal of Electroanalytical Chemistry **468**: 2

Wild, D. (1994); The immunoassay handbook. Stockton press, Houndmills, England

Wink, T., van Zuilen, S. J., Bult, A. and van Bennekom, W. P. (1997); The Analyst 122: 43R

Wissiask, R., Rosenberg, E. and Grasserbauer, M. (2000); Journal of Chromatography A 896: 159

Wittmann, C., Bier, F. F., Eremin, S. and Schmid, R. D. (1996); J. Agric. Food. Chem. 44: 343

Wollenberger, U., Schubert, F., Pfeiffer, D. and Scheller, F. W. (1993); Trends in Biotechnology 11: 255

Wollenberger, U. and Neumann, B. (1997); Electroanalysis (New York) **9**: 366

Yager, J. W., Eastmond, D. A., Robertson, M. L., Paradisin, W. M. and Smith, M. T. (1990); Cancer Res 50 (2): 393

Yi-Feng, T. and Hong-Yuan, C. (2002); Biosensor & Bioelectronics **17**: 19

Zhang, J., Heineman, W. R. and Halsall, B. H. (1999); Journal of Pharmaceutical and Biomedical Analysis 19: 145

Zhao, M., van der Wielen, F. and de Voogt, P. (1999); Journal of Chromatography A 837: 129